

THE ROLE OF HYPOXIA, NEUTROPHIL ELASTASE, AND HIF-1 α IN
HEPATOCELLULAR INJURY

By

Erica Marie Sparkenbaugh

A DISSERTATION

Submitted to
Michigan State University
in partial fulfillment of the requirements
for the degree of

DOCTOR OF PHILSOPHY

Department of Pharmacology and Toxicology

2011

ABSTRACT

THE ROLE OF HYPOXIA, NEUTROPHIL ELASTASE, AND HIF-1 α IN HEPATOCELLULAR INJURY

By

Erica Marie Sparkenbaugh

The liver is sensitive to many toxic insults and diseases, in which hepatocellular injury is mediated by neutrophil (PMN)-mediated inflammation and hypoxia (HX). PMNs cause hepatocyte (HPC) injury through the release of the toxic protease elastase (EL). Primary HPCs are sensitized to the cytotoxic effects of EL when exposed to HX, indicating an interaction between EL and HX. The mechanism of this interaction is not understood, and is the focus of this dissertation.

I tested the hypothesis that the interaction of HX and EL requires reactive oxygen species (ROS), mitogen activated protein kinases (MAPK) and HIF-1 α signaling. Results indicated that ROS were not involved; however lipid peroxidation is an important mediator of cell death in this interaction. Furthermore, HX increased HIF-1 α activation, which was enhanced by cotreatment with EL and resulted in transcription of the cell death proteins Nix and BNIP3. The transactivation of HIF-1 α was mediated in part by p38 MAPK signaling in HX/EL-cotreatment.

The results indicated that HIF-1 α is a critical mediator of HPC injury in vitro, however it is not known if HIF-1 α can contribute to liver injury in an in vivo model of drug-induced liver injury (DILI). Therefore, I tested the hypothesis that HIF-1 α contributes to HPC injury in a well-studied model of DILI, acetaminophen overdose. To

test this, conditional HIF-1 α knockout mice were utilized. Results indicated that HIF-1 α contributes to early cell death signaling in HPCs, and to the production of pro-inflammatory cytokines, PMN infiltration, and coagulation system activation, all of which contribute to early acetaminophen hepatotoxicity at 6 hours after overdose. However, HIF-1 α knockout mice eventually developed severe liver injury by 24 hours, indicating that HIF-1 α might have a protective role at later times.

In summary, the mechanism of the cytotoxic interaction of HX and EL was elucidated, and lipid peroxidation, p38 MAPK and HIF-1 α were identified to have critical roles in hepatocellular injury. Furthermore, I have demonstrated a dual role for HIF-1 α in a model of DILI. This indicates that HIF-1 α is a complex transcription factor and could be a central mediator of both hepatocyte damaging and protective pathways in models of toxic liver injury and disease when both PMNs and tissue HX are involved.

ACKNOWLEDGMENTS

To begin, I'd like to thank my mentor Dr. Robert Roth. My decision to come to MSU was partially due to my interest in the work being published by his laboratory, and I was thrilled to have a chance to rotate with and eventually join the group. Bob's ability to ask subtle questions that require me to think more deeply about my results and interpretation have helped me develop into a better scientist. Bob has also offered support and encouragement during the most difficult times of my graduate research. I also appreciate the fun atmosphere of the lab, including the chats about our weekend bike rides, Friday night happy hours, and our annual kayaking and camping trip.

I'd also like to thank Dr. Patricia Ganey. Patti often provided a different perspective on results that taught me to think about data from multiple angles, thus helping me to become a better scientist. Patti's mentorship has also helped me to become a better writer and presenter. I have been fortunate to have the mentorship of Bob and Patti, who have created a supportive environment. I truly am grateful for the part they have played in both my professional and personal development.

My committee members have also played a significant role in the work presented in this dissertation. Dr. Norbert Kaminski has offered guidance and advice as a committee member, and his suggestions have strengthened the work presented. I have benefitted greatly from having Dr. John LaPres as both a committee member and collaborator. My gratitude extends to many members of his laboratory, including Dr. Ajith Vengellular, Dr. Scott Lynn, and Dr. Yogesh Saini, who have provided scientific support and friendship over the years.

I had the opportunity to collaborate with former laboratory members Dr. Bryan Copple and Dr. Jim Luyendyk when they were at KUMC. They have provided a lot of advice and encouragement over the years, and I have always looked forward to our interactions at scientific meetings.

Within our laboratory, I would like to thank Dr. Jane Maddox, with whom I did my rotation, and our former research assistant Sandra Newport; they trained me in my early days in the laboratory and helped me adjust to the environment as a new graduate student. A former graduate student, Dr. Patrick Shaw, has also served as a great friend and mentor over the years, especially during my early days in the laboratory.

I have also had the pleasure of working with numerous individuals throughout my time in the lab, including Dr. Kassim Traore, Krista Greenwood and Mitchell Nothem. I also need to thank the current and former members of the laboratory. Dr. Francis Tukov, Dr. Sachin Devi, Dr. Steve Bezdecny offered assistance and advice when I first joined, and Dr. Xiaomin Deng and Dr. Wei Zou allowed me to collaborate with them on multiple studies. I would especially like to thank Dr. Rohit Singhal, Dr. Christine Dugan, Aaron Fullerton, Kyle Poulsen, Kevin Beggs, Kaz Miyakawa, Jingtao Lu and Ashley Maiuri, who have been great coworkers and friends. This research would also not have been possible with the assistance of our research assistant Nicole Crisp, and undergraduates Emily Evenson, Allen MacDonald, and Ryan Albee.

The Department of Pharmacology and Toxicology also deserves my thanks. My gratitude goes to Dr. Anne Dorrance and Dr. Carrie Northcott, who have provided me with mentorship and career advice. Additionally, the administrative staff, especially

Diane Hummel, has been extremely helpful to me as I have navigated the academic system. I'd also like to thank the Center for Integrative Toxicology, including Amy Swagart and Carol Chvojka, for their help with travel arrangements and financial issues. I would also like to thank numerous graduate students, specifically Dr. Erika Boerman, Dr. Sachin Kandlikar and Priya Raman, for their friendship and support throughout our graduate career.

I am also extremely grateful to the Society of Toxicology for the many opportunities it has offered me, especially the Michigan regional chapter. I have had numerous opportunities to work alongside excellent scientists and people, and my experiences within SOT as a student representative have played a large role in my scientific and professional development. I would like to especially thank Betty Eidemiller and Dylan Amerine for their help during my time in SOT.

This research would not have been possible without funding from various sources. Thank you to Bob, whose NIH grants supported my research, and the CIT training grant for my stipend. I'd also like to thank the Graduate School at MSU for a dissertation completion fellowship. Finally, I have had financial support from CIT, SOT, and Gordon Research conferences to attend scientific meetings.

I owe a big thank to my friends, who have made each day easier than they could possibly imagine. I am also extremely grateful to my family. I would not be the person I am today without my parents, who have always been encouraging of my academic and scientific interests. My brother Charlie, step-parents, Michele and Jim, and my in-laws,

Ed and Nancy, have been very supportive and willing to help in any way, and I am very grateful.

My deepest thanks go to my husband Dan, who has done 90% of the chores over the years and escorted me to the lab late at night when I didn't want to go in alone. Dan's continuous support, encouragement, and understanding have been the cornerstone of my success.

TABLE OF CONTENTS

LIST OF TABLES.....	x
LIST OF FIGURES	xi
KEY TO SYMBOL OR ABBREVIATIONS	xiii
CHAPTER 1.....	1
General Introduction and Specific Aims	1
1.1 Overview of liver physiology	2
1.2 The biological role of oxygen	5
1.2.1 Normoxia versus hypoxia.....	6
1.2.2 The occurrence of hypoxia and its role in liver disease	8
1.2.3 Hypoxia signaling	9
1.2.4 Pathological responses to hypoxia	19
1.2.5 Summary of hypoxia	27
1.3 Neutrophils in liver disease.....	28
1.3.1 Neutrophil accumulation and activation.....	28
1.3.2 Neutrophil elastase	31
1.3.3 Mechanisms of elastase-mediated cell death.....	31
1.3.4 Role of EL in liver disease and chemical toxicity	35
1.5 The role of hypoxia and neutrophils in liver disease and toxicity.....	36
1.6 Summary	50
1.7 Hypothesis and specific aims.....	52
1.8 Overview and significance of dissertation	53
CHAPTER 2.....	54
2.1 Abstract	55
2.2 Introduction.....	56
2.3 Materials and Methods	59
2.4 Results	65
2.5 Discussion	94

CHAPTER 3.....	100
3.1 Abstract	101
3.2 Introduction.....	102
3.3 Materials and Methods	104
3.4 Results	107
3.5 Discussion.....	120
 CHAPTER 4.....	 126
4.1 Abstract	127
4.2 Introduction.....	128
4.3 Methods	131
4.4 Results	138
4.6 Discussion.....	171
 CHAPTER 5.....	 177
5.1 Summary of research	178
5.1.2 The role of HX and HIF-1 α in an in vitro model of liver injury.....	178
5.1.2 The role of HIF-1 α in an in vivo model of liver injury.....	185
5.2 Considerations for in vitro and cell culture experiments	193
5.3 Major findings and implications.....	195
5.4 Knowledge gaps and future studies.....	197
 REFERENCES	 201

LIST OF TABLES

Table 1: Summary of hypoxia-responsive transcription factors	10
Table 2: The pathways involved in EL- and HX-mediated cell death	51
Table 3: Effect of HX/EL on Lipid Peroxidation in Hepa1c1c7 and HepaC4 cells.	92
Table 4: Hepatic HIF-1 α mRNA expression after APAP overdose.....	141
Table 5: Hepatic BNIP3 mRNA expression after APAP overdose.....	150
Table 6: Hepatic PAI-1 mRNA expression after APAP overdose in HIF-1 α ^{+fl/+fl} and HIF-1 α ^{Δ/Δ} mice.	161
Table 7: Cytokine concentrations in plasma of APAP-treated HIF-1 α ^{+fl/+fl} and HIF-1 α ^{Δ/Δ} mice.....	165

LIST OF FIGURES

Figure 1: Protein structure of HIF-1 α and HIF-1 β	12
Figure 2: Oxygen-dependent regulation of HIF-1 α	15
Figure 3: The TVX/LPS model of IDILI.....	42
Figure 4: The LPS/RAN model of IDILI.....	45
Figure 5: Exposure to HX sensitizes HPC to cell killing by EL.....	48
Figure 6: Hypoxia sensitizes HPCs and Hepa1c1c7 cells to cytotoxicity of EL.....	66
Figure 7: Caspase 3/7 and mitochondrial permeability transition do not contribute to cell death caused by HX/EL cotreatment.....	68
Figure 8: HX/EL cotreatment causes an additive increase in activation of p38, but not JNK or ERK.....	71
Figure 9: Inhibition of p38, but not JNK or ERK, protects Hepa1c1c7 cells from HX/EL interaction.....	73
Figure 10: HX/EL increases nuclear accumulation of HIF-1 α compared to HX alone... ..	77
Figure 11: HX/EL increases mRNA expression of HIF-1 α -regulated genes, Nix and BNIP3.....	79
Figure 12: HX/EL increases expression of BNIP3 protein in a p38-dependent manner	81
Figure 13: HIF-1 β -deficient HepaC4 cells are protected from HX/EL.....	84
Figure 15: Lipid peroxidation contributes to the mechanism of HX/EL-induced cell death in Hepa1c1c7 cells.....	90
Figure 16: ROS and XO are not involved in the interaction of HX/EL.....	108
Figure 17: Intracellular calcium chelation does not protect cells from HX/EL-induced cytotoxicity.....	110
Figure 18: Effect of HIF-1 α inducers in the cytotoxicity of HX/EL.....	114
Figure 19: The role of NF- κ B in HX/EL induced cytotoxicity.....	116
Figure 20: HX/EL downregulates ATF2 activation and cyclin D1 expression.....	118

Figure 21: Conditional HIF-1 α deletion in mice	139
Figure 22: Effect of HIF-1 α deletion on APAP hepatotoxicity.	145
Figure 23: Time course of APAP-induced liver injury in HIF-1 α -deficient mice.	147
Figure 24: Mitochondrial Bax translocation	152
Figure 25: DNA fragmentation after APAP treatment	154
Figure 26: Effect of HIF-1 α deletion on thrombin production and fibrin deposition.	159
Figure 27: Effect of HIF-1 α deletion on PAI-1 production.....	163
Figure 28: Hepatic and plasma concentration of cytokines..	167
Figure 29: Hepatic PMN accumulation after APAP overdose in HIF-1 α ^{+fl/+fl} and HIF-1 α ^{Δ/Δ} mice.....	169
Figure 30: Proposed pathway to HX/EL-induced hepatocyte injury	183
Figure 31: Genetic knockout of EL does not protect from APAP overdose..	186
Figure 32: The proposed dual role of HIF-1 α in APAP overdose.	191

KEY TO SYMBOL OR ABBREVIATIONS

AAT	α 1-antitrypsin
ALT	alanine aminotransferase
ANIT	alpha-naphthylisothiocyanate
APAP	acetaminophen
ARNT	aryl hydrocarbon nuclear translocator
BDEC	bile duct epithelial cell
bHLH	basic helix-loop-helix
BNIP3	Bcl-2/adenovirus E1B 19 kDa protein-interacting protein 3
CsA	cyclosporine A
DILI	drug-induced liver injury
EL	neutrophil elastase
ERK	extracellular regulated kinase
ETC	electron transport chain
GI	gastrointestinal
GSH	oxidized glutathione
GSSG	reduced glutathione
HIF	hypoxia inducible factor
HPC	hepatic parenchymal cell
HRE	hypoxia response element
HX	hypoxia
IADR	idiosyncratic adverse drug reaction
IFN	interferon
IL	interleukin
I-R	ischemia-reperfusion
JNK	jun-kinase
KCs	Kupffer cells
IL-8/KC	interleukin-8/keratinocyte chemoattractant
LDH	lactate dehydrogenase
LPS	lipopolysaccharide
MAPK	mitogen activated protein kinase
mmHg	millimeters of mercury
MPO	myeloperoxidase
NAPQI	<i>n</i> -acetyl- <i>p</i> -benzoquinone imine
NF- κ B	nuclear factor kappa beta
NIX	NIP3-like protein (BNIP3L)
NX	normoxia
O ₂	oxygen
OxR	oxygen replete
ODD	oxygen dependent degradation
P38	p38 protein kinase
PAI-1	plasminogen activator inhibitor-1
PAR	protease activated receptor
PMN	polymorphonuclear lymphocyte, or neutrophil
pO ₂	partial pressure of oxygen

PAS	Per-ARNT-SIM
RANTES	regulated upon activation normal T cell expressed and secreted
pVHL	von-Hippel Lindau tumor suppressor gene product
ROS	reactive oxygen species
SEC	sinusoidal endothelial cell
TAD	transactivation domain
TAM	tamoxifen
TBARS	thiobarbituric acid reactive substances
TNF	tumor necrosis factor
VEGF	vascular endothelial growth factor
XD	xanthine dehydrogenase
XO	xanthine oxidase/oxidoreductase

CHAPTER 1

General Introduction and Specific Aims

1.1 Overview of liver physiology

The liver is situated in the circulation between the gastrointestinal (GI) tract and the rest of the body, and it fulfills a variety of essential roles to metabolism and homeostasis. Blood from the stomach and intestines flows into the liver through the portal vein and enters the sinusoidal system of the liver to be filtered before exiting the liver through the vena cava to the rest of the body. Therefore, the liver is the first organ to encounter ingested nutrients and vitamins, xenobiotics such as drugs and environmental contaminants, and waste products of indigenous intestinal microflora. The cells of the liver efficiently scavenge or take up these substances and chemically alter them for storage, metabolism, or excretion (72).

The liver is the largest internal organ, and it is divided into four lobes: the left and right anatomical lobes on the anterior surface, and the caudate lobe and quadrate lobe on visceral surface. Each of the lobes is organized into functional units called lobules. Hexagonal units of hepatic parenchymal cells (HPCs), or hepatocytes, surround a central vein, which eventually joins the hepatic vein to carry blood out of the liver. This is referred to as the centrilobular region. At the corners of each lobule, portal triads contain branches of the common bile duct, the portal vein and the hepatic artery, through which blood enters the liver. These areas are referred to as periportal regions. Arterial blood and portal venous blood from the GI tract filter through sinusoids, permeable capillaries with large pores, or fenestrae, lined by sinusoidal endothelial cells (SECs), that drain into the central vein. Bile produced by the HPCs is secreted into bile canaliculi, which are thin channels between HPCs, and is carried out of the lobule through the common bile duct and eventually out of the liver.

HPCs perform a variety of functions, including production of plasma proteins such as albumin and other globulins, clotting factors like prothrombin and fibrinogen, bile acids, bilirubin and cholesterol. They have a vital role in glucose metabolism, glycogen storage and gluconeogenesis. HPCs also play an essential role in the elimination of xenobiotics and endogenous substances like steroids; thus, they contain large amounts of phase-I and phase-II enzymes. Phase-I enzymes (eg, cytochromes P450) generate reactive electrophilic metabolites, which can then be processed by phase-II enzymes which add polar groups to generate stable, hydrophilic compounds that can be more readily excreted (72).

Due to its location downstream of the GI tract, the liver is exposed to a variety of exogenous agents, including pathogens, toxins, xenobiotics and their metabolites, and components from the diet. It is enriched with cells of the innate immune system, and contains a large population of resident macrophages called Kupffer cells (KCs) which act as the first line of defense against bacterial pathogens from the GI tract. Other innate immune system cells in the liver include natural killer and natural killer T-cells (109). Activation of the innate immune system in the liver can result in an inflammatory response that is important in eliminating infections. Unfortunately, mediators released during the inflammatory response can also damage HPCs. Inflammatory responses are often accompanied by low oxygen environments during liver disease and toxic reactions. This is due to decreased tissue perfusion caused by coagulation-mediated fibrin deposition (112), edema and accumulation of innate immune cells in the sinusoids (169). Furthermore, the liver is a highly metabolically active tissue and requires efficient delivery of nutrients and oxygen to support its functions; consequently, it is exquisitely

vulnerable to liver diseases and chemical toxicants which disrupt blood flow and/or oxygen utilization (71). The remainder of this Introduction will discuss oxygen homeostasis and the inflammatory response. Specific clinical situations and chemical toxicities in which low oxygen and inflammation play a role will also be discussed. Finally, the overall hypothesis and specific aims will be presented.

1.2 The biological role of oxygen

Oxygen plays a vital role in metabolism and energy production in the body. During external respiration, oxygen is taken into the lungs via ventilation. Pulmonary gas exchange occurs when oxygen diffuses across the alveoli and pulmonary capillaries and into the blood, where it is exchanged for carbon dioxide. Upon entering the blood, oxygen binds to hemoglobin, a protein comprising four subunits each of which contains a heme moiety that includes an atom of ferrous iron, which can reversibly bind an oxygen molecule in a process called “oxygenation.” Oxyhemoglobin can deliver oxygen to the peripheral tissues, where deoxygenation occurs. The difference in partial pressure of oxygen (pO_2) between blood and the site of oxygen utilization within the cell drives oxygen into the tissue via passive diffusion (9).

Mitochondria are the major site of oxygen utilization in cells, due to the electron transport chain (ETC) and oxidative phosphorylation. The ETC comprises complexes I, II, III and IV on the inner mitochondrial membrane. Electron donors such as NADH and $FADH_2$, which are generated mainly in the tricarboxylic acid cycle, are coupled to the transfer of protons (H^+) from the mitochondrial matrix to the intermembrane space, creating a proton gradient. Within the ETC, electrons are transferred to ubiquinone (Q), reducing it to ubiquinol (QH_2). At complex III, electrons are removed from QH_2 and transferred to cytochrome c, which is a water-soluble electron carrier within the intermembrane space. Complex IV, or cytochrome c oxidase, catalyzes the transfer of electrons from cytochrome c to molecular oxygen, which acts as the terminal electron acceptor, thereby creating water molecules. These steps are essential to ATP

production, because it maintains the H^+ gradient across the inner membrane of the mitochondrion that ultimately drives the H^+ -ATPase, resulting in ATP production from ADP and P_i (9, 162).

1.2.1 Normoxia versus hypoxia

Inspired air is composed of roughly 21% oxygen, as well as nitrogen, argon and carbon dioxide. The pressure of inspired air is 760 mmHg, and when it enters the lungs it becomes saturated with water vapor, which has a pressure of 47 mmHg. Each gas in a mixture exerts its own partial pressure, according to Dalton's Law. Since oxygen constitutes 21% of inspired air, the partial pressure of oxygen (pO_2) can be calculated as follows:

$$pO_2 = 0.21 \times (760 - 47) = 150 \text{ mmHg.}$$

Due to gas exchange in the alveoli and to mixing with dead-space gas in the airways, the pO_2 of alveolar air is about 105 mmHg. In the alveoli, oxygen is exchanged for hemoglobin-bound carbon dioxide in red blood cells, and the pO_2 in the arterial blood is approximately 100 mmHg. Blood carries oxyhemoglobin through the circulatory system and to the capillaries of the tissues, where there is a gradient of high pO_2 in the blood to low pO_2 in the tissue. This pO_2 gradient causes oxygen to dissociate from hemoglobin and diffuse through the capillary endothelium into parenchymal cells. The deoxygenated blood draining from tissues mixes with shunted arterial blood in the veins,

and thus the pO_2 in blood draining the average organ (ie, mixed venous pO_2) is around 40 mmHg (9, 102).

The normal pO_2 to which cells are exposed varies among and within different tissues, depending on the metabolic needs of the tissue, the distance of cells from the vascular supply, and whether the cells are positioned upstream or downstream relative to adjacent capillaries. For instance, in the brain, the pO_2 in neurons within 60 microns (μm) of arterial walls ranged from 15-40 mmHg, and neurons within 40 μm of venous drainage was 12-30 mmHg, as measured by platinum polarographic electrodes (178).

In the liver, the pO_2 varies by proximity to blood supply. As mentioned previously, blood from the hepatic artery with a pO_2 of 100 mmHg mixes with blood from the portal vein, which drains from the GI tract and spleen. The pO_2 of blood in the portal vein has been measured as 38 ± 6.8 mmHg in rats (65). Thus, the pO_2 of blood in the portal triad, the sinusoids and central vein are estimated to be 50-65 mmHg, 45 mmHg and 30-40 mmHg, respectively (80, 173). To permit passive diffusion of oxygen into cells, the intracellular pO_2 must be lower than that of the blood by roughly 15 mmHg; therefore the pO_2 in HPCs in the portal triad and central vein is approximately 40-50 mmHg and 15-20 mmHg respectively (87). There are also pO_2 gradients within cells due to constant oxygen consumption by the mitochondria (102, 169).

It is important to note that cells are adapted to the degree of oxygen to which they are usually exposed, and this is considered “normoxia” (NX). It is not clear how cells establish this state of normoxia; however, once the pO_2 in the tissue or cell falls below this normal level, the state is called “hypoxia” (HX) (102). A complete lack of oxygen (ie, $pO_2=0\text{mmHg}$), is termed “anoxia,” which is incompatible with life for an aerobic organism. Due to the central role of oxygen in ATP production in the electron transport chain, HX is sensed by cells as a metabolic crisis that requires them to adapt through increased anaerobic metabolism via glycolysis and other means.

1.2.2 The occurrence of hypoxia and its role in liver disease

Physiologically, there are four types of HX, which are (1) “hypoxic HX,” in which the pO_2 of arterial blood is reduced; (2) “anemic HX,” in which the amount of hemoglobin available to carry O_2 is reduced but arterial pO_2 is normal; (3) “ischemic HX,” in which blood flow to tissue is inadequate despite normal pO_2 and hemoglobin availability; and (4) “histotoxic HX” or “chemical HX,” in which cells cannot utilize oxygen supplied to them due to a toxic agent (9). Strictly speaking, the latter is not HX, since oxygen delivery to cells is normal, although the term is commonly used. Physiologically, histotoxic or chemical HX often results in greater tissue pO_2 due to inability of cells to utilize oxygen. Any mention of HX in this dissertation refers to the first three types, unless chemical HX is specifically stated.

HX occurs during normal physiological events as well as pathological conditions. It is common during embryonic and fetal development, and is important for normal

vasculogenesis, angiogenesis and tubulogenesis (102). HX also occurs during exercise when muscle demand for oxygen exceeds supply and cells switch to anaerobic metabolism to maintain muscle function. Recently, a role for HX has been discovered in many pathological conditions including cardiovascular disease and stroke, chronic pulmonary disease, GI disease, and cancer (154). HX is an important contributor to the pathogenesis of injury in a variety of diseases and chemical toxicities affecting the liver, including hemodynamic shock, fulminant hepatitis, septicemia, cardiac and/or pulmonary failure, and systemic inflammatory response syndrome, among others (1). These and others will be discussed in greater detail later in this Introduction.

1.2.3 Hypoxia signaling

Aerobic respiration and oxidative phosphorylation are essential to energy production in cells. When the oxygen supply cannot meet the energy demands of the cell due to HX, there must be an adaptive response to counteract the reduction in energy production. Cells have evolved numerous adaptive responses to compensate for changes in oxygen demand, including transcriptional regulation of genes through a variety of HX-responsive transcription factors (33). HX-responsive transcription factors, the stimulus for activation and result of signaling are detailed in Table 1.

Table 1: Summary of hypoxia-responsive transcription factors (33)

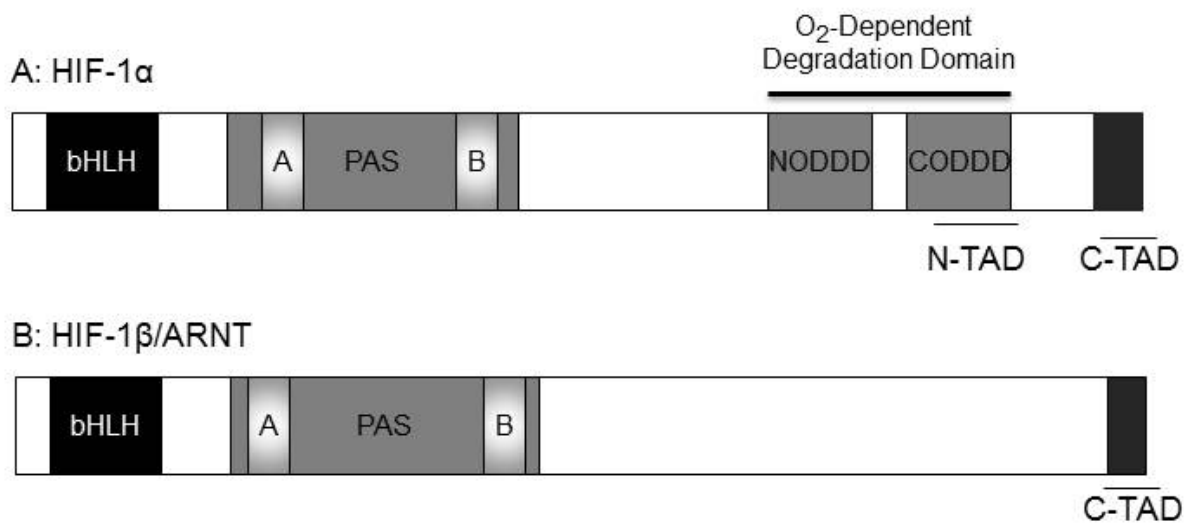
Transcription Factor	Hypoxia-induced Stimulus	Example(s) of Effect
Nuclear Factor kappa-B (NF-κB)	Mitochondrial ROS; Ras/Raf; p42/p44 and PI-3-kinase.	Transcription of COX-2, TNFα, IL-6, and MIP-2, and HIF-1α.
Cyclic AMP Response Element Binding Protein (CREB)	Phosphorylation of CREB.	CREB degradation suppresses expression of inflammatory genes.
Activating Protein-1 (AP-1)	Phosphorylation by JNK, possibly due to ROS formation.	Transcription of Tyrosine Hydroxylase, VEGF, eNOS; interaction with other transcription factors such as HIF-1, GATA-2, NF-1 and NF-κB.
p53	Hypoxia-induced HIF-1a can bind and inactivate Mdm2, a negative regulator of p53.	Transcription of pro-apoptotic genes such as Bax, Bid, Apaf-1, and SUMO.
SP-1 and SP-3	Unknown, reported to be redox sensitive.	Transcription of COX-2, EPO and VEGF.
Early growth response-1 (Egr-1)	Phosphorylation by PKC, Ras/Raf, and ERK, leading to nuclear localization of Egr-1.	Stimulus of the pro-coagulant tissue factor expression, leading to thrombosis and vascular remodeling.
CCAAT/enhancer-binding protein (C/EBPβ)	Phosphorylation by various kinases (PKA, CaMK, MAPK and PKC).	Production of IL-6, via dimerization with other transcription factors.
Hypoxia Inducible Factors (HIFs)	Discussed below.	Discussed below.

The hypoxia-inducible factor system

The hypoxia inducible-factor (HIF) transcription factor system is the most widely studied mechanism of transcriptional response to HX. HIFs are the major cellular sensors of oxygen tension and are regulators of genes involved in systemic responses to HX. HIFs are a family of heterodimeric transcription factors that belong to the basic helix-loop-helix (bHLH) transcription factors that include the PER/aryl hydrocarbon receptor nuclear translocator (ARNT)/single minded (SIM) superfamily of transcription factors (PER/ARNT/SIM or PAS). HIFs are heterodimeric, and are composed of alpha and beta subunits. The beta subunit includes ARNT1 and ARNT2, and is also referred to as HIF-1 β . There are three isoforms of the alpha subunit: HIF-1 α , HIF-2 α , and HIF-3 α . HIF-1 α is the most widely studied isoform, is evolutionarily conserved and constitutively expressed in all cell types, and is the principal regulator of the hypoxic response (Figure 1) (102, 153). The role of HIF-2 α and HIF-3 α in oxygen sensing will be discussed below.

Figure 1: Protein structure of HIF-1 α and HIF-1 β . HIF-1 α and HIF-1 β contain an N-terminal basic helix-loop-helix (bHLH) for DNA binding and dimerization. They also contain the Per-Arnt-Sim (PAS) domain for dimerization. HIF-1 α has an N-terminal and a C-terminal oxygen-dependent degradation domain (NODDD and CODDD). Finally, both HIF-1 α and HIF-1 β contain transactivation domains (TAD).

Figure 1

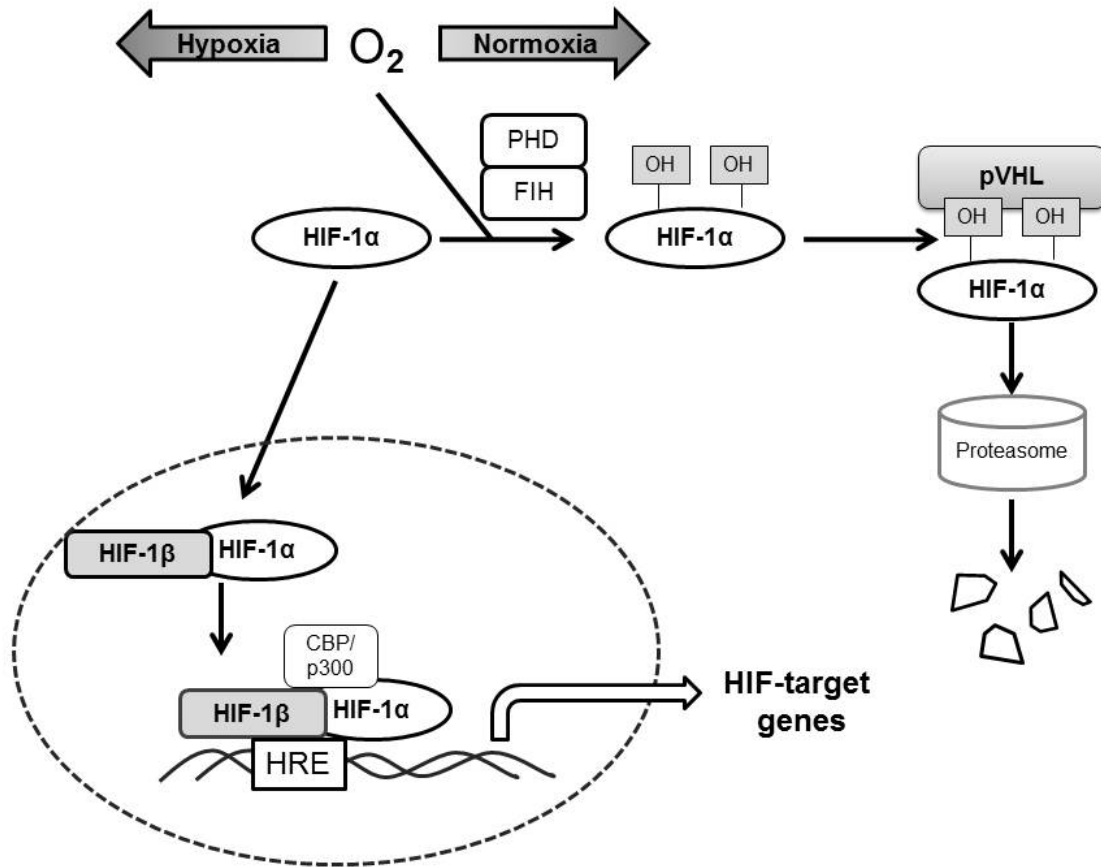


The N-terminal basic domain of HIF-1 α is necessary for DNA binding, and the HLH domain is the primary dimerization interface; both are required for the formation of functional DNA binding complexes (91, 153). The PAS region comprises two adjacent repeats called PAS A and PAS B. PAS domains act as the secondary dimerization interface, allow binding with a second bHLH/PAS partner in the nucleus. Alpha-HIFs differ from other bHLH/PAS proteins by containing two oxygen dependent degradation (ODD) domains and an N-terminal and C-terminal transactivation domain (N-TAD and C-TAD, respectively). HIF-1 α protein levels in cells are dependent on cellular pO₂ and are regulated post-translationally (102, 153).

Oxygen-dependent regulation of HIF-1 α protein consists of several steps and proteins (Figure 2). Four hydroxylase enzymes, known as prolyl hydroxylase domain (PHD)-containing proteins, control the stability of HIF-1 α by modifying two prolyl residues within the ODD domains. The PHD enzymes are dioxygenases that require oxygen, 2-oxoglutarate (alpha-ketoglutarate), ascorbate and iron; the enzyme catalyzes the splitting of molecular oxygen and couples it to the hydroxylation of the HIF-1 α substrate and the decarboxylation of 2-oxoglutarate to succinate and CO₂. One oxygen atom is incorporated into a hydroxyl group on each of two proline residues (Pro402 and Pro564 in humans) within the ODD domains of HIF-1 α (152). Hydroxylation of these residues on HIF-1 α facilitates interaction with the von Hippel-Lindau tumor suppressor gene product (pVHL), part of the E3 ubiquitin ligase complex, which targets HIF-1 α for ubiquitination and proteasomal degradation (102, 137, 152, 153).

Figure 2: Oxygen-dependent regulation of HIF-1 α . HIF-1 α protein is constitutively expressed. At normoxia, prolyl hydroxylase (PHD) uses oxygen to hydroxylate proline residues on HIF-1 α . This recruits the von Hippel Lindau (pVHL), an ubiquitin ligase, which targets HIF-1 α for degradation by the proteasome. Factor inhibiting HIF (FIH) uses oxygen to hydroxylate asparagine residues on HIF-1 α and prevent binding to transcriptional coactivators. In contrast, during hypoxia, HIF-1 α can accumulate in the cytoplasm and translocate to the nucleus where it heterodimerizes with HIF-1 β , forming the functionally competent HIF-1 transcription factor. HIF-1 binds coactivators such as CBP and p300. This complex binds to hypoxia response elements (HRE) on DNA and thereby directs transcription of over 100 genes.

Figure 2



A second level of oxygen-dependent regulation of HIF-1 α transcriptional activity is controlled by the enzyme Factor Inhibiting HIF (FIH), which catalyzes the hydroxylation of an asparaginyl residue (Asn 803 in humans) in the C-TAD of HIF-1 α . This inhibits the binding of coactivator molecules such as p300/CBP and reduces the ability of HIF-1 α to direct transcription (102, 137, 152, 153).

During HX, PHD and FIH enzyme activities are reduced; this process will be discussed in detail in the next section. As a result, HIF-1 α is able to accumulate within cells and enter the nucleus, where it heterodimerizes with ARNT to form the functional HIF-1 transcription factor. HIF-1 binds to coactivators such as p300/CBP, and the resulting transcriptional complex binds to HX response elements (HRE) in DNA, which have a consensus sequence of G/ACGTG (115). HIF-1 α has been shown to regulate over 70 genes in the human hepatoma cell line HepG2 (102, 177).

Hypoxia-mediated PHD and FIH enzyme inhibition

In the setting of HX, PHD and FIH activities are diminished, and HIF-1 α is stabilized and activated to induce transcription; however, the exact mechanism by which PHD and FIH enzymes sense changes in oxygen tension is unknown. There are three theories as to how this occurs. The first is that PHD and FIH enzymes require oxygen for their catalytic activity, and HX simply imparts a loss of substrate. This prevents PHD- and FIH-mediated hydroxylation of HIF-1 α , allowing for accumulation and transactivation (102). The second theory implicates the ETC as the primary oxygen sensor. The mechanism of HX-induced reactive oxygen species (ROS) generation will be discussed below. Briefly, excess ROS generation during HX has been reported to

contribute to HIF-1 α stability and transcription of HIF-regulated genes, and numerous studies have reported that HX-induced HIF-1 α stability and HRE-reporter gene activity are enhanced by mitochondrial ROS (mROS) (15, 16, 93, 95, 150). However, as oxygen levels continue to decline to near anoxia, HIF-1 α can be stabilized in the absence of functional mitochondria (95) suggesting that multiple mechanisms modulate HIF-1 α stabilization depending on the severity of hypoxic stress. A third theory also implicates the ETC, and states oxygen consumption by the ETC reduces cytoplasmic oxygen concentration, thus inhibiting PHD and enhancing HIF-1 α accumulation (22).

Regardless of the mechanism of oxygen sensing, the expression and activity of HIF-1 α protein is tightly regulated by intracellular oxygen tension. The response is also very rapid; incubation of HeLa cells in gassing mixtures with pO₂ ranging from 1.4 – 35 mmHg caused HIF-1 α protein accumulation as early as 2 mins after treatment. In these studies, binding of HIF-1 α to DNA occurred within 7.5 mins of HX exposure (82). HIF-1 α is also quickly degraded, with a half-life of less than 5 mins during reoxygenation (82). This indicates that HIF-1 α protein levels and DNA binding are tightly controlled, and suggests that sustained HIF-1 α activation might be detrimental to cells (102). HIF-1 α protein levels and activity are also regulated by various non-hypoxic stimuli, including growth factors, hormones, cytokines, and coagulation factors (93).

HIF-2 α and HIF-3 α

HIF-1 α and HIF-2 α share 48% amino acid sequence identity and therefore have similar domain architecture and are similarly regulated; however, they have discrete functions. HIF-2 α can activate target genes that are distinct from HIF-1 α -regulated

genes and is selectively expressed during embryogenesis in vascular endothelial cells, catecholamine-producing cells, kidney, and lung (153). Little is known about the role of HIF-3 α . It has been found to be expressed in adult thymus, lung, brain, heart and kidney. It can bind ARNT and HREs in DNA, but little is known about its transcriptional targets (91). For this dissertation, only HIF-1 α will be considered.

1.2.4 Pathological responses to hypoxia

As mentioned previously, many pathological conditions of the liver can result in tissue HX. These include ischemia/reperfusion, sepsis, drug-induced liver injury (DILI), cholestasis and fibrosis, as discussed in detail below. The injury that is produced when oxygen availability is limited to the highly aerobic liver tissue has been intensively studied. Most recently, the focus has been on the pathological role of HIF-1 α signaling, however some of the first studies into the mechanism of HX-mediated cell death focused on cellular energy metabolism, mitochondrial function, and membrane integrity. Other studies have investigated the role of oxidative stress, mitogen activated protein kinase (MAPK) signaling and activation of transcription factors separate from HIF-1 α .

Hypoxic cell injury: loss of energy metabolism and membrane integrity

Initial studies into the mechanism of HX-mediated HPC death focused on the morphological changes to cellular membranes and organellar structure. The majority of these studies were performed in isolated primary rat HPCs. In an early study, liver ischemia was induced by clamping the hepatic artery and portal vein of a rat for 3 hours, and livers were isolated and analyzed thereafter. This severe ischemia resulted in degradation of membrane phospholipids and subsequent loss of membrane integrity

(19). In subsequent studies, isolated rat HPCs were exposed to anoxia ($pO_2 < 1$ mmHg), and detailed time courses of morphological changes were delineated. Membrane bleb formation occurred early, 23 mins after anoxia and blebs began to coalesce at 30 mins. Subsequently, HPCs began to swell at 54 mins and finally rupture by 60 mins. Membrane rupture resulted in leakage of cytoplasmic contents and uptake of dyes such as trypan blue and propidium iodide (59). These morphological changes were associated with many biological changes. Exposure of primary rat HPCs to anoxia ($pO_2 < 1$ mmHg in the culture medium) resulted in a time-dependent decrease in cellular adenosine triphosphate (ATP) concentration; ATP levels were completely abolished within 120 mins of exposure to anoxia (92). Supplementation of culture medium with the glycolytic substrate fructose protected cells from HX-induced cell death; this was attributed to attenuation of ATP depletion, prevention of reductive stress, and protection from the loss of membrane integrity and reductive stress. Additionally, a variety of radical scavengers, including caffeic acid, quercetin and 4-OH Tempo protected HPCs from anoxia-induced cell death. The iron chelator desferroxamine (DFX) was also protective, as well as the xanthine oxidase inhibitor oxypurinol. These data suggested that cell death caused by severe HX or anoxia involves reductive stress and mitochondrial dysfunction. Indeed, HPCs depleted of glutathione (GSH), an important radical scavenger, were more susceptible to anoxia-induced cell death (92). The role of oxidative stress in HPC death during HX will be discussed below.

This process of severe HX or anoxia--induced cell death has been classified as oncotic necrosis. It begins with membrane bleb formation, nonspecific DNA hydrolysis, and swelling of intracellular organelles such as the mitochondria and endoplasmic reticulum. The next step is mitochondrial dysfunction, characterized by permeability transition of the inner mitochondrial membrane and failure of oxidative phosphorylation and ATP production. The membrane blebs eventually fuse, and the lack of ATP prevents membrane repair; as a result the blebs burst and there is loss of cellular membrane integrity, which causes cytoplasmic contents to leak. Organelles are nonviable at this stage. A similar series of events has been characterized in primary HPCs subjected to chemical HX induced by cyanide/iodoacetate treatment (107) Cells that have undergone oncosis appear as necrotic tissue, which leads to inflammation and organ failure (143). Indeed, in vivo models of ischemia-reperfusion (I-R) liver injury are characterized by increased plasma alanine aminotransferase (ALT) activity, a marker of HPC damage, and by the presence of necrotic HPCs in the liver (55).

Another pathway to cell death is apoptosis, which is a specific program of events carried about in an energy-dependent manner. Briefly, intrinsic apoptosis involves activation of a cascade of cysteine-aspartate proteases (caspases) which carry out degradation of cellular proteins and DNA. The cell and organelles shrink and the nuclei condense. Eventually, small buds called apoptotic bodies break off from the cell; these are removed by phagocytic cells of the innate immune system (116). There is evidence that some HPCs undergo apoptotic cell death during ischemic injury, but this is most often observed in models of ischemia/reperfusion, rather than ischemia alone. The current consensus is that there is a programmed series of events that includes

mitochondrial dysfunction, appearance of autophagosomes, and cellular swelling and membrane rupture that results in an oncotic necrotic morphology. This is distinct from apoptotic cell death because of the loss of ATP precludes the apoptotic response. This process has been termed necrapoptosis, and occurs in I-R injury (55, 71, 75).

It is important to point out that the mechanisms of HPC death described above have been defined in cells exposed to severe HX, anoxia or chemical HX, and in general, this appears to be a frank necrotic injury. This is different from the necrapoptosis associated with I-R injury. Furthermore, both of these pathways might be distinct from the injury caused by a modest HX, which is associated with oxidative stress, MAPK signaling and HIF-1 α -mediated gene transcription, as described below.

Mitochondrial ROS production

It is clear that oxygen is important for the appropriate function of the ETC and consequent ATP production. When oxygen is not available as the final electron acceptor, the excess electrons are transferred to form oxygen-containing free radicals and other reactive compounds, collectively called reactive oxygen species (ROS). The superoxide anion ($O_2^{\bullet-}$) is formed upon one electron reduction of molecular oxygen (O_2). Superoxide is a free radical, due to its unpaired electron, and can give rise to other ROS such as hydrogen peroxide (H_2O_2), hydroxyl radical (OH^{\bullet}), peroxynitrite ($ONOO^-$), and hypochlorous acid ($HOCl$). The appearance of ROS during a state of HX is counterintuitive but has been reported in many cell types, including pulmonary myocytes, HeLa cells, adipocytes and HPCs in particular (93).

Exposure of primary HPCs and the transformed liver cell lines Hep3B and HepG2 to moderate HX (10 mmHg in the cell culture atmosphere) increased generation of ROS as measured by dichlorofluorescein (DCF) fluorescence, a marker of H₂O₂ production (15, 16). To determine the source of ROS, Hep3B cells without mitochondrial DNA [respiration-deficient, or rho-zero (ρ0) cells] were subjected to HX (10 mmHg in the cell culture atmosphere). These cells did not generate ROS (Chandel 1998) indicating that the mitochondrial ETC is a significant source of ROS in HX. Furthermore, inhibitors of complex III prevented HX-induced ROS production, indicating that the site of ROS generation during HX is complex III of the ETC (57, 95).

ROS contribute to cell death by damaging DNA, proteins and polysaccharides, and by causing lipid peroxidation (93). Oxidative stress can also lead to mitochondrial permeability transition (MPT), which contributes to loss of ATP stores, membrane failure and necrotic cell death (106, 143). Indeed, abrogation of oxidative stress with antioxidants protects both primary rat HPCs and HepG2 cells from HX-induced cell death (156).

In addition to direct oxidative damage to cell proteins and structural components, another consequence of ROS generation is depletion of cellular stores of reduced glutathione (GSH) (44, 92, 111, 117). GSH is an important reducing agent in biochemical processes; it detoxifies xenobiotics and is an intracellular antioxidant (111, 117). HX-induced ROS can decrease GSH stores through oxidation of GSH to form GSSG, enhanced efflux of GSH from cells, and/or decreased GSH synthesis (111, 117). Loss of GSH has been implicated in the mechanism of HX-induced HPC and HepG2

cell death. Administration of cell-permeable GSH ethyl ester (GSHEE) can replenish GSH stores and prevent HX-induced cell death. Additionally, selective depletion of mitochondrial GSH with diethylmaleate/buthionine-L-sulfoximine increased the sensitivity of cells to HX-induced oxidative stress and cell death (111). This indicates that mitochondrial GSH plays a critical role in protecting cells from HX-induced cell death, likely due to its antioxidant properties.

The mitochondria are not the only potential source of ROS during HX. The enzyme xanthine oxidase (XO) catalyzes the oxidation of hypoxanthine to xanthine and then to uric acid, in the process generating H_2O_2 and $O_2^{\bullet-}$. XO is an important source of ROS in HX; inhibition of the enzymes with BOF-4272, allopurinol or its metabolite oxypurinol, protects HPC from ROS production and cell death during HX (88). Another potential source of ROS is NADPH oxidase; inhibition of this enzyme prevents HIF-1 α activation in response to nonhypoxic stimuli, and overexpression of the NADPH subunit NOX1 increases HIF-1 α levels in lung epithelial cells. This suggests that NADPH oxidase is an important regulator of the HIF-1 α pathway in response to nonhypoxic conditions; however, its role in HX is less clear (93). ROS are also important second messenger molecules and modulate various intracellular signaling pathways, including activation of mitogen activated protein kinases (MAPK) or inactivation of phosphatases. ROS-mediated kinase activation has been shown to contribute to HIF-1 α stabilization and gene transcription, as discussed below (93).

Hypoxia and MAPK activation

The MAPKs are a family of proteins that act as key signaling intermediates that transmit both extracellular and intracellular signals to intracellular targets by phosphorylation of serine and threonine residues on target proteins. They affect almost all cellular activities, including mitosis, gene expression, movement, metabolism and cell death (84). Family members include extracellular signal regulated kinases (ERKs), and the two stress activated protein kinases, c-jun N-terminal kinase (JNK) and p38. Signals are sent via activation of MAPK kinase kinases, which phosphorylate MAPK kinases, which in turn activate the three MAPKs. In general, ERK is activated by mitogenic growth factors, and ERK signaling controls cell differentiation. In contrast, JNK and p38 are activated in response to a variety of noxious stimuli, including ultraviolet light, osmotic stress, oxidative stress, and cytokines; JNK and p38 play important roles in cytokine production and activation of cell death pathways (84).

As mentioned previously, ROS generated during HX can also act as second messenger molecules. Indeed, many groups have demonstrated that HX-induced ROS can activate JNK (122) and p38 (120) MAPKs. Others have demonstrated that moderate HX (35 mmHg in cell culture atmosphere) leads to selective phosphorylation of the p38 α and p38 γ isoforms, but not p38 β , p38 β 2, or p38 δ . Inhibition of p38 α but not p38 γ prevented HIF-1 α -mediated transcription (23), suggesting a role for p38 in the regulation of HIF-1 α stabilization or transactivation. Further support for this was found in primary HPC, in which HX-induced cell death depended on p38-mediated, HIF-1 α -induced BCL2/adenovirus E1B 19kDa interacting protein 3 (BNIP3) expression (120), suggesting an integral role for p38 in the HIF-1 α -mediated cell death response. Indeed,

phosphorylation of HIF-1 α by p38 enhanced its interaction with the transcriptional coactivators CBP and p300, thereby enhancing transactivation (121).

HIF-1 α regulated gene transcription

HX-induced HIF-1 α activation is necessary for cells to adapt to decreased oxygen availability; these responses can lead to cell survival or cell death, depending on the duration and severity of HX, among other environmental factors (102). The initial adaptive response is necessary to address the energy deficit created by HX and occurs through HIF-1 α -mediated transcription of genes involved in anaerobic glycolysis, including aldolase A, lactate dehydrogenase, pyruvate kinase and glucose transporters, among others. HIF-1 α also directs transcription of vascular endothelial growth factor (VEGF) and erythropoietin (EPO) which can enhance perfusion and oxygen delivery to tissues by stimulating angiogenesis and red blood cell production, respectively (121). In cases of severe or prolonged HX or additional stress, these changes cannot address the metabolic imbalance. In this case, HIF-1 α stimulates the activation of several cell death pathways, seemingly as a means of eliminating cells stressed beyond recovery. HIF-1 α directs the transcription of various pro-apoptotic proteins of the B-cell chronic lymphocyte leukemia/lymphoma (BCL) family members, including BNIP3, Nix, and Noxa (102, 177). These proteins can contribute to cell death by autophagy, apoptosis or oncosis (163).

HIF-1 α also contributes to cell death via modulation of the cell cycle. HX inhibits the G1/S transition of the cell cycle in a HIF-1 α -dependent manner in several cell types by increasing the expression of the cyclin-dependent kinase inhibitors, p21 and p27

(52). HX downregulates the expression of cyclin D1 in PC12 cells (23). HIF-1 α negatively regulates cyclin D1 expression directly, by binding to two HREs in the cyclin D1 promoter and recruiting histone deacetylase 7 to suppress transcription of the gene (183). Cyclin D1 is required for the transition from the G1 to S phase of the cell cycle (23), which contributes to cell proliferation and regeneration of HPCs after injury or toxic insult (39). Downregulation of cyclin D1 induces cell cycle arrest and apoptosis in the hepatoma cell lines, HepG2 and Hep3B (127). Furthermore, HIF-1 α can also interact with and stabilize p53, leading to cell cycle arrest and apoptosis (14).

1.2.5 Summary of hypoxia

In summary, HX is a significant component of many diseases and toxicities of the liver, leading to energy deficit in HPCs. HPCs have evolved a variety of mechanisms to adapt to decreased oxygen availability. The initial response is loss of ATP production and mitochondrial dysfunction, ROS production and activation of signaling pathways such as MAPKs. Additionally, HIF-1 α and other transcription factors are activated during HX and direct transcription of genes that allow cells either to adapt to HX or to die. Cell death due to HX is often due to oncotic necrosis, but in some cell types it can be an organized, apoptotic process. It is important to investigate the mechanism by which HX can cause cell death as a means of developing therapies for the treatment and prevention of HX-mediated HPC injury.

1.3 Neutrophils in liver disease

Many of the conditions associated with HX are also accompanied by a neutrophil (or polymorphonuclear lymphocyte [PMN])-mediated inflammatory response in the liver. PMNs significantly contribute to the pathogenesis of liver injury in various diseases and chemical toxicities (70, 139). They contribute to such conditions as I-R and obstructive cholestasis injury due to surgery or shock (56). Furthermore, PMNs cause liver injury during sepsis or endotoxemia and various chemical toxicities, such as alcoholic hepatitis (164) and alpha-naphthyl isothiocyanate (ANIT) hepatotoxicity (35). There is also evidence that PMNs contribute to acetaminophen-induced liver injury, but their role is controversial (68). Research from our laboratory has identified PMNs as a key mediator of injury in inflammation-drug interaction models of idiosyncratic DILI (IDILI) (38, 112, 159, 192). The following sections will discuss the mechanisms of PMN activation and PMN proteases and their role in toxic liver injury and diseases.

1.3.1 Neutrophil accumulation and activation

Tissue injury and xenobiotic-induced stress can activate sinusoidal endothelial cells (SECs) in the liver. These cells express P-selection, which engages ligands on the surface of circulating PMNs. This process causes PMNs to roll along the endothelial surface. Activated SECs and Kupffer cells release a variety of cytokines and chemokines, including tumor necrosis factor-alpha (TNF α), interleukin (IL)-1, IL-8 (the murine homolog of IL-8 is keratinocyte chemoattractant [KC]), and platelet activating factor (PAF), among others. These cytokines and chemokines induce the expression of E-selectin and inter-cellular adhesion molecule-1 (ICAM-1) on the surface of SECs, which bind to L-selectin and β 2 integrin (CD11b/CD18) on the surface of PMNs,

respectively. These interactions initiate firm adhesion of PMNs to the endothelium, which facilitates the sequestration of PMNs in liver sinusoids. Due to the low shear stress of the sinusoids, accumulation of PMNs can occur without the activation of ICAM-1 and β 2 integrin in a model of endotoxemia. However, CD18 is required for PMN activation and extravasation into the parenchyma (74). Activation of CD11b/CD18 recruits components of NADPH oxidase to the cell surface. The primed and partially activated PMNs can receive signals from homeostatically altered cells in the parenchyma. These signals include the chemokines IL-8/KC, macrophage-inflammatory protein-2 (MIP-2), and cytokine-induced neutrophil chemoattractant-1 (CINC-1), which induce PMNs to release the contents of intracellular granules that contain collagenases and serine proteases. These PMN proteases degrade the vascular basement membrane, allowing PMNs to extravasate from the sinusoids and transmigrate into the parenchyma (43, 70, 76).

Upon entering the parenchyma, PMNs become fully activated and release a variety of mediators that can be toxic to HPCs. In fact, extravasation into the tissue and close proximity to HPCs is required for PMN-mediated cytotoxicity (70). PMNs actually adhere to HPCs via interactions of CD11b/CD18 on PMNs with ICAM-1 on HPCs (76). Multiple stimuli, including the binding of CD11b/CD18 on the surface of PMNs activate the NADPH oxidase enzyme complex to generate superoxide anion and its dismutation product, H_2O_2 , a highly diffusible oxidant which is an important mediator of PMN cytotoxicity. Activation of CD11b/CD18 also induces degranulation of three types of secretory vesicles contained within PMN: primary (or azurophilic) vesicles, secondary (or specific) vesicles, and tertiary (or gelatinous) vesicles (43). The primary vesicles

contain myeloperoxidase (MPO) enzyme, which generates hypochlorous acid (HOCl), another diffusible oxidant and chlorinating agent. HOCl can generate toxic chloramines, which create chlorotyrosine residues and other HOCl-modified proteins, which are toxic to HPC in models of I-R injury and endotoxemia (70).

The primary granules also contain three serine proteases: cathepsin G, proteinase 3 and neutrophil elastase (EL) at very high concentrations, around 1 pg enzyme per cell (43, 97, 184). These proteases are capable of degrading extracellular matrix components to facilitate PMN transmigration into sites of inflammation and are involved in killing of bacterial pathogens and parenchymal cells (30, 43, 63, 76).

It has been widely demonstrated that mediators released from activated PMNs are cytotoxic to a variety of cell types in vitro, including endothelial cells (100, 135, 138, 189), epithelial cells (51, 165, 167), and primary HPCs (58, 63, 118). Early investigations studied the effects of PMN activation in coculture with HPCs, which resulted in death of HPCs. Initially, it was thought that ROS produced by activated PMN were the cytotoxic mediators; however, treatment with antioxidants and inhibitors of MPO and NADPH oxidase did not prevent HPC injury. This suggested that another cytotoxic component was released by activated PMNs. Treatment with broad spectrum serine protease inhibitors implicated the neutrophilic proteases; further studies with specific inhibitors of the three proteases ultimately identified EL as the primary cytotoxic mediator of HPC death released by activated PMNs. Furthermore, purified EL is cytotoxic to HPCs in vitro (63, 118).

1.3.2 Neutrophil elastase

EL is a 29 kDA protein with a catalytic site containing aspartate, histidine and serine residues (97). It acts optimally at pH 8.0 – 8.5, and although it is a promiscuous protease with many substrates, it prefers small hydrophobic residues such as valine, alanine, cysteine, methionine, isoleucine, leucine, and serine as cleavage sites. Because EL has potent catalytic activity and broad substrate specificity, it is involved in many fundamental biological pathways, including coagulation and fibrinolysis, angiogenesis, inflammation, and complement activation (97). Excessive EL release degrades extracellular matrix components such as collagens and laminins, thereby damaging organs through endothelial cell injury (168). EL plays an integral role in inflammation by its ability to proteolytically cleave various proteins. It can directly activate some cytokines, such as IL-6, and inactivate others, such as TNF α (60, 133). It can also activate blood coagulation factors (60) and fibrinolysis (49, 186). Furthermore, EL can induce transcription and release of the chemokine IL-8/KC from airway epithelial cells (18, 182). There are many endogenous inhibitors of EL, including α 2-macroglobulin, α 1-proteinase inhibitor, secretory leukocyte protease inhibitor (SLPI), monocyte neutrophil elastase inhibitor (MNEI) and elafin (97, 184). The liver is an important source of EL inhibitors, which likely keep the actions of EL local and prevent its potentially damaging effects.

1.3.3 Mechanisms of elastase-mediated cell death

The mechanism of EL-induced cell death has been well studied yet is not completely understood. It is clear that the pathway to cell death depends on cell type and culture conditions. Early studies indicated that EL caused cell death directly though

membrane damage that led to cytolysis and necrosis (2). As mentioned previously, EL cleaves extracellular matrix components, which leads to cell detachment and deformation of cell membrane that is cytotoxic (175). Electron microscopic evaluation of primary HPCs exposed to EL indicated mitochondrial swelling, dilation of the endoplasmic reticulum, and nuclear alterations (118). More recent work has indicated that EL can activate cell death signaling pathways, such as oxidative stress, MAPK activation, and apoptosis.

EL-induced oxidative stress

Early studies into the mechanism of EL-mediated cell death indicated that EL can cause oxidative stress through multiple pathways, including ones involving the mitochondria or xanthine oxidase (2, 30, 45, 46). EL converts the enzyme xanthine dehydrogenase (XD) to xanthine oxidase (XO) in pulmonary artery endothelial cells and in a cell-free in vitro system (135). XD to XO conversion occurs through reversible oxidation of sulfhydryl residues. XO converts hypoxanthine to xanthine and then to uric acid, generating H_2O_2 and $O_2^{\bullet-}$ in the process; therefore, increased XO activity can lead to oxidative injury in cells. Treatment with the XO inhibitors allopurinol and its metabolite oxypurinol prevented ROS production and cell death due to EL. The injury was characterized as oncotic necrosis because there was loss of membrane integrity and leakage of cellular contents (135, 176). The exact mechanism by which EL causes XD to XO conversion is not known, though it is dependent on the proteolytic activity of the enzyme. The fact that EL can cause conversion of XD to XO in a cell-free system suggests that EL might enter endothelial cells and act directly on the enzyme, though it

is a large molecule (29 kDA) and is not likely to cross the membrane passively. There is some evidence that EL can enter HUVEC cells and activate signaling pathways (138), but it is unknown whether EL can cross the plasma membranes of HPC. Nevertheless, XO activity is an important contributor to EL-induced cell injury (135, 142, 176).

EL can also cause oxidative stress through the mitochondrial pathway. In human fetal lung fibroblasts, EL caused concentration-dependent increases in both total ROS (measured by DCF fluorescence) and mitochondrial ROS (measured by the mitochondria-specific ROS indicator MitoTracker Red), which led to lipid peroxidation and cell death, however the mechanism by which EL incites ROS is not known (2). Sivelestat, a selective inhibitor of the proteolytic activity of EL, attenuated ROS production and was protective, suggesting that the proteolytic activity of the enzyme is required for this pathway. Inhibition of the mitochondrial ETC with rotenone also attenuated ROS production and prevented EL-induced cell death, as did treatment with catalase to decompose H₂O₂ (2).

In similar studies, EL caused mitochondrial ROS production in the A549 respiratory epithelial cell line and in normal human bronchial epithelial cells (45, 46). In these studies, EL increased ROS (measured by DCF fluorescence), and treatment with the antioxidant and iron chelator DFX or dimethylthiourea (an OH[•] radical scavenger) attenuated the increase in ROS and prevented cell death. Taken together, these data suggest that ROS are important mediators of EL-induced cell death.

Activation of apoptosis

EL has also been shown to cause apoptosis of lung epithelial cells through activation of caspases and mitochondrial permeability transition (51). EL treatment resulted in apoptosis of bovine pulmonary artery endothelial cells (189). Similarly, in a human epithelial cell line, EL treatment resulted in mitochondrial dysfunction and activation of the intrinsic apoptotic pathway (51). More recent studies have demonstrated that EL can activate protease-activated receptor-1 (PAR-1) on the surface of human lung epithelial cells by cleavage of the tethered ligand, which results in apoptosis through NF- κ B and p53-dependent pathways (165, 167).

The MAPK proteins are also important downstream targets of EL exposure in a variety of cell types. In lung epithelial cells, EL leads to activation of ERK (130), JNK and p38 (18, 98). In endothelial cells, EL caused phosphorylation and activation of both JNK and p38 and led to p38-dependent apoptosis (138).

It is clear that the exact mechanism of EL-mediated injury is cell-type specific, however one commonality among studies is that it is dependent on the proteolytic activity of the enzyme. As mentioned previously, EL is a highly promiscuous enzyme with many substrates. It has been hypothesized that EL might activate or inactivate a cell surface receptor to induce cell death signaling; one putative target is PAR-1 (165). Other potential targets include growth factor receptors, which may be more relevant to the mechanism of EL-induced cytotoxicity in vivo, where growth factor signaling plays an important role in recovery from injury. In many of the studies performed in endothelial cells and HPC, EL-induced cell death was measured by leakage of lactate

dehydrogenase (LDH) or alanine aminotransferase (ALT), respectively, into the culture medium, indicating loss of membrane integrity (63, 175). This, along with the morphological changes of mitochondrial and endoplasmic reticulum swelling (118), suggests that EL-mediated cell death is oncotic necrosis; however, the possibility of apoptosis has not been ruled out, since membrane damage can occur as a secondary phenomenon in this cell death pathway as well.

It is obvious that EL can change cellular homeostasis in many ways, including making cells more vulnerable to oxidative stress through conversion of xanthine dehydrogenase to xanthine oxidase. It can also damage membranes and make cells more sensitive to other environmental stresses, such as HX. Finally, EL can activate cell death signaling pathways which can lead to apoptosis and secondary necrosis.

1.3.4 Role of EL in liver disease and chemical toxicity

PMNs are implicated in the pathogenesis of various liver diseases and chemical toxicities, and excess EL activity has been linked to the mechanism in many cases. For instance, HPC produce the major endogenous inhibitor of EL, α 1-antitrypsin (AAT), which inhibits EL enzymatic activity by covalent binding. AAT deficiency strongly increases the risk for chronic liver disease, hepatic inflammation, cirrhosis, fibrosis and hepatocellular carcinoma in humans (42, 60). Indeed, EL is an important mediator of HPC death in other liver diseases such as endotoxemia (10, 99), hepatitis B (168), and I-R (128, 172), as well as many chemical toxicities, including alcoholic hepatitis (164) and alpha-naphthyl isothiocyanate (ANIT) hepatotoxicity (35, 61). For the purpose of this dissertation, EL-mediated liver pathology will only be discussed in context with concurrent HX.

1.5 The role of hypoxia and neutrophils in liver disease and toxicity

Sepsis or Endotoxemia

Sepsis is a condition in which there is a whole body inflammatory response, often due to the presence of a pathogen in the blood. Severe bacterial infection leads to endotoxemia, which is the presence of endotoxin (or lipopolysaccharide [LPS], a component of gram negative bacterial cell walls) in the blood. In some cases, endotoxemia can lead to septic shock, or severe hypotension. The end result of sepsis in the liver is coagulopathy and ischemia, and an inflammatory response that recruits and activates PMNs to release EL. Sivelestat, a specific inhibitor of EL, prevents liver injury in experimental models of sepsis. Additionally, EL inhibition reduces inflammatory cytokine production and PMN recruitment (171). This indicates that that EL has multiple roles in sepsis: it enhances the inflammatory response and damages HPC directly.

HX has also been observed in livers during sepsis, due to hypotension, coagulation, microvascular dysfunction, or sinusoidal blockade by PMNs (13). Decreased hepatic pO₂ during sepsis has been measured in several studies. In male rats, intraperitoneal injection of *E. coli* endotoxin decreased mean hepatic tissue pO₂ from 25.2 mmHg to 3.8 mmHg within 6 hrs (141). In mice, endotoxin caused a 75% reduction in pO₂ of blood in sinusoids and hepatic parenchymal tissue (80).

Cholestasis and fibrosis

Cholestasis is a condition in which bile flow from the liver is reduced. It can arise from liver ischemia in certain circumstances. Indeed, experimental liver ischemia

caused increased serum concentrations of liver enzymes, bilirubin and bile salts, as well as reduced bile flow in mice (48).

PMNs and EL are also involved in cholestatic liver injury. For instance, in a mouse model of obstructive jaundice using bile duct ligation, cholestatic liver injury is accompanied by PMN recruitment (179). In a similar model of cholestasis, CD18 antiserum, which prevents PMN infiltration and activation in the liver, significantly reduced hepatic necrosis after bile duct ligation (56). ANIT is a xenobiotic that injures bile duct epithelial cells to release large amounts of bile acids into the hepatic parenchyma, resulting in cholestasis and hepatocyte death dependent on inflammatory mediators, including PMNs (35). Inhibition of PMN infiltration and activation by administration of CD18 antiserum, attenuated ANIT toxicity and cholestasis (96). Although a specific role for EL in cholestatic injury has not been reported, AAT deficiency is often associated with cholestasis in humans (42), providing some support that EL might play a role in this injury.

Liver fibrosis occurs in chronic disease due to deposition of extracellular matrix and results from a variety of liver disorders such as steatohepatitis and primary biliary cirrhosis. HX and HIF-1 α contribute to progression of fibrosis in multiple ways: through stimulation of epithelial-to-mesenchymal transition of HPCs which results in an increase in the number of collagen-producing myofibroblasts in the liver (25), and through production of profibrotic factors from hepatic parenchymal (28) and non-parenchymal cells (26).

Ischemia-Reperfusion

I-R injury is perhaps the most well-studied clinical condition in which both HX and EL are important contributors to hepatocyte death. I-R occurs during hepatic resection, liver transplantation, and hypotensive shock following surgery (4, 56, 75). Tissue storage during transplant or stoppage of perfusion during surgery creates a hypoxic environment for HPC, which is followed by reoxygenation during tissue reperfusion. There are two stages in the I-R stress which ultimately cause HPC death. The initial ischemia activates KCs to secrete cytokines and produce ROS; additionally, ischemia alters HPC function by increasing ROS production via XO and mitochondrial dysfunction. Cytokines and chemokines released by KCs recruit and sequester PMNs into the liver sinusoids. This is followed by reoxygenation due to tissue reperfusion. At this point, reoxygenation of HPCs actually exacerbates ROS production as well as activates PMNs in the liver. As described earlier, activated PMNs secrete ROS and proteases. During reperfusion, HPCs are killed by a variety of mechanisms, including ROS and EL generated by PMNs, as well as internal ROS and prolonged HX. The type of cell death has been characterized as oncotic necrosis due to appearance of swollen cells with damaged membranes. There is also a small population of HPCs that die due to apoptosis, however the extent to which apoptosis plays a role in liver failure is not completely understood (71).

There is extensive evidence that HX is an important mediator of HPC death after I-R (56, 71). Additionally, HIF-1 α accumulation occurs in livers prior to HPC death (34), and I-R leads to increased hepatic expression of HIF-1 α -regulated genes, including those that can signal for cell death such as BNIP3 (120).

The role for PMNs in I-R liver failure is well established; inhibition of PMN recruitment and activation protects against liver injury in many I-R models (70, 71). Furthermore, a specific role for EL has also been found. The selective EL inhibitor sivelestat protects mice and rats from liver injury in experimental models of I-R (3, 124). Sivelestat also reduces the recruitment of PMNs and production of inflammatory cytokines, indicating that EL has dual roles in liver injury during I-R, similar to sepsis. Taken together, it is clear that both HX and EL are significant components of I-R pathophysiology.

Drug induced liver injury

HX and PMNs are involved in the pathogenesis of a variety of chemical-induced liver injury and DILI models. In rodent models of alcoholic liver disease, HX has been observed in livers after chronic and acute ethanol feeding (5, 6). A recent report demonstrates that chronic ethanol feeding induces HIF-1 α activation in HPC, and HPC-specific deletion of HIF-1 α protects mice from hepatic steatosis, lipid accumulation and liver injury (125). Moreover, PMN activation, as measured by plasma EL concentration, was correlated with disease severity in people with alcohol-induced chronic liver damage (164).

Halothane hepatitis is another classic example of DILI; HX was one of the earliest factors identified to play a role in HPC injury (161) in halothane hepatitis. A recent report identified PMNs as important mediators of halothane hepatitis; anti-CD18 antibody attenuated severe liver injury in a mouse model (41).

Acetaminophen (*N*-acetyl-*p*-aminophenol, [APAP]) overdose is the leading cause of DILI in the United States (104). The mechanisms of APAP-induced liver injury are well-studied, and will be discussed further in Chapter 4. Briefly, in overdose, APAP is metabolically bioactivated in HPCs to a reactive intermediate, *n*-acetyl-*p*-benzoquinone imine (NAPQI). NAPQI binds covalently to intracellular proteins and causes their dysfunction, depletes cellular GSH stores and induces ROS, all of which contribute to necrosis of HPCs (31, 73). APAP also induces an inflammatory response that recruits PMNs into the liver (101). The role of PMNs in the pathogenesis of APAP-induced liver injury is controversial, with evidence both for and against a contribution to hepatotoxicity (68). APAP overdose also causes coagulation system activation and fibrin deposition in the liver, which might lead to tissue HX (50). Indeed, there are recent reports of the development of hypoxia and ROS-dependent HIF-1 α accumulation in livers after APAP overdose (17, 77). The role of HIF-1 α in APAP-induced liver injury will be discussed in detail in Chapter 4 of this dissertation.

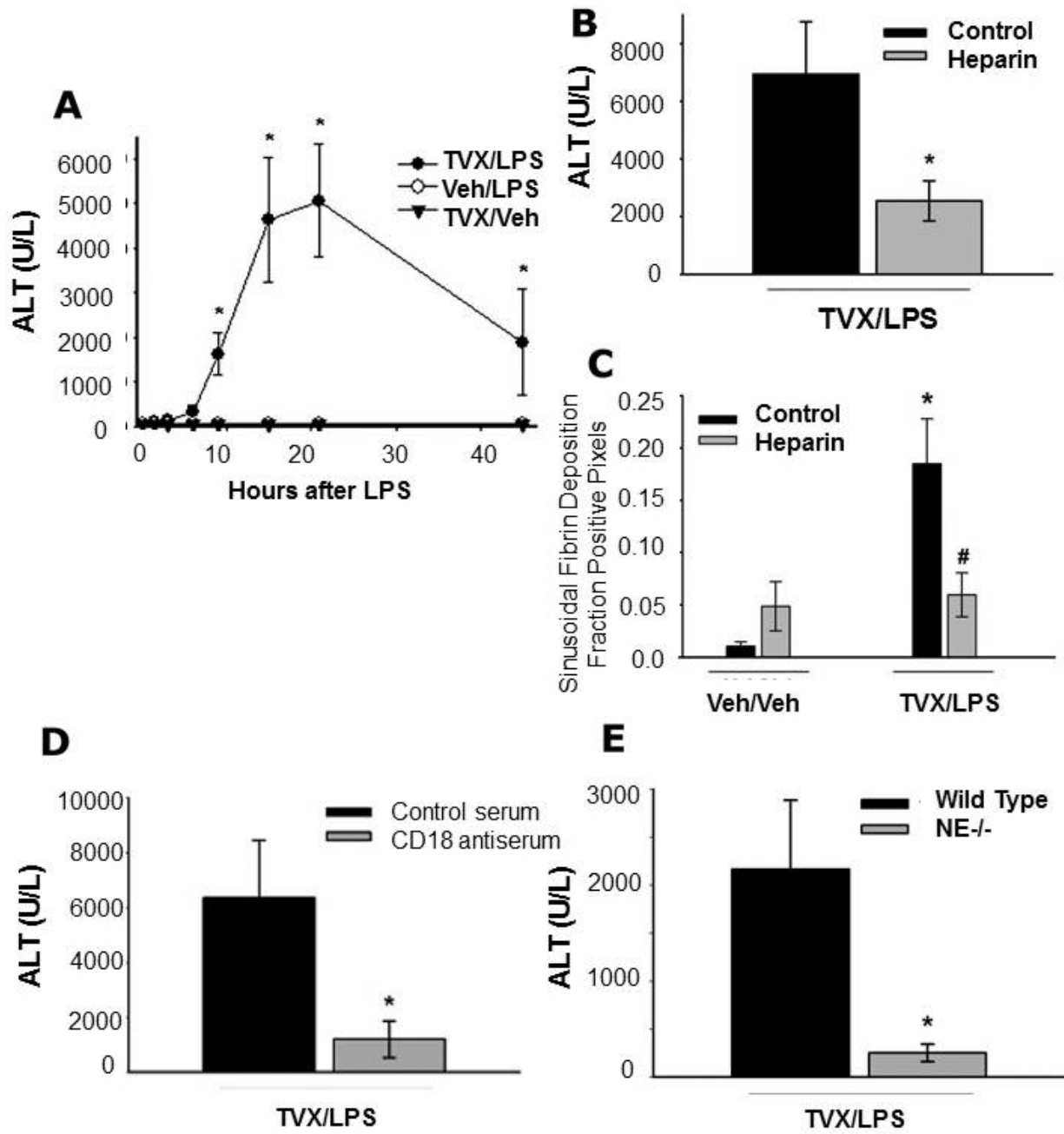
Idiosyncratic DILI (IDILI)

IDILI is a subset of DILI which occurs in a minority of patients, with variable time to onset and no apparent dose-dependence, and it is not detected in routine animal testing (144). Drugs with idiosyncratic potential in humans include chlorpromazine, halothane, sulindac, and trovafloxacin (TVX), among others. Rodent models of IDILI have been developed in which administration of a nonhepatotoxic dose of LPS to induce mild inflammation precipitates a toxic reaction to an otherwise nontoxic dose of drug.

Recently, a role for HX and EL has been observed in a mouse model of IDILI using LPS and TVX; TVX is a fluoroquinolone antibiotic associated with severe idiosyncratic liver injury in humans. In this model, mice treated with a nontoxic dose of TVX (150 mg/kg, per os) followed three hours later with a nontoxic dose of LPS (2.0×10^6 EU/kg) developed severe liver injury 15 hrs after treatment (Figure 3A). Prior to the onset of liver injury, there was coagulation system activation and fibrin deposition in the livers of TVX/LPS-treated mice (Figure 3B). Sinusoidal fibrin deposition can impair hepatic blood flow and oxygen delivery to HPCs, resulting in HX. Heparin, which prevents coagulation system activation, attenuated fibrin deposition (Figure 3B) and protected mice from the TVX/LPS-mediated liver injury (158) (Figure 3C). These data suggest a role for coagulation-mediated HX in the pathogenesis of TVX/LPS hepatotoxicity. Further studies in this model suggested a role for PMNs in TVX/LPS hepatotoxicity. Inhibition of PMN activation by administration of anti-CD18 antibody prevented liver injury (Figure 3D). Furthermore, mice deficient in neutrophil EL were protected from TVX/LPS-induced liver injury (Figure 3E) (159).

Figure 3: The TVX/LPS model of IDILI. Male C57/BL6 mice were treated with 150 mg/kg TVX and 3 hours later with 2×10^6 EU/kg LPS. (A) Plasma ALT activity was significantly increased starting 9 hrs after LPS administration and peaked 15 hrs after treatment (157). (B) Heparin also protected animals from TVX/LPS hepatotoxicity at 15 hrs after LPS. (C) Pretreatment with heparin, an anticoagulant, reduced hepatic fibrin deposition (158). (D) Pretreatment with CD18 antiserum protected mice from TVX/LPS hepatotoxicity. (E) Mice deficient in neutrophil elastase (NE^{-/-}) were protected from TVX/LPS hepatotoxicity (159).

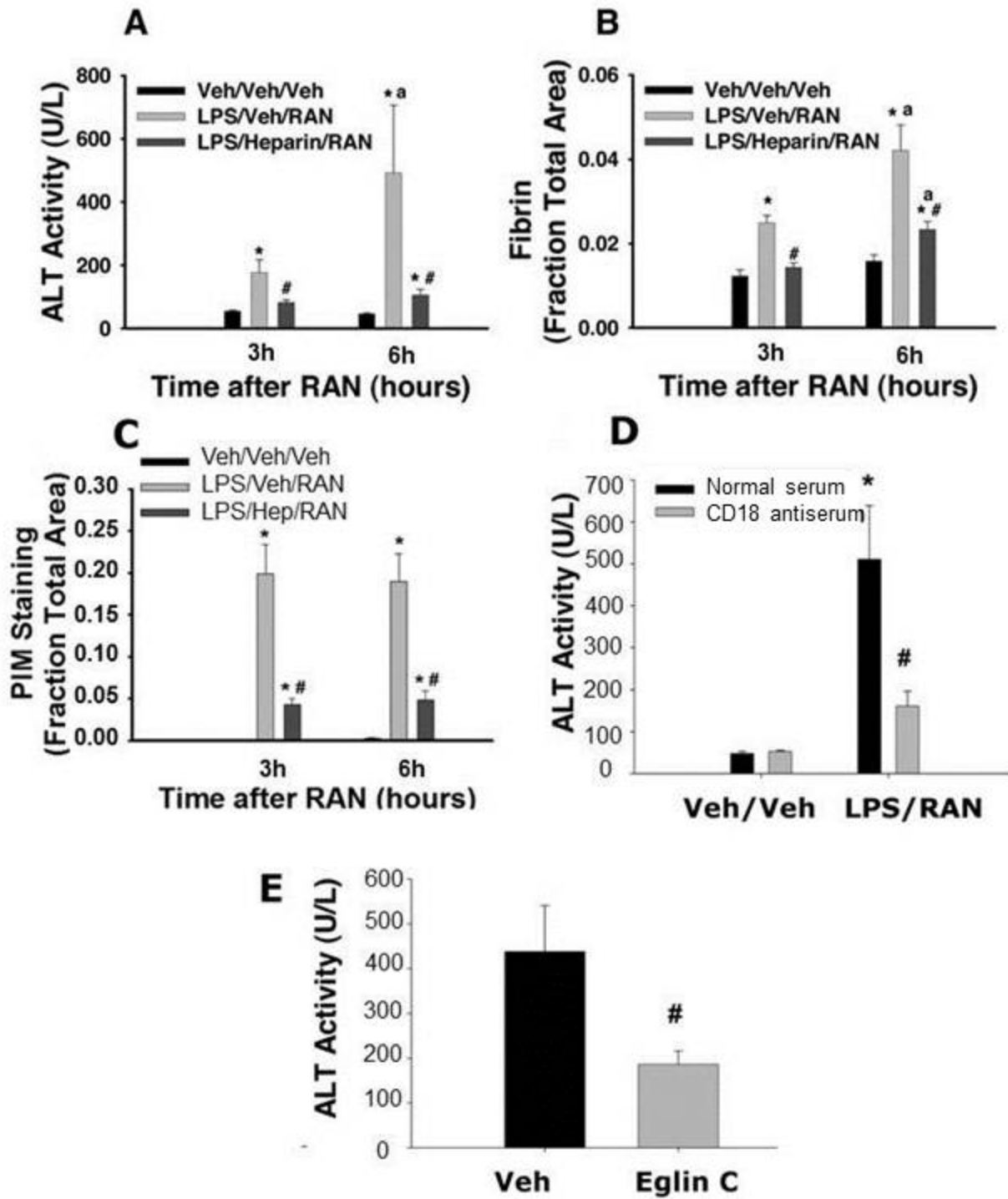
Figure 3



A similar mechanism of liver injury was observed in a rat model using LPS and ranitidine (RAN), an H₂ receptor antagonist associated with IDILI in humans. Rats treated with a non-hepatotoxic dose of LPS followed 2 hrs later by a nontoxic dose of RAN (30 mg/kg) developed hepatocellular necrosis 6 hrs after RAN treatment compared to those treated with LPS or RAN alone (Figure 4A). LPS/RAN treatment caused coagulation system activation and sinusoidal fibrin deposition 3 and 6 hrs after treatment with RAN (Figure 4B). Coagulation and fibrin deposition led to liver HX as measured by pimonidazole staining (Figure 4C) (112). Pimonidazole is a small molecule that forms protein adducts when the pO₂ in a cell is less than 10 mmHg and can be detected immunohistochemically as a biomarker of tissue HX. Inhibition of coagulation system activation with heparin protected rats from liver injury, fibrin activation and tissue HX (Figure 4A-C) (112). Concurrently, evidence of activated PMNs was observed in the livers of LPS/RAN-cotreated rats as increased immunohistochemical staining for HOCl-adducted proteins (37). Additionally, CD18 antiserum prevented PMN accumulation and activation, and protected rats from liver injury (Figure 4D). In further studies, the selective EL inhibitor eglin c also protected rats from LPS/RAN-mediated liver injury (Figure 4E) (37), suggesting a role for EL in the pathogenesis. Interestingly, CD18 antibody or eglin c treatment also attenuated coagulation system activation and fibrin deposition, which indicates that tissue HX and EL are tightly linked in this model (37).

Figure 4: The LPS/RAN model of IDILI. Male Sprague-Dawley rats were treated with a nontoxic dose of LPS, followed 2 hrs later by 30 mg/kg RAN. Pretreatment with the anticoagulant heparin attenuated (A) liver injury 3 and 6 hrs after RAN, and reduced fibrin deposition (B) and hepatic HX (C) (112). Inhibition of PMN accumulation and activation with CD18 antiserum protected rats from LPS/RAN hepatotoxicity (D) (37). Inhibition of EL activity with eglin c also protected rats from LPS/RAN-induced liver injury (E).

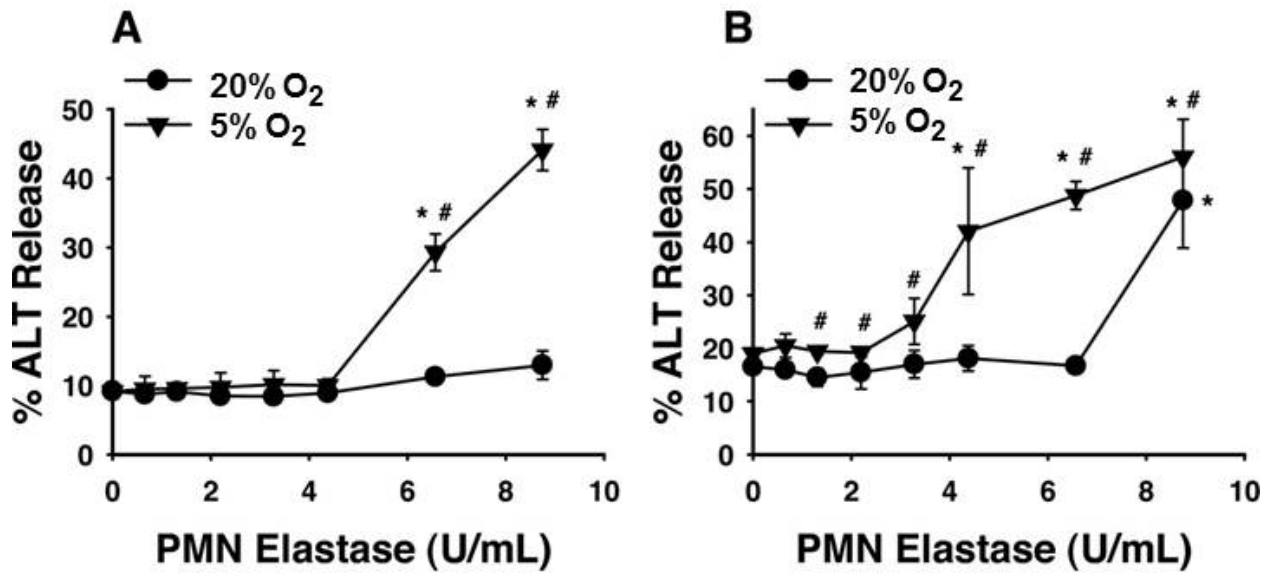
Figure 4



Taken together, these findings support the view that HX and EL are important mediators of liver injury. Similar mechanisms were identified in other LPS/xenobiotic interaction models, including LPS/monocrotaline (29), LPS/diclofenac (36) and LPS/sulindac (193). Additionally, in vitro experiments indicated that HX renders primary rat HPCs more sensitive to cytotoxicity induced by drugs such as diclofenac (36) and sulindac (193). These observations led to the hypothesis that HX and EL can act synergistically to cause HPC injury. Indeed, exposure to nontoxic HX (35 mmHg pO₂ in atmosphere) rendered HPC more sensitive to otherwise nontoxic concentrations of EL (112). Furthermore, HX shortened the time to EL-mediated cytotoxicity (Figure 5). These data indicate that there is a cytotoxic interaction between HX and EL in HPCs.

Figure 5: Exposure to HX sensitizes HPC to cell killing by EL. Primary rat HPCs were treated with 0 – 9 U/mL EL in an oxygen replete [20% O₂ (150 mmHg)] or hypoxic [5% O₂ (35 mmHg)] atmosphere for (A) 2 hrs or (B) 8 hrs. Cytotoxicity was assessed by release of alanine aminotransferase (ALT) into the cell culture medium and is represented as percent of total cellular ALT (112).

Figure 5



1.6 Summary

It is obvious that HX and EL are both important pathological mediators of liver injury in multiple clinical and experimental conditions, including chemical toxicities. It has been demonstrated that HX can sensitize cells to the cytotoxicity of EL in primary rat HPCs (Figure 5) (112), which points to a direct cytotoxic interaction between HX and EL. Furthermore, HX- and EL-mediated cell death signaling pathways share many commonalities, including mitochondrial dysfunction, oxidative stress, and MAPK-dependent cell death, indicating multiple potential points of interaction. A summary of these pathways is provided in Table 2. The experimental work described in this dissertation is meant to elucidate the mechanism of this interaction.

Table 2: The pathways involved in EL- and HX-mediated cell death

Target	Elastase effects	Hypoxia effects
Mitochondria	<ul style="list-style-type: none"> - ROS production enhanced lipid peroxidation and cell death of lung epithelial cells (2, 46) 	<ul style="list-style-type: none"> - Generation of ROS from complex III of the ETC (15) - Oxidative damage to DNA, proteins, and lipid structures (93) - Activation of MPTP (106, 143) - ROS-mediated HIF-1α stabilization (93)
Xanthine Oxidase	<ul style="list-style-type: none"> - Conversion of XD to XO - Production of ROS - Cell death (135, 176) 	<ul style="list-style-type: none"> - Conversion of XD to XO - Production of ROS - Cell death (88)
MAPK	<ul style="list-style-type: none"> - Activation of ERK, JNK and p38 in lung epithelial cells (18, 98, 130) - P38-dependent apoptosis of endothelial cells (138) 	<ul style="list-style-type: none"> - JNK mediates activation of other HX-responsive transcription factors (33, 122) - p38 mediates HIF-1α transactivation and BNIP3 production (120)
NF-κB	<ul style="list-style-type: none"> - Upregulated p53 activity, which led to Bax- and Puma-dependent apoptosis of lung epithelial cells (167) - Apoptosis (138) 	<ul style="list-style-type: none"> - Upregulation of HIF-1α mRNA expression (174) - Apoptosis of Raw 264.7 macrophages (47)
Caspases	<ul style="list-style-type: none"> - Caspase 3/7-dependent apoptosis (138) 	<ul style="list-style-type: none"> - Caspase 3 activation (94)
Calcium	<ul style="list-style-type: none"> - No evidence for role of calcium 	<ul style="list-style-type: none"> - Calpain-dependent necrosis of HepG2 cells (94)
HIF-1α	<ul style="list-style-type: none"> - No direct evidence for EL-mediated HIF-1α activation 	<ul style="list-style-type: none"> - Activation of HIF-1α-mediated transcription of cell death genes BNIP3 and Nix in hepatocytes (120)

1.7 Hypothesis and specific aims

The overall hypothesis is that HX and EL synergize to cause cell death that depends on oxidative stress, MAPK and HIF-1 α . These factors were chosen based on their central roles in the mechanisms of HX- and EL-mediated cell death individually. The goal of the specific aims proposed is to determine which factors are critical for the development of HX/EL-induced cell death and how each factor influences the others in the cascade resulting in cytotoxicity. This general hypothesis will be tested by specific hypotheses represented in the following aims:

Aim 1 Hypothesis: HX sensitizes primary rat HPCs and the transformed hepatocyte cell line Hepa1c1c7 to cell death caused by EL through ROS generation that is critical to the development of cell death (Chapter 2 and 3).

Aim 2 Hypothesis: The cytotoxic interaction of HX/EL depends on MAPK signaling (Chapter 2).

Aim 3 Hypothesis: Hypoxia-inducible factor-1 α signaling contributes to cell death caused by the cytotoxic interaction of HX and EL (Chapter 2)

Aim 4 Hypothesis: HIF-1 α is a critical mediator of hepatotoxicity in a model of drug-induced liver injury with acetaminophen (APAP) (Chapter 4).

1.8 Overview and significance of dissertation

The studies proposed in this dissertation will outline mechanisms by which HX and EL cotreatment causes hepatocellular injury. This is especially important considering the vast number of liver pathologies in which HX and PMNs play a central role, including cholestasis, fibrosis and I-R. Furthermore, identification of common cell death signaling mechanisms induced by HX and EL will aid in predicting the toxicity of xenobiotics. Finally, it will elucidate the role of the critical transcription factor HF-1 α in the development of APAP hepatotoxicity, the leading cause of liver failure in the United States.

CHAPTER 2

Sparkenbaugh, E.M., Ganey, P.E. and Roth, R.A. Hypoxia sensitization of hepatocytes to neutrophil elastase-mediated cell death depends on MAPKs and HIF-1 α . Submitted to A J Phys Gastroint and Liver Phys 10-2011

2.1 Abstract

The liver is sensitive to pathological conditions associated with tissue HX and the presence of activated neutrophils that secrete the serine protease EL. We demonstrated previously that cotreatment of rat HPCs with nontoxic levels of HX and EL caused synergistic cell death. HX is sensed by hypoxia-inducible factor-1 α (HIF-1 α), a transcription factor which heterodimerizes with HIF-1 β /ARNT and directs expression of many genes, including the pro-cell death gene BNIP3. Since cell death from either EL or HX also requires MAPK activation, we tested the hypothesis that the cytotoxic interaction of HX and EL depends on MAPK and HIF-1 α signaling. Treatment of Hepa1c1c7 cells with EL in the presence of HX (2% O₂) resulted in synergistic cell death. EL reduced p-ERK in both oxygen-replete and HX cells, and ERK inhibition enhanced the cytotoxicity of EL alone. HX/EL cotreatment caused an additive increase in p-p38, and p38 inhibition attenuated cell death caused by this cotreatment. EL enhanced HX-induced HIF-1 α accumulation and transcription of the HIF-1 α -mediated cell death gene BNIP3, and p38 inhibition attenuated BNIP3 expression and production. Cytotoxicity and BNIP3 expression from cotreatment with EL and HX was reduced in HIF-1 β -deficient HepaC4 cells compared to Hepa1c1c7 cells. These data suggest that p38 signaling contributes to HX/EL-induced cell death via modulation of HIF-1 α -mediated gene transcription. Finally, lipid peroxidation was enhanced in HX/EL cotreated cells compared to either treatment alone. Vitamin E treatment attenuated lipid peroxidation and protected cells from the cytotoxicity of HX and EL, suggesting that lipid peroxidation plays a role.

2.2 Introduction

PMN-mediated inflammation and tissue HX play a role in HPC injury that results in liver failure in a variety of conditions, including septic shock (80, 171), I-R injury (70, 75), alcoholic liver injury (5, 170), and several drug-inflammation models in which an inflammatory stress synergizes with nontoxic doses of drugs with idiosyncratic liability in humans to result in liver injury in rodents (36, 112, 157, 193). In these models, prevention of hepatic PMN accumulation or reduction in liver HX affords protection from injury (37, 112, 193), suggesting interdependence of these factors in pathogenesis. One way by which PMNs might contribute to injury is through the release of the cytotoxic protease EL. In support of this hypothesis, inhibition of EL by cotreatment with eglin C or genetic knockout of EL prevented liver injury in some models of inflammatory stress/drug interaction (37, 159). In vitro, exposure of primary rat HPCs to modest HX (5% O₂) enhanced the cytotoxicity of EL and shortened the time until onset of cell death (112), further indicating that there is an interaction in the pathway(s) by which HX and EL cause injury. The mechanism of this interaction is not known.

EL is cytotoxic to many primary and transformed cell types in vitro, including lung epithelial cells (135, 165) and primary HPCs (63, 118), however the mechanism is not well understood. In primary HPCs, it induces morphological changes such as mitochondrial, endoplasmic reticular and nuclear swelling consistent with oncotic necrosis (118). In transformed lung epithelial cells, EL activates MAPKs and NF- κ B in a PAR-dependent fashion, resulting in MAPK- and NF- κ B-dependent apoptosis (166, 167). Thus, the mechanism of EL cytotoxicity might depend on cell type, but it is clear

that EL can cause cell membrane dysfunction and activate cell death signaling pathways.

During inflammatory episodes, a reduction in tissue pO_2 (ie, HX) can occur from decreased tissue perfusion due to vascular obstruction from coagulation-mediated fibrin deposition (112) or to increased metabolic demand of innate immune cells (89). In addition, EL inhibits endothelial cell production of nitric oxide (NO) and prostacyclin, thereby inhibiting vasodilation and reducing blood flow to hepatic tissue, further contributing to the development of HX (129).

Hypoxia-inducible factor (HIF) has been widely studied as a factor used by cells to sense and respond to changes in oxygen tension. HIF comprises alpha and beta subunits which heterodimerize to form a competent transcription factor (154). There are three isoforms of the alpha subunit, HIF-1 α , HIF-2 α and HIF-3 α , of which HIF-1 α is the best characterized. The beta subunit, HIF-1 β , is also known as the aryl hydrocarbon receptor nuclear translocator (ARNT). HIF-1 α is constitutively expressed in the cytoplasm, and under normal oxygen tension it is continually degraded. When oxygen is limited, HIF-1 α can accumulate and translocate to the nucleus where it heterodimerizes with HIF-1 β /ARNT, binds to hypoxia response elements in the DNA, and directs transcription of over 100 genes (154). HIF-1 α -directed genes control many pathways, including angiogenesis, erythropoiesis, energy metabolism, and glycolysis, all of which can enhance oxygen delivery or energy production in hypoxic environments. However, if HX is severe or prolonged, HIF-1 α can also activate transcription of cell

death genes, including BCL2/adenovirus E1B interacting protein 3 (BNIP3) and Nix (102).

HX injures HPCs through a variety of pathways in addition to HIF-1 α . It causes mitochondrial dysfunction, loss of ATP production, and eventual loss of plasma membrane integrity (92). Exposure of primary HPCs or the transformed hepatocyte cell line HepG2 to low oxygen ($pO_2 < 10$ mmHg in the cell culture atmosphere) increases mitochondrial reactive oxygen species (ROS) production (15), which contributes to HX-mediated cell death by damaging DNA, proteins and polysaccharides and initiating lipid peroxidation (93). Recent studies indicated that the the HX phase of hypoxia/reoxygenation injury involves lipid peroxidation and membrane damage in mouse embryonic fibroblasts (187). Furthermore, HX activates the MAPKs (155). In particular, activation of p38 MAPK enhances gene transcription by HIF-1 α (121) as well as HX-induced death of primary HPCs (120).

There is significant overlap in the mechanisms by which HX and EL lead to HPC injury separately; however, the mechanism by which HX sensitizes HPCs to killing by EL is not known. We hypothesized that the synergistic cytotoxicity of HX and EL requires MAPKs and HIF-1 α signaling. The results from these studies offer insight into mechanisms of HPC death that can lead to liver failure in situations in which tissue HX and PMN-associated inflammation occur.

2.3 Materials and Methods

Materials

Unless otherwise noted, all materials were purchased from Sigma-Aldrich (St. Louis, MO). Antibiotic-antimycotic (ABAM) and Dulbecco's Modified Eagles Medium (DMEM) were purchased from Invitrogen (Carlsbad, CA). Heat-inactivated fetal bovine serum (FBS) was purchased from Fisher Scientific. SB203580, U0126, SP600125 and 2-(4-Methyl-8-(morpholin-4-ylsulfonyl)-1,3-dioxo-1,3-dihydro-2H-pyrrolo[3,4-c]quinolin-2-yl)ethyl acetate, a nonpeptidyl pyrroloquinoline caspase inhibitor (CI) were purchased from Calbiochem (San Diego, CA).

Elastase

Human sputum elastase (Elastin Products Company, Owensville, MO) was resuspended in PBS and stored at -20°C until use. The enzymatic activity of EL was determined using the colorimetric elastase substrate, MeOSuc-Ala-Ala-Pro-Val-pNA (Calbiochem, San Diego, CA). One unit of EL was defined as the amount of enzyme required to cause a change of absorbance of 1.0 at 410 nm in 10 min at 37°C.

Hypoxia Exposures

For HX exposures, cells were placed in heated, humidified hypoxic glove boxes (Coy Laboratories, Grass Lake, MI) at 5% CO₂. Primary HPCs were exposed to 5% O₂, and Hepa1c1c7 cells were exposed to 2% O₂ in the atmosphere. Chamber pO₂ was monitored continually to ensure consistent oxygen exposure.

Cell Culture

Primary rat HPCs were isolated as previously described (112). Mouse Hepa1c1c7 and HepaC4 cells (ATCC, Manassass, VA) were maintained in DMEM supplemented with 10% FBS and 1% ABAM. Confluent cell cultures were detached from the plate with 0.25% trypsin-EDTA. For protein and RNA isolation, cells were seeded at 1×10^6 cells/well in 6-well tissue culture dishes (Costar, Lowell, MA), and for cytotoxicity experiments, cells were seeded at 4×10^4 cells/well in white-walled 96-well plates (Costar, Lowell, MA). Cells were allowed to adhere overnight at 20% O₂.

Cytotoxicity Assessment

HPCs were plated at 2.5×10^5 cells/well in 12-well tissue culture plates in Williams' Medium E (WME) (Invitrogen, Carlsbad, CA) containing 10% FBS for 3 hrs. After attachment, cells were washed twice with serum-free WME and treated with various concentrations of EL in either OxR or HX environment for 8 hrs. At 8 hrs, medium and cell lysates were collected and analyzed for ALT activity as described previously (112).

Hepa1c1c7 and HepaC4 cells were allowed to adhere and were washed with serum-free DMEM to remove any traces of FBS, which can neutralize the proteolytic activity of EL. Cells were treated with various concentrations of EL in serum-free DMEM in either OxR (20% O₂, 5% CO₂, 37°C) medium or medium that had been incubated overnight in a hypoxic atmosphere (5% or 2% O₂, 5% CO₂, 37°C) and placed in either the OxR or HX incubator.

For experiments using Hepa1c1c7 and HepaC4 cells, cell death was assessed with the Cytotox-Glo Luminescent Assay (Promega Corporation, Madison, WI) according to the manufacturer's directions. Briefly, it is a luminescent assay that measures the activity of an intracellular protease that has been released from membrane-compromised cells. The dead cell protease activity is measured in the medium and in the cell lysate, and data are represented as percent of total dead cell protease released (% enzyme release).

For MAPK inhibitor studies, stock solutions of SB203580, UO126 and SP600125 were prepared in DMSO and stored at -20°C. Cells were washed twice with serum-free DMEM and treated with either 5 or 10 µM inhibitor (0.1% DMSO vehicle) for 2 hrs in an oxygen replete incubator. For CI studies, a stock solution of CI was prepared in DMSO and stored at -20°C. Cells were washed twice with serum-free DMEM and treated with 40 µM CI (0.2% DMSO vehicle) for 1 hr under OxR conditions. For alpha-tocopherol (vitamin E) studies, a stock solution of vitamin E was prepared in DMSO and stored at -20°C. Cells were washed twice with serum-free DMEM and treated with 50 µM vitamin E (0.01% DMSO vehicle) for 30 min in OxR conditions. Finally, for cyclosporine A (CsA) studies, cells were pretreated with 2.5 µM CsA (0.01% DMSO vehicle) for 2 hrs in OxR conditions. After pretreatment with inhibitor, cells were treated with EL and transferred to hypoxic glove boxes for 24 hrs.

Protein Isolation

Hepa1c1c7 and HepaC4 cells were plated in 6-well tissue culture plates until 80-90% confluent. They were washed twice with serum-free DMEM and treated with EL in

OxR or HX serum free DMEM. At various times after treatment, the serine protease inhibitor phenylmethylsulfonylfluoride (PMSF) was added to the media at a final concentration of 1 μ M to neutralize EL activity. Cells were then scraped and collected via centrifugation (2000 rpm for 2 min). The pellet was washed with ice-cold PBS. Whole cell extracts were prepared by sonication (two 5s pulses) of pellets in ice-cold Harlow Buffer containing HALT protease and phosphatase inhibitors (Thermo Scientific, Rockford, IL). Lysates were collected by centrifugation at 10,000 x g for 10 minutes. Cytoplasmic and nuclear extracts were prepared by lysing cells on ice for 10 min with lysis buffer A (10 mM HEPES, 1.5 mM $MgCl_2$, 10 mM KCl, 0.5 mM DTT, 0.05% IGEPAL, pH 7.9) containing HALT protease and phosphatase inhibitors. Lysates were centrifuged (3000 rpm for 10 min), and supernatant was collected in prechilled tubes as the cytoplasmic fraction. Nuclear pellets were resuspended with lysis buffer B (5 mM HEPES, 1.5 mM $MgCl_2$, 0.2 mM EDTA, 0.5 mM DTT, 26% glycerol v/v, pH 7.9), and NaCl was added to a final concentration of 300 mM. The pellets were sonicated (two 5s pulses) then allowed to sit on ice for 30 min. Nuclear fraction supernatant was collected in prechilled tubes after centrifugation (22,000 x g, 25 min). Protein concentration was determined by the bicinchoninic acid (BCA) assay (Thermo Scientific, Rockford, IL).

Western Analysis

For MAPK and BNIP3 detection, 20 μ g of protein were separated on 10% SDS-PAGE gel. For HIF-1 α detection, 25 μ g of cytoplasmic and nuclear protein were loaded onto a 10% SDS-PAGE gel. Proteins were transferred to polyvinylidene fluoride (PVDF) membranes (Millipore, Billerica, MA). Membranes were washed with tris-

buffered saline (TBS) containing 0.1% Tween-20 (TBST) and blocked for 1 hr with 5% BSA for MAPK and BNIP3 detection or 5% milk for HIF-1 α detection. Blots were probed with p-p38, p-ERK1/2, p-JNK, and BNIP3 primary antibodies (Cell Signaling Technology, Beverly, MA) (1:1000 in 5% BSA) or HIF-1 α antibody (Novus Biologicals, Littleton, CO) (1:500 in 5% milk) at 4°C overnight. Membranes were washed with TBST, probed with secondary goat anti-rabbit HRP conjugated antibody (Santa Cruz Biotechnology, Santa Cruz, CA) (1:2000 – 1:10,000) in 5% BSA or milk in TBST. HRP was visualized with the HyGlo Chemiluminescent HRP Antibody Detection Reagent and exposed to HyBlot CL Film (Denville Scientific, Metuchen, NJ).

Membranes were stripped using Restore Western Blot Stripping Reagent (Thermo Scientific, Rockford, IL) and reprobed for total p38, ERK1/2, JNK (Cell Signaling technology, Beverly, MA), β -actin (Abcam, Cambridge, MA) (1:5000 in 5% BSA) or lamin (AbCam, Cambridge, MA) (1:10,000 in 5% BSA). HIF-1 α western blots were stripped, and reprobed for tubulin (cytoplasmic, 1:1000 in 5% BSA) or lamin (nuclear, 1:10,000 in 5% BSA), to serve as loading controls and determine purity of each fraction.

RNA Isolation and RT-PCR

Cells were treated with various concentrations of EL in OxR or HX conditions for various times. After treatment, EL was neutralized with 1 μ M PMSF, and cells were collected by centrifugation. Total RNA was isolated with TRIzol reagent (Invitrogen Corporation, Carlsbad, CA) according to manufacturer's directions. RNA quantity and quality was assessed by Nanodrop 2000 (Thermo Scientific, Rockford, IL). cDNA was

prepared from 1 µg RNA with iScript cDNA Synthesis Kit (Bio-Rad Laboratories, Hercules, CA). The expression level of specific genes was analyzed using SYBR green (Applied Biosystems, Foster City, CA). Copy number was determined by comparison to standard curves of the respective genes. Expression level was normalized to the hypoxanthine guanine phosphoribosyl transferase (HPRT) gene. PCR primers were used as follows: mouse BNIP3: forward, 5'- atccaaagctgcttaaatcggcgc-3' and reverse 5'- agcatgtcaaggaggcaggcttta-3'; mouse Nix: forward, 5'- tgctgcgtctctaagcatgaggaa-3' and reverse, 5'- aggccagcacatgagaaaggaaga-3'; and HPRT: forward, 5'- aggagtctgttgatgttgccagt-3' and reverse, 5'- gggacgcagcaactgacatttcta-3'.

Malondialdehyde (MDA) Measurement

Hepa1c1c7 cells were treated with 0 or 7.5 U/mL EL in an OxR or hypoxic environment for 16 hr. After treatment, cells were collected by centrifugation and sonicated (two 5s pulses) in cold 50 mM potassium phosphate buffer (pH 7.4, 1 mM EDTA). Thiobarbituric acid reactive substances (TBARS) were detected in cell lysates with a kit (Cayman Chemical, Ann Arbor, MI) using MDA for the standard curve. Results are expressed as MDA equivalents. In some experiments, cells were pretreated for 2 hrs with 10 µM SB203580 or for 30 min with 50 µM vitamin E. MDA concentration was also assessed in Hepac4 cells.

Statistical Analyses

All data are expressed as mean ± SEM. The results were analyzed using two- and three-way ANOVA as appropriate and Tukey's post hoc test to compare groups. P<0.05 was of the criterion for significance.

2.4 Results

Cytotoxicity of EL and HX in primary HPCs and Hepa1c1c7 cells

Primary HPCs were not sensitive to concentrations of EL up to 17 U/ml 8 hrs after treatment. Similar to previously published results (112), 5% O₂ was modestly cytotoxic to HPCs, and it significantly enhanced the cytotoxicity of EL at 8.5 and 17 U/ml (Figure 6A). There was a statistically significant interaction between HX and EL treatments, indicative of a synergistic response.

In Hepa1c1c7 cells, EL caused cytotoxicity at concentrations greater than 7.5 U/mL at 24 hrs, and HX (2% O₂) alone was modestly cytotoxic (Figure 6B). Cotreatment of Hepa1c1c7 cells with HX and EL resulted in a significant increase in cell death over either treatment alone, and there was a significant interaction between 2% O₂ and concentrations of EL 7.5 U/mL and greater (Figure 6B). Neither HX, EL, nor HX/EL-cotreatment caused significant cytotoxicity at 6, 12, or 18 hrs, indicating that cytotoxicity developed rapidly between 18 and 24 hrs of treatment in HX/EL-cotreated cells (data not shown).

EL caused concentration-dependent caspase 3/7 activation 6 hrs after treatment that was not affected by HX (Figure 7A). Pretreatment with a nonpeptidyl caspase 3/7 inhibitor had no effect on the cytotoxicity of EL; however it did attenuate cytotoxicity caused by HX alone. Caspase inhibition did not protect cells from the cytotoxic interaction (Figure 7B). Furthermore, pretreatment with 2.5 μM CsA to inhibit mitochondrial permeability transition did not prevent cell death (Figure 7C).

Figure 6: Hypoxia sensitizes primary HPCs and Hepa1c1c7 cells to cytotoxicity of EL. (A) Primary rat HPCs were treated with 0, 8.5, or 17 U/mL EL in either OxR or HX environment (5% O₂ in atmosphere) for 8 hrs, and cytotoxicity was assessed from release of ALT into the medium. Data represent mean ± SEM of 3 separate experiments performed in duplicate. (B) Hepa1c1c7 cells were exposed to 0-30 U/mL EL in either OxR or HX (2% O₂) environment for 24 hrs, and cell death was assessed by leakage of a cell death enzyme into medium. Data represent mean ± SEM of 8 experiments performed in triplicate. a: p<0.05 vs. 0 U/mL EL in OxR; b: p<0.05 vs. 0 U/mL EL in HX; c: p<0.05 vs. same [EL] in OxR; #: significant interaction between treatments.

Figure 6

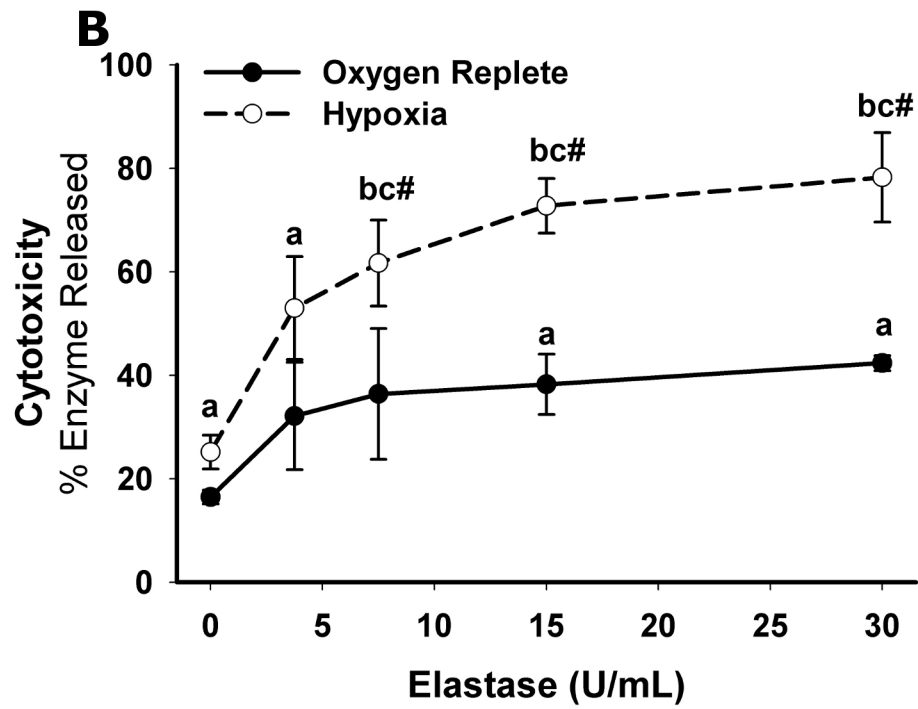
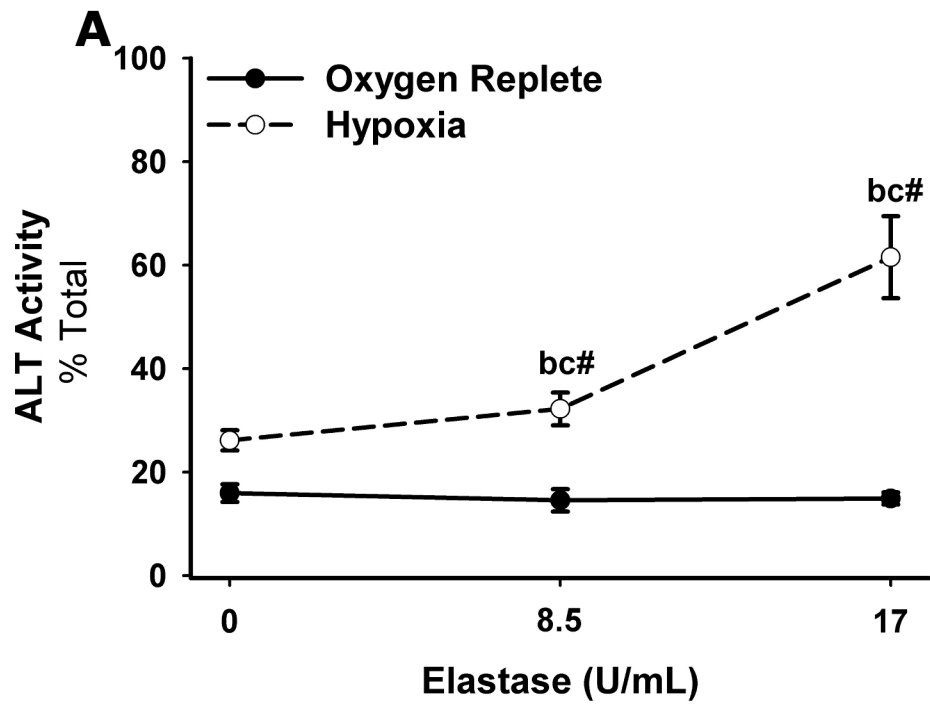
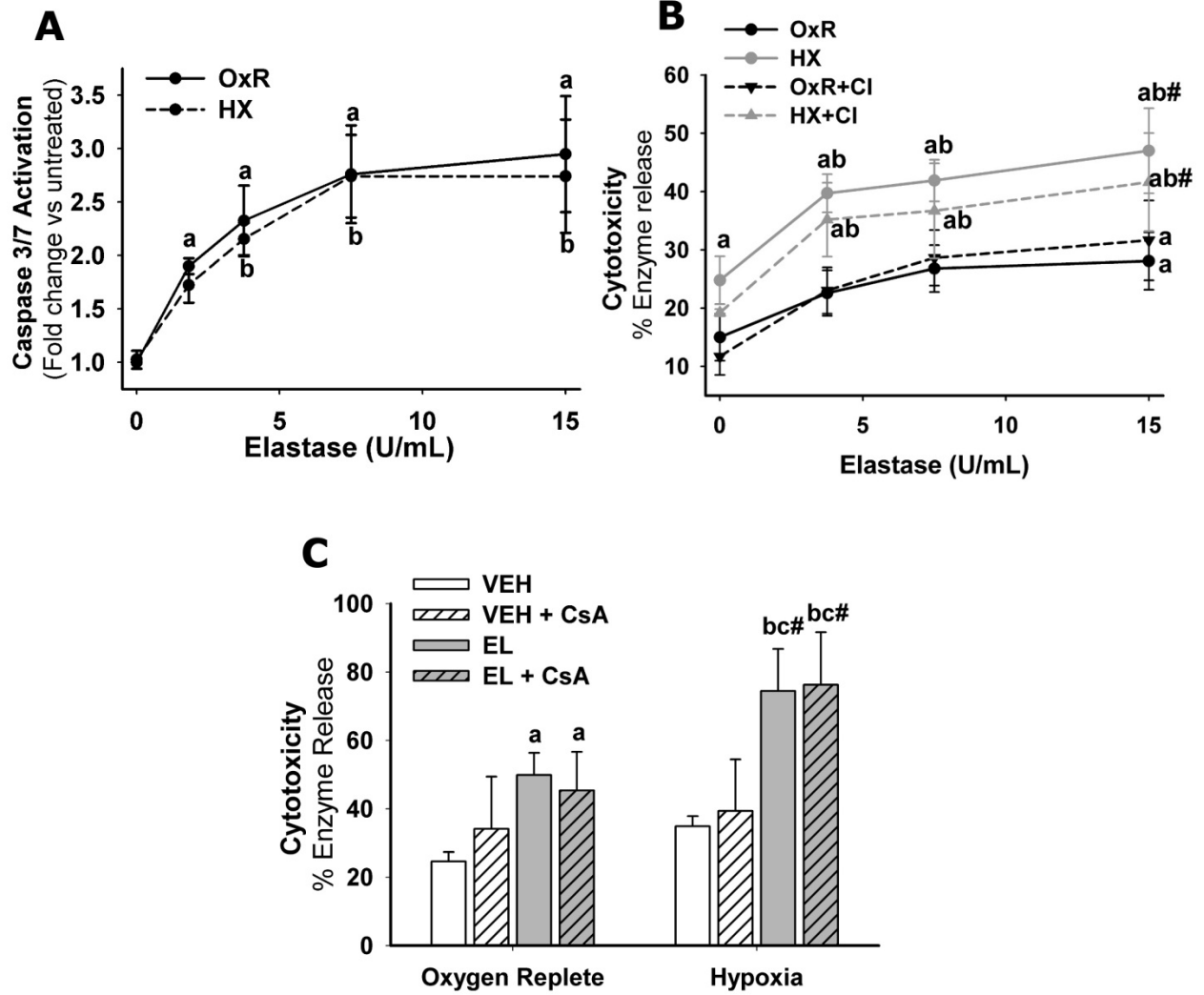


Figure 7: Caspase 3/7 and mitochondrial permeability transition do not contribute to cell death caused by HX/EL cotreatment. (A) Hepa1c1c7 were treated with 0, 1.875, 3.75, 7.5 or 15 U/mL EL in either OxR or HX environment for 6 hrs, and caspase 3/7 activity was assessed. Data represent mean \pm SEM of three separate experiments performed in triplicate. (B) Hepa1c1c7 cells were pretreated with Cl (40 μ M), then treated with 0-15 U/mL EL in OxR or HX environment for 24 hrs, and cell death was assessed. Data are mean \pm SEM of 4 separate experiments in triplicate. (C) Cells were pretreated with CsA (2.5 μ M) and treated with 0 or 7.5 U/mL EL in OxR or HX environment for 24 hrs, and cytotoxicity was assessed. Data represent means \pm SEM of 3 experiments in triplicate. a: $p < 0.05$ vs. 0 U/mL EL in OxR; b: $p < 0.05$ vs. 0 U/mL EL in HX; c: $p < 0.05$ vs 7.5 U/mL EL in OxR; #: significant interaction between EL and HX.

Figure 7



MAPK phosphorylation

Phosphorylation of ERK, JNK and p38 was assessed 30 min after treatment with HX and EL. Phosphorylation of ERK was modestly increased by HX. Interestingly, EL decreased p-ERK irrespective of cotreatment with HX (Figure 8A). Phosphorylation of ERK was abolished by U0126, which inhibits the upstream MAPK kinases, MEK1 and MEK2, specific for ERK phosphorylation (Figure 8A). JNK phosphorylation was not consistently affected by EL or HX, and it was inhibited with 5 μ M SP600125, which prevents JNK-dependent phosphorylation of downstream mediators such as c-Jun (Figure 2.3A). EL and HX each increased p-p38, and there was an additive increase in p-p38 caused by cotreatment (Figure 8A). Densitometry indicated that both EL and HX increased the ratio of p-p38:total p38 from 1 to 1.7 \pm 0.4 and 2.0 \pm 0.3, respectively, and cotreatment increased the ratio to 3.0 \pm 0.76 (Figure 8B). P38 phosphorylation was reduced by 10 μ M SB203580, which targets p38 and its downstream substrates.

Inhibition of ERK with U0126 increased the cytotoxicity of EL alone but had no significant effect on the interaction of HX/EL (Figure 9A). JNK inhibition using SP600125 had no effect on cell death in any treatment group (Figure 9B). Inhibition of p38 with SB203580 had no effect on cytotoxicity caused by HX or EL, but it significantly attenuated cytotoxicity in HX/EL-cotreated cells to the level of either EL or HX alone (Figure 9C).

Figure 8: HX/EL cotreatment causes an additive increase in activation of p38, but not JNK or ERK. (A) cells were treated with either VEH or 7.5 U/mL EL for 30 min in either OxR or HX environment, and phospho- and total ERK 1/2 (44 kDa and 42 kDa), JNK (42 kDa), and p38 (38 kDa) were determined by Western blot analysis. Some cells were pretreated with U0126 (5 μ M), SP600125 (5 μ M), or SB203580 (10 μ M) to inhibit ERK, JNK or p38, respectively. (B) Densitometry was performed on phospho- and total p38 bands. Data represent the mean \pm SEM of the ratio of phospho-p38: total p38 of 6 separate experiments. a: $p < 0.05$ vs. VEH in OxR; b: $p < 0.05$ vs. VEH in HX.

Figure 8

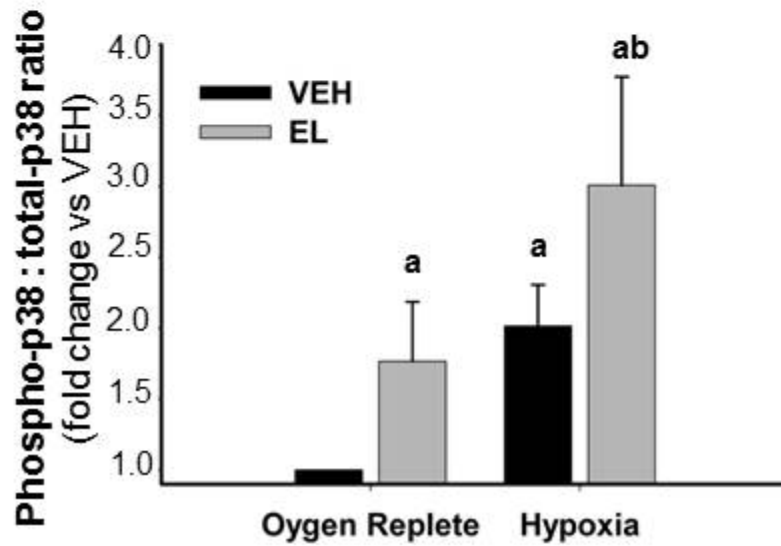
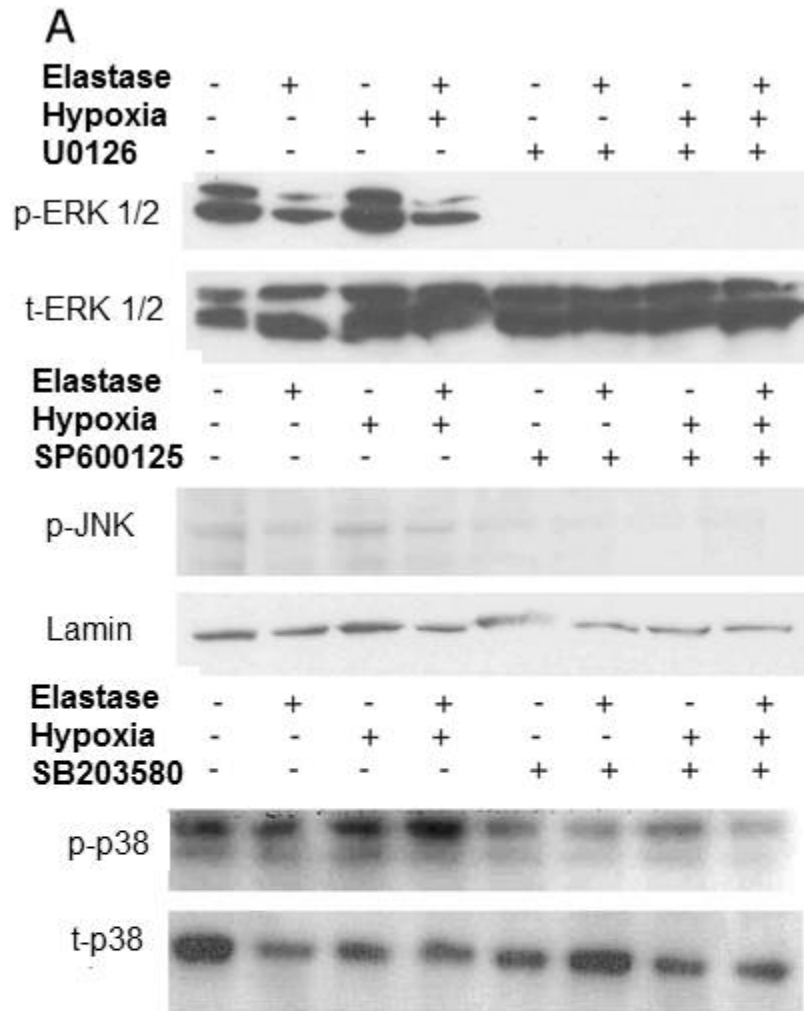
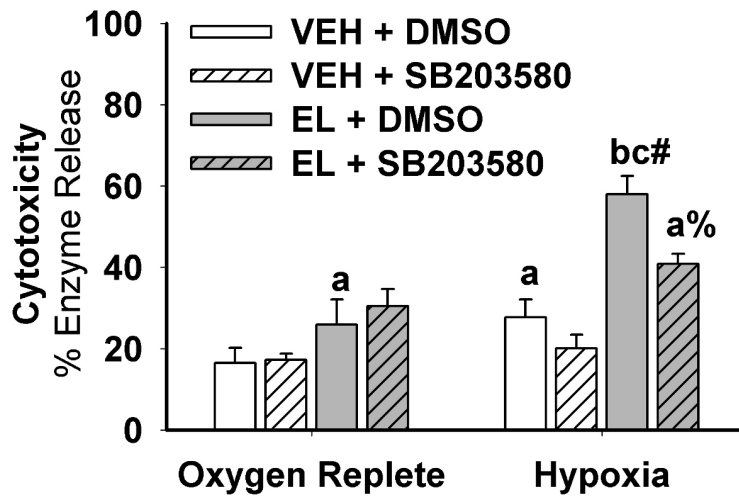
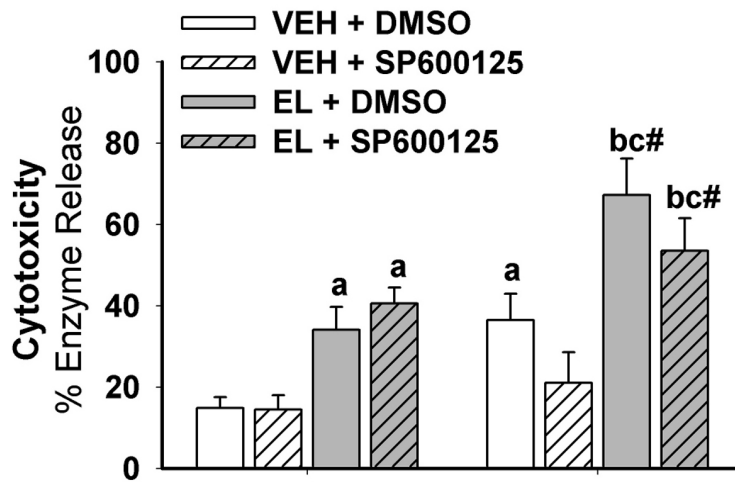
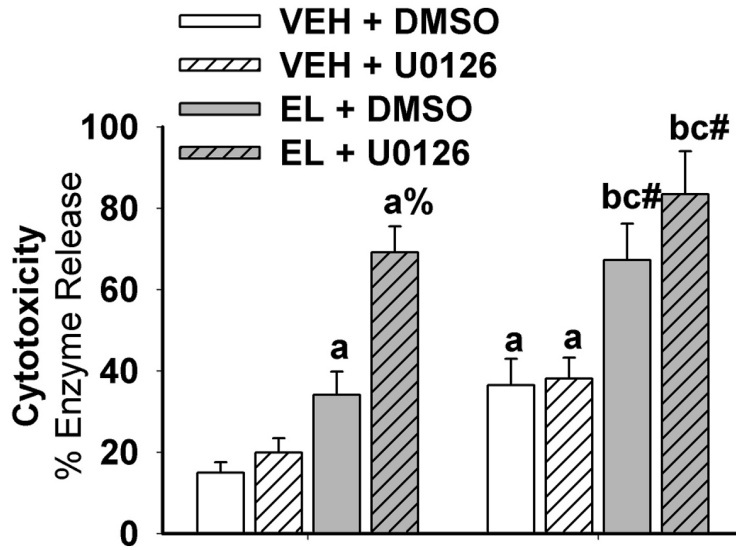


Figure 9: Inhibition of p38, but not JNK or ERK, protects Hepa1c1c7 cells from HX/EL interaction. Cells were pretreated for 2 hrs with (A) 5 μ M U0126 or Vehicle (0.05% DMSO) to inhibit ERK phosphorylation, (B) 5 μ M SP600125 to inhibit JNK activity, or (C): 10 μ M SB203580 to inhibit p38 activity. Cells were then treated with VEH or 7.5 U/mL EL in OxR or HX for 24 hrs, and cytotoxicity was assessed. Data represent mean \pm SEM of 5-8 experiments performed in triplicate. a: $p < 0.05$ vs. VEH in OxR; b: $p < 0.05$ vs. VEH in HX; c: $p < 0.05$ vs. EL in OxR; %: $p < 0.05$ vs. same treatment group without inhibitor; #: significant interaction between HX and EL.

Figure 9



HIF-1 α accumulation and activation

HIF-1 α protein was measured in cytosolic and nuclear fractions 30 and 60 mins after treatment. EL did not alter HIF-1 α protein levels in either fraction. HX increased HIF-1 α protein in the cytosolic and nuclear fractions, and EL cotreatment further enhanced HIF-1 α accumulation in both fractions (Figure 10A). Blots were stripped and reprobed for both tubulin and lamin to determine the purity of the cytoplasmic and nuclear fractions, respectively. HIF-1 α and lamin band intensity were quantified in nuclear fractions. At 60 min, HX significantly increased the ratio of HIF-1 α :lamin by 6-fold compared to untreated cells. HX/EL cotreatment further enhanced the HIF-1 α :lamin ratio by nearly 14-fold over control, and there was a significant interaction between EL and HX treatments (Figure 10B).

BNIP3 and Nix mRNAs were assessed 8 hrs after treatment. EL did not affect expression of Nix (Figure 11A); however, it did increase BNIP3 mRNA expression (Figure 11B). HX increased both BNIP3 and Nix mRNA expression, and that effect was enhanced by cotreatment with EL (Figure 11A and 11B). Inhibition of p38 signaling had no effect on the increases in BNIP3 mRNA expression caused by either HX alone or EL alone, but it did reduce the increased BNIP3 expression after HX/EL cotreatment (Figure 11B).

BNIP3 protein levels were monitored 12 hrs after treatment. EL caused a modest increase in BNIP3 protein. HX caused a more pronounced increase in BNIP3, and this was enhanced by cotreatment with EL (Figure 12A). The intensity of BNIP3 protein was assessed by densitometry and expressed relative to lamin (loading control).

EL significantly increased the BNIP3:lamin ratio from 1.0 to 3.1 +/- 0.9. HX increased the BNIP3:lamin ratio to 8.7 +/- 3.5, and cotreatment with EL enhanced it further to 16.5 +/- 6.6 (Figure 12B). Inhibition of p38 phosphorylation attenuated the increase in BNIP3 protein due to HX, and there was even greater reduction of BNIP3 protein in HX/EL cotreated cells (Figure 12C).

Figure 10: HX/EL increases nuclear accumulation of HIF-1 α compared to HX alone. (A) Cells were treated with VEH or 7.5 U/mL EL in either OxR or HX environment for 60 min, and cytoplasmic and nuclear protein extracts were probed for HIF-1 α (105 kDa), lamin (70 kDa), or tubulin (50 kDa) protein via Western Blot. (B) Intensity of HIF-1 α and lamin were measured with Image J software. Data represent the mean of the HIF-1 α :lamin ratio \pm SEM of 4 separate experiments. a: $p < 0.05$ vs. VEH in OxR; b: < 0.05 vs. VEH in HX; c: $p < 0.05$ vs EL in OxR; #: significant interaction between HX and EL.

Figure 10

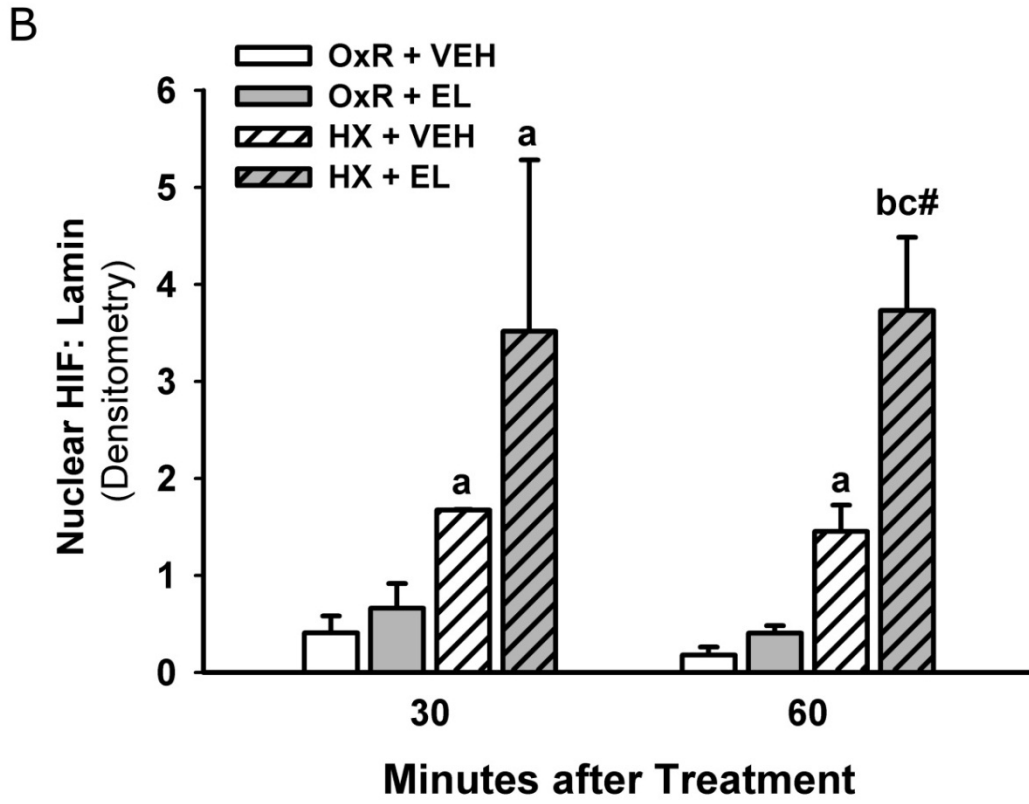
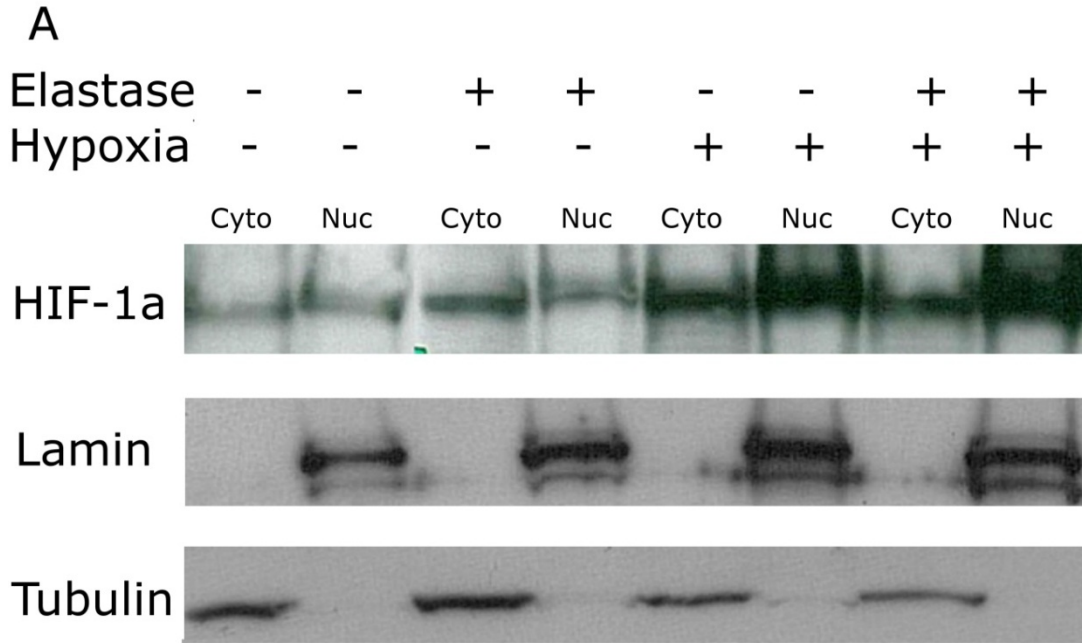


Figure 11: HX/EL increases mRNA expression of HIF-1 α -regulated genes, Nix and BNIP3. Cells were treated with VEH or 7.5 U/mL EL in OxR or HX conditions for 8 hrs, and RNA was isolated. (A) Detection of Nix. (B) Detection of BNIP3. In some experiments, cells were pretreated with 10 μ M SB203580 to inhibit p38 activity. a: p<0.05 vs. VEH in OxR; b: p<0.05 vs. VEH in HX; c: p<0.05 vs. EL in OxR; %: p<0.05 vs. same treatment without inhibitor; #: significant interaction between HX and EL.

Figure 11

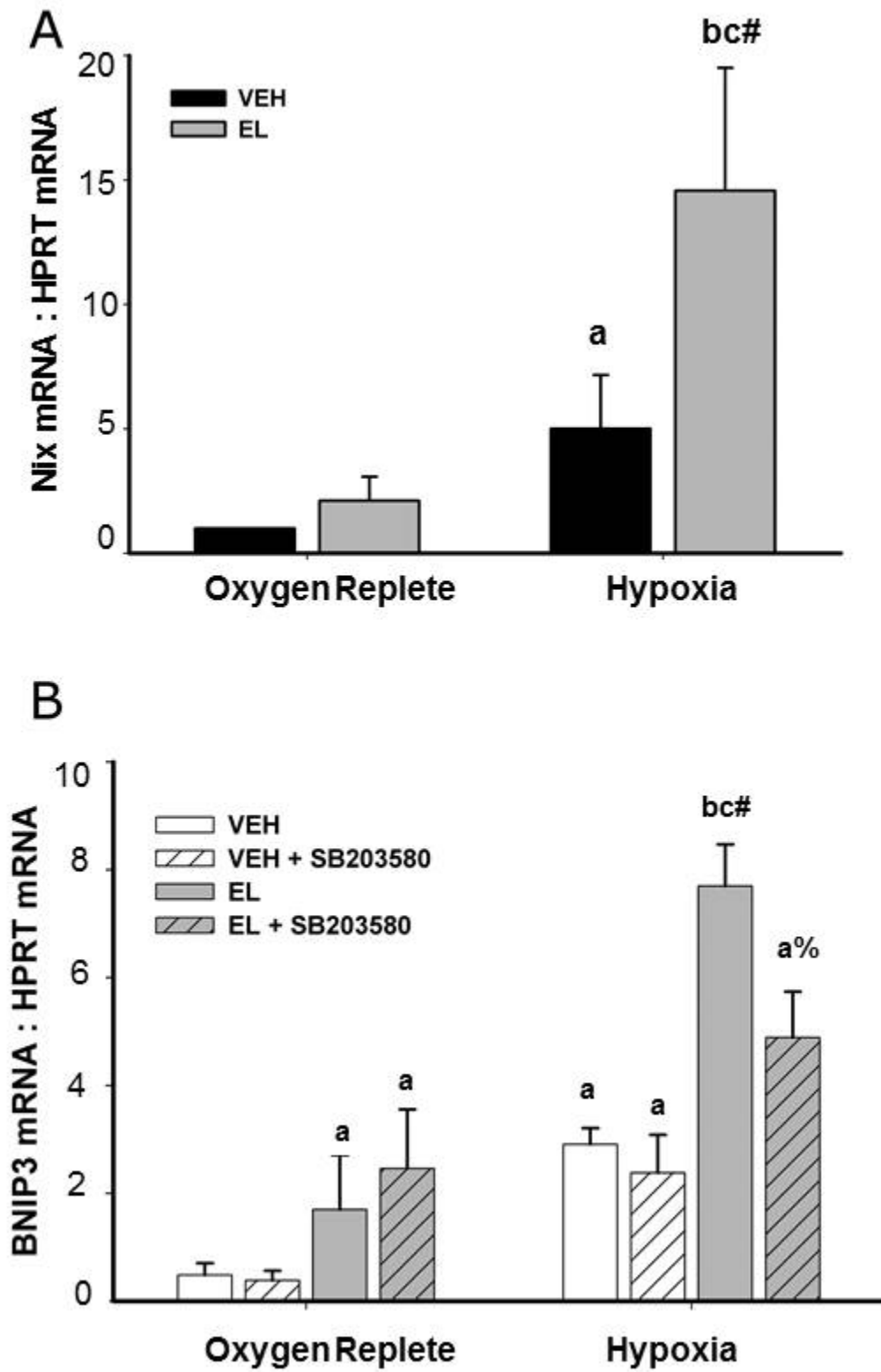
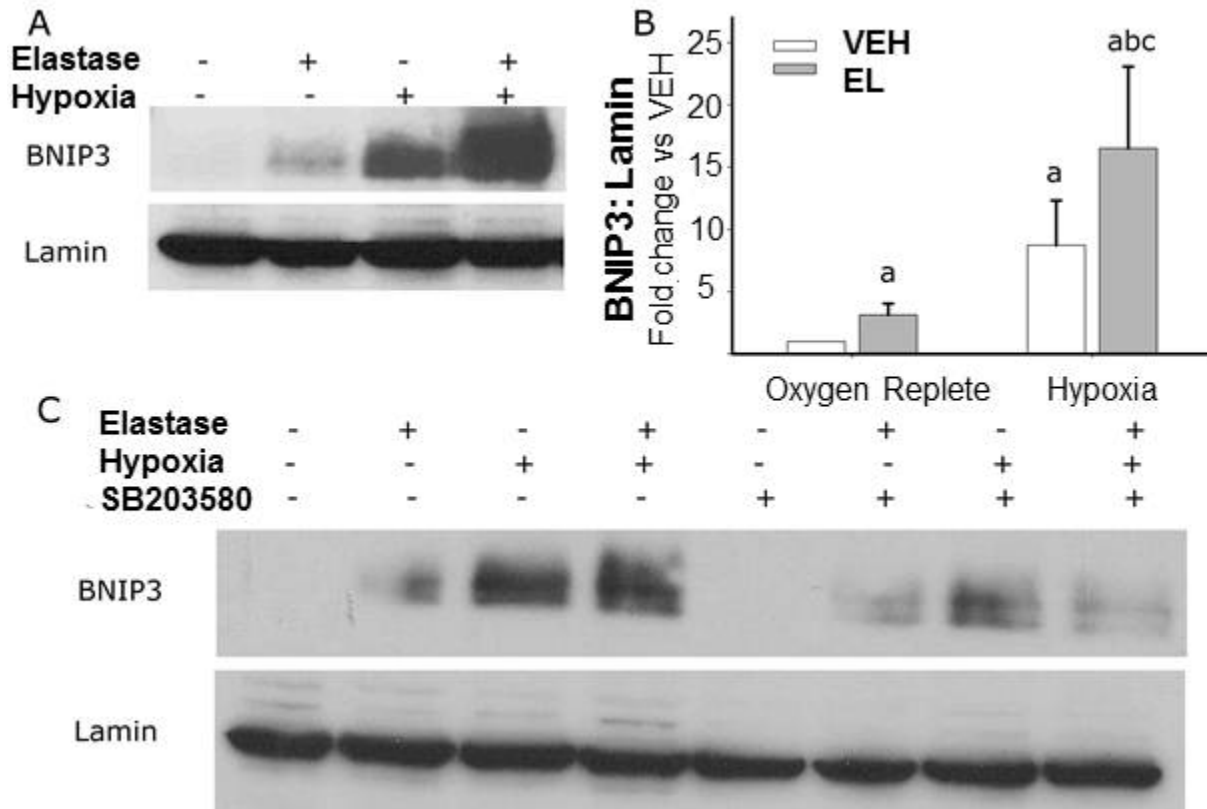


Figure 12: HX/EL increases expression of BNIP3 protein in a p38-dependent manner. (A) Hepa1c1c7 cells were treated with VEH or 7.5 U/mL EL in OxR or HX environment for 12 hrs, and BNIP3 (25 kDa) and lamin (70 kDa) protein were detected via Western blot. (B) BNIP3 and lamin intensity were measured with densitometry using Image J software, and data represent the mean of BNIP3:lamin ratio \pm SEM of 8 separate experiments. (C) Cells were pretreated for 2h with DMSO (0.01% final concentration) or 10 μ M SB203580 to inhibit p38, then treated with VEH or 7.5 U/mL EL in OxR or HX conditions for 12h. BNIP3 protein was detected via western blot. a: $p < 0.05$ vs. VEH in OxR; b $p < 0.05$ vs. VEH in HX; c: $p < 0.05$ vs. EL in OxR.

Figure 12



HIF-1 α signaling

To determine the role of HIF-1 α in the cytotoxicity of HX/EL, HepaC4 cells were used. These cells are deficient in HIF-1 β /ARNT, the heterodimeric partner of HIF-1 α required for competency as a transcription factor. As in Hepa1c1c7 cells, EL caused significant cytotoxicity in HepaC4 cells. However, HX alone was not cytotoxic in HepaC4 cells, and there was no interaction between HX and EL (Figure 13).

BNIP3 mRNA and protein expression were also assessed in HepaC4 cells. In contrast to Hepa1c1c7 cells (Figure 11B), EL did not alter the expression of BNIP3 mRNA in HepaC4 cells (Figure 14A). HX enhanced the BNIP3:HPRT ratio from 0.41 +/- 0.12 in untreated cells to 1.54 +/- 0.78, however this difference was not statistically significant. The BNIP3:HPRT ratio in HX/EL-cotreated HepaC4 cells was 1.99 +/- 0.57, which was not different from cells treated with either OxR or HX conditions alone. Inhibition of p38 had no effect on BNIP3 mRNA expression by any treatment (Figure 14A). In HepaC4 cells, the HX-mediated increase in BNIP3:HPRT ratio was significantly less than that in Hepa1c1c7 cells (1.54 +/- 0.78 versus 2.91 +/- 0.28; Figure 11B and 14A). Despite the modest increase in BNIP3 mRNA, there were no detectable increases in BNIP3 protein caused by any treatment after 12 hrs in HepaC4 cells (Figure 14B).

Figure 13: HIF-1 β -deficient HepaC4 cells are protected from the cytotoxicity of HX/EL. Hepa1c1c7 and HepaC4 cells were treated with VEH or 7.5 U/mL EL in OxR or HX conditions for 24h, and cytotoxicity was assessed. Data represent mean \pm SEM of 4 experiments in triplicate. a: $p < 0.05$ vs. VEH in OxR; b: $p < 0.05$ vs. EL in OxR; c: $p < 0.05$ vs. VEH in HX; %: $p < 0.05$ vs. same treatment in Hepa1c1c7 cells; #: significant interaction between treatments.

Figure 13

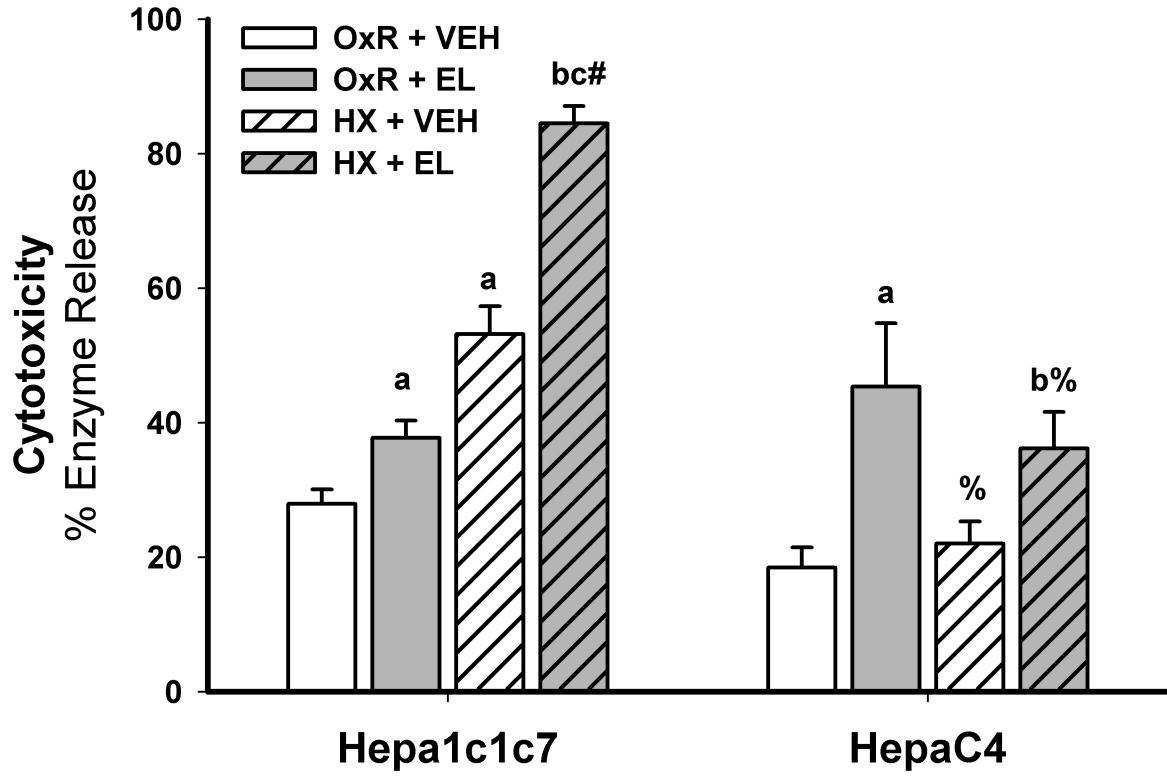
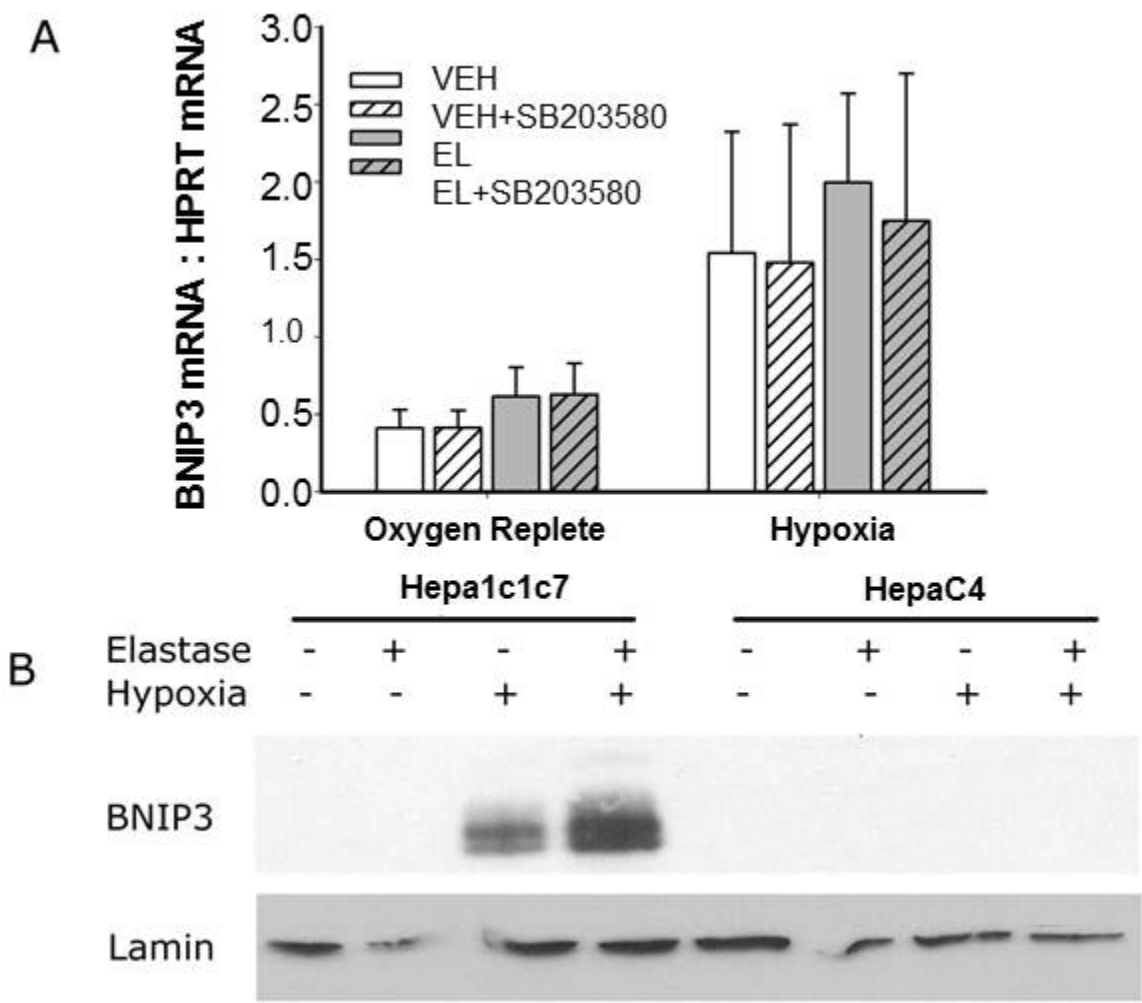


Figure 14: HepaC4 cells do not express BNIP3 mRNA or protein after HX/EL cotreatment. (A) HepaC4 cells were pretreated with 0.01% DMSO or 10 μ M SB203580 then treated with VEH or 7.5 U/mL EL in OxR or HX conditions for 8 hrs, and RNA was collected. Expression of BNIP3 and HPRT mRNA was assessed by q-RT-PCR. Data represent the mean of the ratio of BNIP3 mRNA : HPRTmRNA \pm SEM of 4 experiments in duplicate. (B) Hepa1c1c7 and HepaC4 cells were treated with VEH or EL in OxR or HX for 12 hrs and whole cell lysates were probed for BNIP3 protein and lamin.

Figure 14



Lipid Peroxidation

The lipid-soluble antioxidant vitamin E protected Hepa1c1c7 cells from cytotoxicity of HX/EL (Figure 15A), whereas water-soluble antioxidants such as 4-OH Tempo, n-acetylcysteine, and desferrioxamine were not protective (data not shown). To determine if oxidative stress occurred, H₂O₂ was measured with the DCFH-DA assay. In our system, there were no detectable increases in H₂O₂ production due to any treatment (data shown in Figure 16B). Vitamin E pretreatment had no effect on p38 phosphorylation (Figure 15B).

Lipid peroxidation was assessed by measuring cellular malondialdehyde (MDA) concentration. EL increased MDA concentration in cells (Table 3). Although HX alone had no effect, it significantly enhanced MDA concentration in EL-cotreated cells. In cells treated with vitamin E, HX/EL treatment significantly increased MDA compared to any treatment alone; however, this increase was significantly less than that in HX/EL-treated cells without added vitamin E (Table 3). Inhibition of p38 signaling by itself increased MDA concentration in OxR conditions, but the increase due to EL that occurred in control cells did not occur in cells treated with SB203580. It also reduced lipid peroxidation in HX/EL-cotreated cells compared to controls (Table 3).

Lipid peroxidation was also assessed in HepaC4 cells. Within these cells, there were no treatment-related changes in MDA concentration. When compared to Hepa1c1c7 cells, basal MDA concentration was slightly greater in HepaC4 cells as well as in HX-treated HepaC4 cells. There was no significant difference in MDA

concentration between HepaC4 and Hepa1c1c7 cells due to HX/EL cotreatment (Table 3).

Figure 15: Lipid peroxidation contributes to the mechanism of HX/EL-induced cell death in Hepa1c1c7 cells. (A) Cells were pretreated with 0.05% DMSO or 50 μ M Vitamin E for 30 min, and then treated with VEH or 7.5 U/mL EL in OxR or HX environment for 24 hrs after which cytotoxicity was assessed. Data represent mean \pm SEM of 3 experiments in triplicate. (B) Hepa1c1c7 cells were treated with VEH or 7.5 U/mL EL in OxR or HX atmosphere for 30 mins, and whole cell extracts were probed for phospho- and total p38 (38 kDa). a: $p < 0.05$ vs. VEH in OxR; b: $p < 0.05$ vs. VEH in HX; c: $p < 0.05$ vs. EL in OxR; %: $p < 0.05$ vs. same treatment without inhibitor.

Figure 15

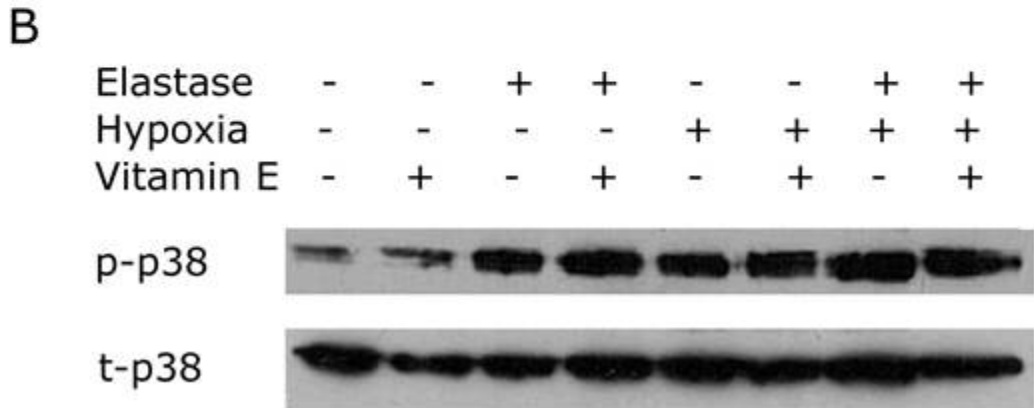
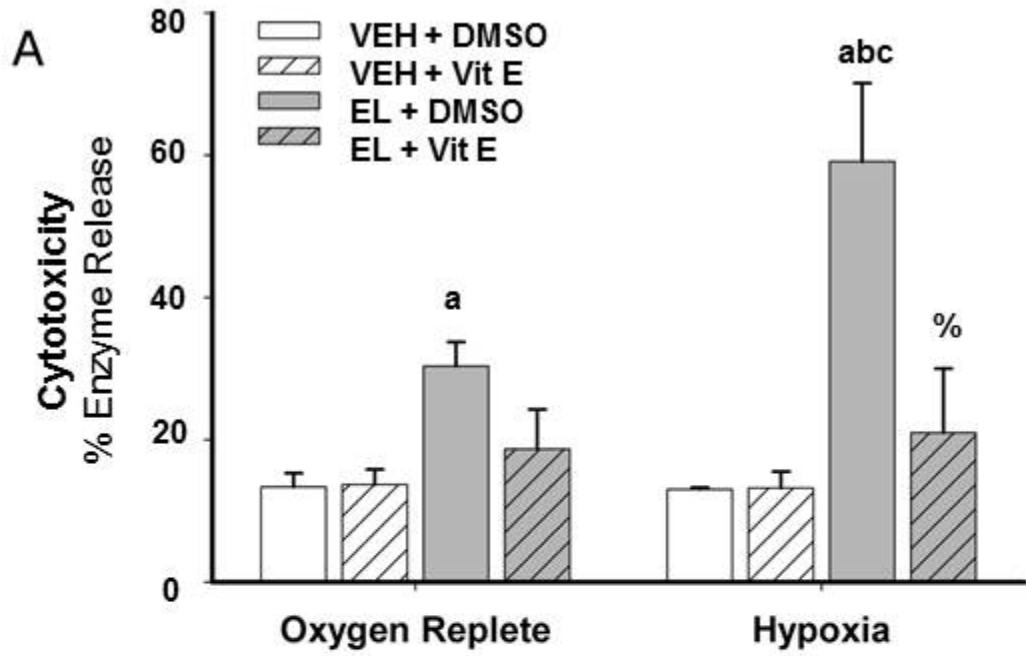


Table 3: Effect of HX/EL on Lipid Peroxidation in Hepa1c1c7 and HepaC4 cells.

Hepa1c1c7 cells were treated with VEH or 7.5 U/mL EL in OxR or HX for 16 hrs and were assessed for TBARS (MDA equivalents). In some experiments, cells were pretreated with 50 μ M vitamin E for 30 min or 10 μ M SB203580 for 2 hrs. MDA concentration was also assessed in HepaC4 cells (rightmost column). Values presented are means \pm SEM for n=3-5 experiments. a: p<0.05 vs. VEH in OxR; b: p<0.05 vs. EL in OxR; c: p<0.05 vs. VEH in HX; #: significant interaction between treatments; %: p<0.05 vs. same treatment in control cells.

Table 3

	Malondialdehyde (μM)			
	Hepa1c1c7 Cells			HepaC4 Cells
Treatment	Control	Vitamin E	SB203580	
OxR + VEH	0.60 \pm 0.22	0.72 \pm 0.41	2.64 \pm 1.08[%]	1.41 \pm 0.57
OxR + EL	1.22 \pm 0.28^a	1.05 \pm 0.54	0.43 \pm 0.21[%]	1.45 \pm 0.49
HX + VEH	0.72 \pm 0.22	0.37 \pm 0.06	0.57 \pm 0.28	2.18 \pm 0.48[%]
HX + EL	3.40 \pm 0.62^{bc#}	1.40 \pm 0.33^{ab%}	2.02 \pm 1.23^{bc%}	2.62 \pm 1.60

2.5 Discussion

HX and PMNs are important mediators of hepatocyte death in many models of inflammatory liver injury, and we have demonstrated previously that HX sensitizes primary rat HPCs to the cytotoxicity of PMN-derived EL (112), a finding which we confirmed in this study (Figure 6A). In order to characterize the mechanism of this interaction in more detail, we extended this observation to Hepa1c1c7 cells. The response to HX has been well characterized in Hepa1c1c7 cells and in the HIF-1 β /ARNT-deficient variant, HepaC4 (20, 149). Similar to primary HPCs, Hepa1c1c7 cells were also sensitive to EL alone. Exposure to HX (2% O₂) significantly enhanced cell death caused by EL at concentrations as low as 3.75 U/mL EL (Figure 6B), and there was a cytotoxic interaction between these treatments.

EL causes caspase-dependent apoptosis of lung epithelial cells (51, 166). HX is also associated with caspase activation in cardiac fibroblasts (21). Therefore, we examined the role of intrinsic apoptosis and the effector caspases 3 and 7 in the mechanism of HX/EL-induced cell death. EL caused a concentration-dependent increase in caspase 3/7 activation that was not enhanced by HX (Figure 7A); however, caspase inhibition did not protect Hepa1c1c7 cells from the cytotoxic interaction of HX with EL (Figure 7B). CsA also did not afford protection (Figure 7C). These results suggest that neither caspase signaling nor mitochondrial permeability transition contributes to HX/EL-induced cell death; thus, the mode of cell death does not appear to be apoptotic.

The role of the MAPKs in cell death is complex and depends on cell type. Both HX and EL activate MAPKs in several cell types, and the result of activation is often cell death and/or activation of HIF-1 α or other transcription factors (121). ERK is generally activated by growth factors and mitogens and is involved in cell growth, differentiation, and survival pathways, whereas JNK and p38 are activated by inflammatory cytokines and various cell stresses and are involved in inflammation, apoptosis and oncotic cell death (151). In studies presented here, there were no consistent changes in phosphorylation of JNK by any treatment (Figure 9A). Furthermore, JNK inhibition had no effect on the cytotoxicity of any treatment, suggesting that JNK does not play a role in the cytotoxic interaction of HX and EL.

Interestingly, there was a high basal level of p-ERK that was reduced by EL. HX increased p-ERK, but this was also reduced by cotreatment with EL (Figure 8A). This is consistent with a report in which EL reduced p-ERK in endothelial cells (138). Inhibition of ERK enhanced cell death from EL alone (Figure 9A). This suggests that ERK plays a protective role, and that EL-mediated reduction in ERK phosphorylation can contribute to EL-induced cell death. ERK inhibition had no effect on HX/EL-induced cell death, which suggests that during HX, EL-mediated effects on ERK are less critical to cell death. ERK signaling protects cortical neurons from HX-induced apoptosis by inhibiting Bad and releasing the anti-apoptotic protein Bcl-2 (83). Interestingly, ERK inhibition did not enhance the cytotoxicity of HX in Hepa1c1c7 cells (Figure 9A), which is consistent with the mode of cell death not being apoptotic.

HX and EL each increased activation of p38, and there was an additive increase in p-p38 due to cotreatment (Figure 8B). Depending on the concentration-response

relationship for p-p38-mediated events, it is possible that this additive increase in p-p38 is sufficient to alter downstream signaling to enhance cytotoxicity in HX/EL-cotreated cells. Inhibition of p38 attenuated the cytotoxicity HX/EL cotreatment, although it had no effect on the modest cytotoxicity of either HX or EL alone (Figure 9C). This suggests that p38 is important to the signaling in HX/EL-cotreated cells that leads to cell death, and that this role is unique compared to the mechanism of either insult alone.

One mechanism by which p38 might be involved in the interaction of HX/EL is through its ability to modulate the transactivation of HIF-1 α . p38 can directly phosphorylate HIF-1 α to stabilize its interaction with HIF-1 β or the interaction with transcriptional coactivators (121). Consistent with this hypothesis, p38 was necessary not only for cytotoxicity in HX/EL-cotreated cells, but also for the increase in BNIP3 mRNA (Figure 11B) and protein (Figure 12C) under these conditions.

HepaC4 cells are deficient in HIF-1 β /ARNT, thus they are deficient in HIF-1 α signaling and transactivation. HIF-1 β expression is required for the formation of the HIF-1 DNA binding complex (149), as well as for HIF-1 α -mediated transcription (20) in hepatoma cells. In HepaC4 cells, EL alone caused modest cytotoxicity (Figure 13) to a similar level as seen in Hepa1c1c7 cells (Figure 6B), indicating that the cytotoxicity of EL is not mediated through HIF-1 α signaling. Interestingly, HX alone did not cause any cytotoxicity in HepaC4 cells, and there was no increase in cell death upon HX/EL cotreatment. These data suggest that HIF signaling is required for the cytotoxic interaction of HX/EL. Furthermore, despite a modest increase in BNIP3 mRNA expression in both HX- and HX/EL-treated HepaC4 cells (Figure 14), there was no detectable BNIP3 protein. These data verify that HIF-1 α signaling is impaired in

HepaC4 cells. They also suggest that BNIP3 might have a causative role in the HX/EL cytotoxicity. The mechanism by which BNIP3 and Nix cause cell death depends on cell type and experimental conditions. For example, in primary mouse HPCs, HX-induced BNIP3 expression contributes to a mode of cell death that resembles oncotic necrosis and is independent of caspase activation and mitochondrial permeability transition (120). This is consistent with data presented in the current studies, as there was no evidence for a role of caspases or MPT (Figure 7). Furthermore, p38 signaling was required for HX-mediated BNIP3 expression and cell death of primary HPCs (120), which is also consistent with our results.

In Hepa1c1c7 cells, cotreatment with HX/EL enhanced lipid peroxidation compared to EL treatment alone, and vitamin E reduced the lipid peroxidation (Table 3). Furthermore, vitamin E protected against the cytotoxicity from HX/EL exposure (Figure 15A), suggesting that lipid peroxidation plays a role in the interaction. Lipid peroxidation is an important mechanism of HPC death due to ischemia/reperfusion (124) and sepsis, conditions in which HX and EL are involved. Pharmacological inhibition of EL attenuated lipid peroxidation and liver injury in both mouse (124) and rat (129) models of I-R.

There was no measurable increase in ROS production (DCF fluorescence) due to any treatment in this system (Figure 16B). This is in contrast with previous studies in which HX increased ROS production from HepG2 and Hep3B hepatocellular carcinoma cells (15). EL is associated with ROS production in A549 lung epithelial cells (46). One potential reason for the lack of increase in ROS production is that hepatomas have inherently higher levels of ROS than normal HPCs (160). This raises a question about

the source of radicals for initiation of lipid peroxidation in this model, which is not known. Others have demonstrated that HX-induced ROS can activate p38 in various cell types (23, 120), but this does not appear to be the case in Hepa1c1c7 cells in this study, since no ROS were detected. Since vitamin E did not attenuate p38 activation (Figure 15B), radicals involved in lipid peroxidation do not appear to contribute to p38 activation. However, inhibition of p38 signaling attenuated the HX/EL-mediated increase in MDA concentration (Table 3), suggesting that p38 might contribute to cell death through lipid peroxidation in addition to its role in enhancing HIF-1 α -mediated gene transcription.

In HepaC4 cells, the basal MDA concentration was greater than in Hepa1c1c7 cells, but this apparent difference was not statistically significant. MDA concentration was significantly greater in HX-treated HepaC4 cells than in Hepa1c1c7 cells; however, there was no difference in MDA concentration caused by HX/EL cotreatment between Hepa1c1c7 and HepaC4 cells (Table 3). This indicates that HX enhancement of EL-induced lipid peroxidation is not mediated through HIF-1 α signaling.

Based on our results, a working hypothesis for the mechanism by which HX and EL interact to cause HPC death is presented. HX and EL cotreatment results in early activation of p38 and accumulation of HIF-1 α protein. P38 contributes to the transactivation of HIF-1 α and thereby to the expression of cell death factors such as BNIP3 in HX/EL-cotreated cells. EL-mediated lipid peroxidation also contributes to cell death, and HX enhances this response by a mechanism that depends at least in part on p38. These data offer insight into the mechanism by which HX and EL released by activated PMNs synergize in contributing to cell death. Understanding the intracellular

signaling that results in HPC death is crucial to developing treatments to prevent liver failure in I-R, sepsis and DILI.

CHAPTER 3

**Other pathways investigated while exploring the mechanism of the cytotoxic
interaction of HX/EL in Hepa1c1c7 cells**

3.1 Abstract

Cotreatment of Hepa1c1c7 cells with HX and EL resulted in synergistic cell death dependent on p38, HIF-1 α and lipid peroxidation (Chapter 2). However, a variety of other pathways have been implicated in either HX- or EL-mediated cell death alone. These include oxidative stress, intracellular calcium and NF- κ B-mediated gene transcription, which were investigated in HX/EL-cotreated cells. We also examined the role of non-hypoxic HIF-1 α activation via cobaltous chloride (CoCl₂) and DFX cotreatment with EL. We investigated activating transcription factor 2 (ATF2), a transcription factor activated by p38. Finally we measured cyclin D1, a gene involved in cell cycle regulation.

3.2 Introduction

HX-induced cell death is a well-studied process, and many pathways leading to cell death have been implicated in various cell types in the literature. Additionally EL-induced cell signaling and cell death is well characterized, and many pathways are activated by EL in various cell types. Interestingly, there is significant overlap in the pathways activated by HX and EL, which are summarized in Table 2.

One commonly identified target of HX and EL is the mitochondrial ETC. The mechanism by which HX perturbs the ETC and how it is involved in HX-induced cell death is described in detail in Section 1.2.4. The role of the ETC and ROS in EL-induced cell death is described in Section 1.3.3.

Another source of ROS is xanthine oxidase (XO), which catalyzes the oxidation of hypoxanthine to xanthine and uric acid, generating H_2O_2 and $\text{O}_2^{\bullet-}$ as products of the process. EL reversibly converted xanthine dehydrogenase (XD) to XO in pulmonary artery endothelial cells and in a cell-free system. The enhanced XO enzyme activity increased ROS generation, and inhibition of XO by allopurinol or its metabolite oxypurinol prevented ROS generation and EL-mediated cell death (135, 176). Interestingly, HX can also convert XD to XO to increase XO activity and ROS generation (126). Inhibition of XO with BOF-4272, allopurinol or oxypurinol reduced ROS production and prevented cell death in HPCs exposed to HX (88).

There is also evidence that both HX and EL can regulate NF- κ B signaling. EL activated NF- κ B in lung epithelial cells, and pharmacologic inhibition of NF- κ B prevented EL-induced apoptosis (167). NF- κ B signaling increased p53 activation,

which led to the expression of pro-apoptotic proteins PUMA and Bax. PUMA and Bax cause MPTP and activation of caspase 3-induced apoptosis.

HX activates NF- κ B signaling in PMNs (174), macrophages (105) and other cells. In some cases, HX-induced ROS activate NF- κ B, which enhances transcription of HIF-1 α (174) and other inflammatory genes, such as TNF α , IL-6 and MIP-2 (81, 105). Finally, HX caused NF- κ B-dependent apoptosis in Raw 264.7 macrophages (47). As presented in Section 2.4, EL caused concentration-dependent caspase 3/7 activation which was not enhanced by cotreatment with HX, and caspase inhibition failed to attenuate the cytotoxic HX/EL interaction, suggesting that there is no role for apoptosis in the interaction (Figure 8). It is, however, possible that NF- κ B participates in the interaction of HX/EL independently of apoptosis.

We also investigated activating transcription factor-2 (ATF2), which is phosphorylated and activated by JNK and p38 (12). p38 activation was increased by HX/EL cotreatment, and p38 inhibition protected cells from HX/EL-induced cell death (Figure 9Figure 10). ATF2 controls a variety of downstream genes, most notably those that regulate cell cycle progression and apoptosis (140).

The purpose of this chapter is to illustrate various pathways not included in Chapter 2 that were investigated while studying the mechanism of the cytotoxic interaction of HX/EL in Hepa1c1c7 cells. We hypothesized that ROS, NF- κ B and ATF2 play a role in HX/EL-induced cell death.

3.3 Materials and Methods

Cell Culture and Cytotoxicity Assessment

Please refer to Section 2.3 for information on this topic. For cell treatments, serum-free DMEM was placed in either an oxygen replete (OxR, 20.5% O₂) incubator or hypoxia (HX, 2% O₂) incubator overnight in order to equilibrate to the desired pO₂.

Materials

Unless otherwise noted, all cell culture materials were purchased from Invitrogen (Carlsbad, CA). In some studies, Hepa1c1c7 cells were pretreated with the following agents: 4-OH Tempo, allopurinol, 1,2-Bis(2-aminophenoxy)ethane-N,N,N',N'-tetraacetic acid tetrakis (acetoxymethyl ester) (BAPTA-AM), CoCl₂, DFX (Sigma Aldrich, St. Louis, MO), (E)-2-Fluoro-4'-methoxystilbene (NF-κB activation inhibitor) and caffeic acid phenylethyl ester (CAPE) (EMD Biosciences, San Diego, CA). The NF-κB activation inhibitor is a cell-permeable resveratrol analog shown to inhibit TNFα-induced NF-κB reporter activity in HEK cells with an IC₅₀ of 0.15 μM. A concentration of 50 μM was chosen because it was non-toxic to Hepa1c1c7 cells. The specific target of this molecule is not known. CAPE is a specific inhibitor of NF-κB activation, and cells were pretreated for 2 hrs with 50 μM CAPE, a concentration shown to inhibit NF-κB activation in HepG2 cells (86). NF-κB activity was not assessed in Hepa1c1c7 cells after treatment to determine the efficacy of CAPE and the NF-κB activation inhibitor.

Xanthine Oxidase Enzyme Assay

Hepa1c1c7 cells were seeded into 6-well plates. Confluent cultures were washed twice with serum-free DMEM and treated with 0 or 7.5 U/mL EL in either OxR or HX conditions. After 16 hrs of treatment, FBS was added to the wells at a final concentration of 1% to neutralize EL activity. Cells were collected by scraping and centrifugation (2000 rpm, 3 mins). The cell pellet was sonicated (5s) in 100 mM Tris-HCl buffer containing HALT protease inhibitor (Thermo Scientific, Rockford, IL) then centrifuged (10,000 x g for 15 mins). The supernatant was assayed using the Xanthine Oxidase Assay Kit (Cayman Chemical Company, Ann Arbor, MI) per the manufacturer's instructions.

Western Analysis

Hepa1c1c7 cells were plated in 6-well plates. Upon reaching confluence, cells were washed twice with SF-DMEM, and whole cell extracts were collected as described in Section 2.3. Proteins (20 µg) were separated on 10% SDS gels then transferred to PVDF membranes. Membranes were blocked in 5% BSA in TBST, and then incubated overnight with phospho-ATF2 antibody (1:1000, Cell Signaling Technology, Beverly, MA) in 5% BSA in 0.1% TBST. Membranes were washed three times in 0.1% TBST then incubated for 1 hr in secondary goat anti-rabbit HRP conjugated antibody (1:5000, Santa Cruz Biotechnology, Santa Cruz, CA). HRP was detected with HyGlo Chemiluminescent HPR Antibody Detection Reagent and exposed to HyBlot CL Film (Denville Scientific, Metuchen, NJ). Membranes were stripped using Restore Western Blot Stripping Reagent (Thermo Scientific, Rockford, IL) and after blocking were re-probed for total ATF2 (1:1000, Cell Signaling Technology, Beverly, MA).

RNA Isolation and RT-PCR

RNA was extracted as described in Section 2.3. The expression of specific genes was analyzed using SYBR green (Applied Biosystems, Foster City, CA). Copy number was determined by comparison to standard curves of the respective genes. Expression level was normalized to the hypoxanthine guanine phosphoribosyl transferase (HPRT) gene. PCR primers were used as follows: mouse Cyclin D1: forward, 5'-attggtctttcattgggcaacggg-3' and reverse, 5'- ggccaattgggtgggaaagtcaa-3' and mouse PCNA: forward, 5'-aaagatgccgtcgggtgaatttc-3' and reverse, 5'-aatgtcccattgccagctctcc-3' (Integrated DNA Technologies, Coralville, IA).

Statistical Analysis

Unless otherwise noted, all data are expressed as mean \pm SEM. The results were analyzed using two- and three-way ANOVA as appropriate and Tukey's post hoc test to compare groups. $P < 0.05$ was of the criterion for significance.

3.4 Results

Role of ROS and XO in HX/EL-induced cell death

In Hepa1c1c7 cells, 7.5 U/mL EL caused modest cytotoxicity 24 hrs after treatment. HX (2% O₂ in the atmosphere) was not cytotoxic, however, HX enhanced the cytotoxicity of EL, and there was a significant interaction between treatments. Pretreatment with the superoxide dismutase inhibitor 4-OH Tempo (1 mM) did not protect Hepa1c1c7 cells from the cytotoxicity of EL or HX/EL cotreatment, and it enhanced the toxicity of HX alone (Figure 16A). This concentration of 4-OH Tempo has been demonstrated to attenuate oxidative stress and cell death in HepG2 cells (190). The production of H₂O₂ was assessed via DCF fluorescence. H₂O₂ production was not affected by EL, HX, or HX/EL cotreatment in Hepa1c1c7 cells (Figure 16B). To determine if there is a non-mitochondrial source of ROS generation during HX/EL cotreatment, the activity of XO was monitored 16 hrs after treatment. Both HX and EL increased XO enzyme activity, and there was an additive increase in XO activity in HX/EL-cotreated cells (Figure 16C). Cells were pretreated with the XO inhibitor allopurinol at a concentration (1 mM) demonstrated to inhibit XO activity in endothelial cells exposed to EL (134). XO inhibition did not attenuate the cytotoxicity of EL or HX alone, and it did not prevent the cytotoxic interaction of HX/EL (Figure 16D).

Role of intracellular calcium in HX/EL induced cell death

Cells were pretreated with the intracellular calcium chelator BAPTA-AM (10 μM) then exposed to EL, HX, or HX/EL cotreatment. This concentration of BAPTA-AM was

Figure 16: ROS and XO are not involved in the interaction of HX/EL. (A) Hepa1c1c7 cells were pretreated for 2 hrs with 4-OH Tempo (1mM), then treated with EL, HX or HX/EL, and cytotoxicity was assessed at 24 hrs. Data represent mean \pm SEM of four individual experiments performed in triplicate. (B) Hepa1c1c7 cells were loaded with 10 μ M DCFH-DA for 30 minutes, then washed and treated with EL, HX or HX/EL for 6 hrs, and DCF fluorescence was assessed. Data represent the mean \pm SD of two separate experiments performed in triplicate. (C) Whole cell lysates were assessed for XO enzyme activity 16 hrs after treatment. Data represent mean \pm SEM of seven individual experiments. (D) Cells were treated with allopurinol (1 mM) then treated with EL, HX or HX/EL and cytotoxicity was assessed at 24 hrs. Data represent mean \pm SEM of four separate experiments in triplicate. a: $p < 0.05$ versus 0 U/mL EL in OxR; b: $p < 0.05$ versus 0 U/mL EL in HX; c: $p < 0.05$ versus 7.5 U/mL EL in OxR; #: significant interaction between HX and EL (two-way ANOVA).

Figure 16

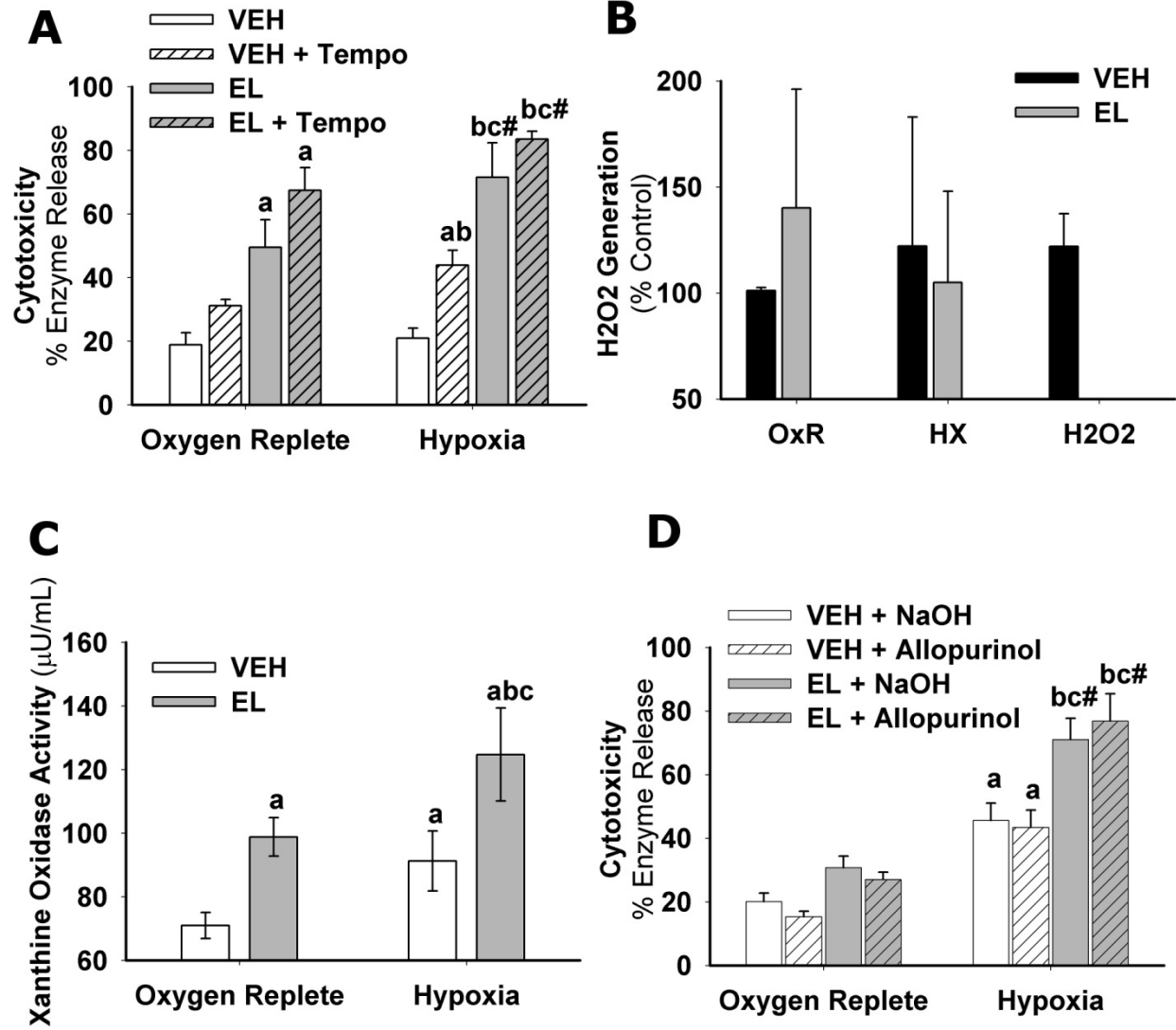
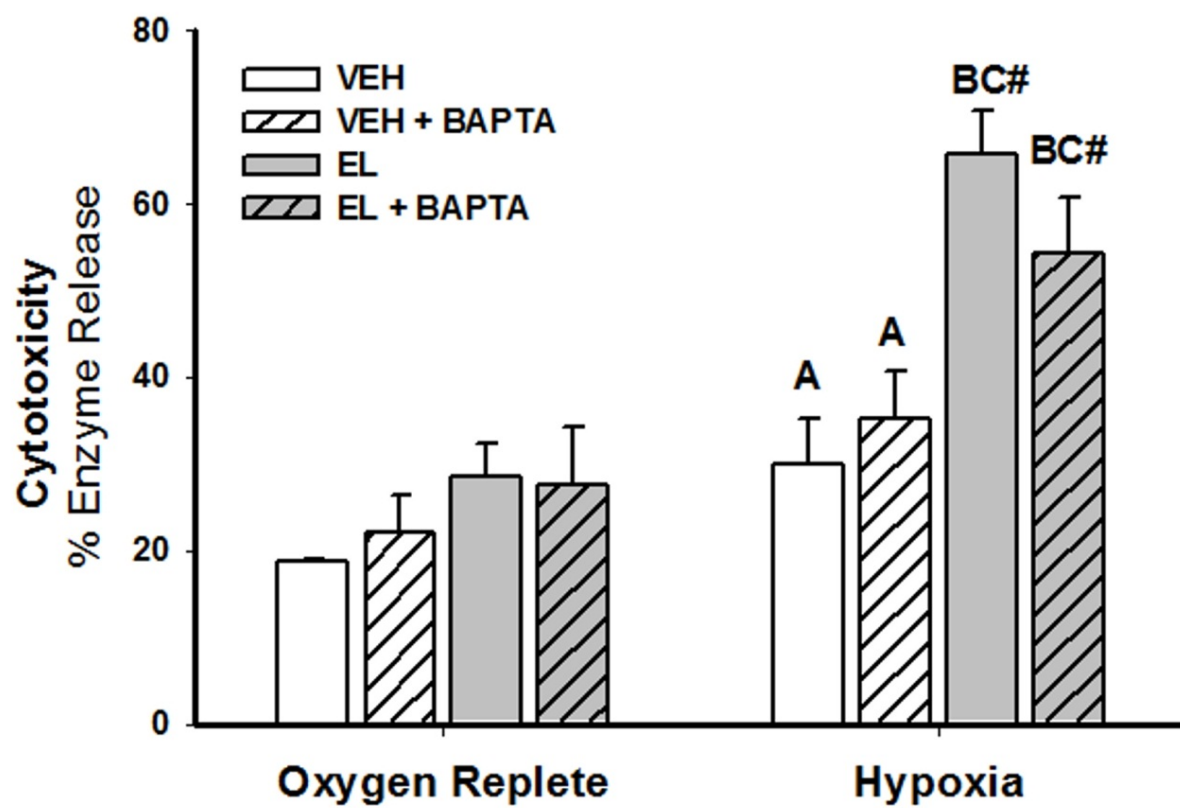


Figure 17: Intracellular calcium chelation does not protect cells from HX/EL-induced cytotoxicity. Cells were plated in 96-well plates, and treated with 10 μ M BAPTA for 2 hrs, then placed in an OxR or HX environment and treated with VEH or 7.5 U/mL EL, and cell death was assessed 24 hrs after treatment. Data represent mean \pm SEM of four separate experiments performed in triplicate. A: $p < 0.05$ versus 0 U/mL EL in OxR; B: $p < 0.05$ versus 0 U/mL EL in HX; C: $p < 0.05$ versus 7.5 U/mL EL in OxR; #: significant interaction between HX and EL (two-way ANOVA).

Figure 17



previously demonstrated to chelate intracellular calcium in HepG2 cells and protect them from bile acid-induced cell death (53). BAPTA-AM did not prevent cell death caused by HX/EL cotreatment (Figure 17)

Effect of HIF-1 α activation

Cobaltous chloride can activate HIF-1 α signaling in a variety of cell types and is often used as a “HX mimetic” in in vitro experiments (177). Exposure of Hepa1c1c7 cells to 100 μ M CoCl₂ failed to increase but rather attenuated the modest cytotoxicity caused by EL or HX, and completely protected cells from HX/EL cotreatment (Figure 18A). The iron chelator desferrioxamine (DFX) is also used as a HX mimetic; the depletion of iron inhibits PHD enzyme and allows HIF-1 α to accumulate in cells and become activated (62). Treatment with 200 μ M DFX had no effect on cytotoxicity caused by HX, EL or HX/EL cotreatment (Figure 18B). To ensure that HIF-1 α was activated by treatment with CoCl₂ and DFX, BNIP3 mRNA was measured 8 hrs after treatment. Indeed, CoCl₂ enhanced BNIP3 mRNA alone, and cotreatment with EL increased BNIP3 mRNA expression further. Conversely, DFX had no effect on BNIP3 mRNA, and it did not modulate BNIP3 expression when cotreated with EL (Figure 18C).

Role of NF- κ B in HX/EL cytotoxicity

Cells were pretreated with the NF- κ B activation inhibitor (50 μ M) for 2 hrs and then treated with EL, HX or HX/EL. Treatment with this inhibitor had no effect on the cytotoxicity caused by HX/EL (Figure 19A). A second inhibitor of NF- κ B signaling, CAPE (200 μ M) also had no effect on HX/EL-induced cell death (Figure 19B). In these

studies, HX did not enhance the cytotoxicity of EL to the same degree as in other sets of experiments, so it is difficult to make conclusions based on these studies. However, there was no evidence that NF- κ B inhibition by either the activation inhibitor or CAPE had any effect on the level of cytotoxicity of any of the treatment groups.

Role of cell cycle in HX/EL cytotoxicity

Due to evidence implicating p38 in HX/EL-induced cytotoxicity (Chapter 2, Figure 10), the activation of activating transcription factor-2 (ATF-2) was measured. ATF-2 is phosphorylated by p38 and has been implicated in cell death (12). Neither HX nor EL affected the basal level of p-ATF-2 in cells 2 or 4 hrs after treatment; however HX/EL cotreatment significantly reduced p-ATF2 (Figure 20A). Measurement of p-ATF2 and t-ATF2 intensity with densitometry confirmed these results (Figure 20B). ATF-2 can regulate the transcription of various genes involved in cell cycle progression, such as cyclin D1 (140). EL decreased cyclin D1 mRNA expression 8h after treatment by about 20%. HX alone had no effect on cyclin D1 expression, however HX/EL cotreatment significantly reduced cyclin D1 mRNA by 70% (Figure 20C).

Figure 18: Effect of HIF-1 α inducers in the cytotoxicity of HX/EL. (A) Cells were treated with CoCl₂ (100 μ M) in the presence of EL, HX or HX/EL, and cytotoxicity was assessed at 24 hrs. Data represent mean \pm SEM of three separate experiments performed in triplicate. (B) Cells were treated with DFX (1 mM), then EL, HX or HX/EL and cytotoxicity was assessed at 24 hrs. Data represent mean \pm SEM for four separate experiments performed in triplicate. (C) Cells were treated with VEH, CoCl₂ or DFX then treated with 0 or 7.5 U/mL EL for 8 hrs in OxR environment, after which the mRNA expression of BNIP3 and HPRT were assessed. Data represent the mean ratio of BNIP3:HPRT \pm SEM for three separate experiments. A: p<0.05 versus 0 U/mL EL in OxR; B: p<0.05 versus 0 U/mL EL in HX; C: p<0.05 versus 7.5 U/mL EL; #: significant interaction between HX and EL (two-way ANOVA). In panel C, A: p<0.05 versus VEH/VEH, B: p<0.05 versus 7.5 U/mL in VEH; C: p<0.05 versus VEH in CoCl₂; #: significant interaction between EL and CoCl₂ (two-way ANOVA).

Figure 18

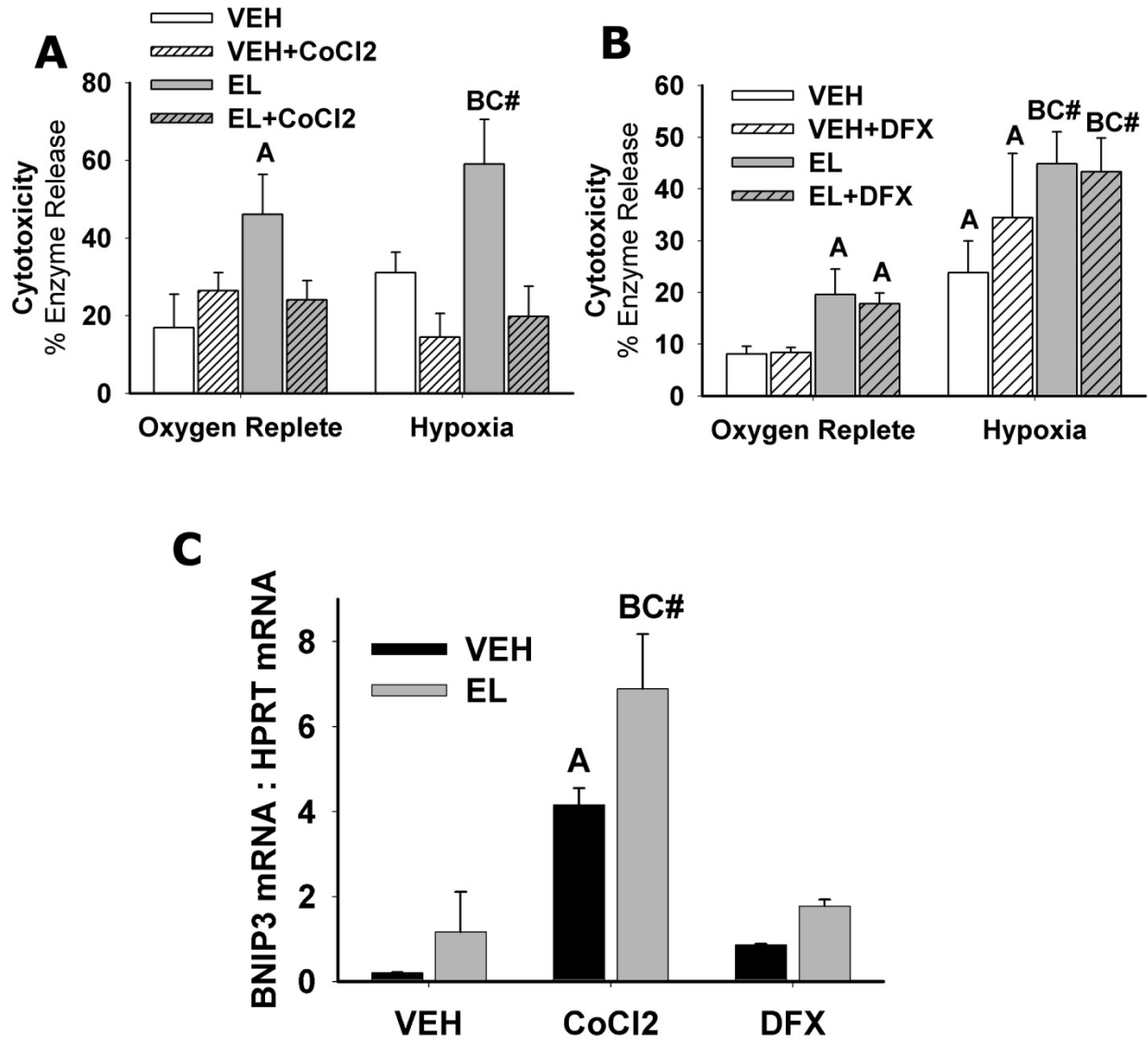


Figure 19: The role of NF- κ B in HX/EL-induced cytotoxicity. (A) Cells were pretreated with NF- κ B activation inhibitor (50 μ M) for 2 hrs then treated with EL, HX or HX/EL for 24 hrs, and cytotoxicity was assessed. (B) Cells were pretreated with CAPE (200 μ M) for 2 hrs, and cytotoxicity was assessed 24 hrs after treatment with EL, HX or HX/EL. Data represents mean \pm SEM for three separate experiments performed in triplicate. A: $p < 0.05$ versus 0 U/mL in OxR.

Figure 19

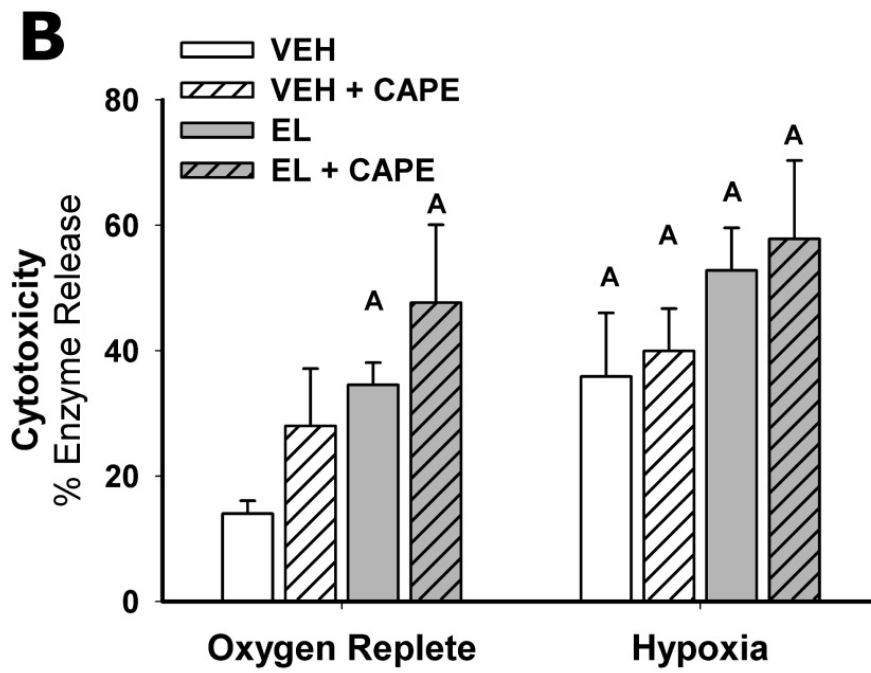
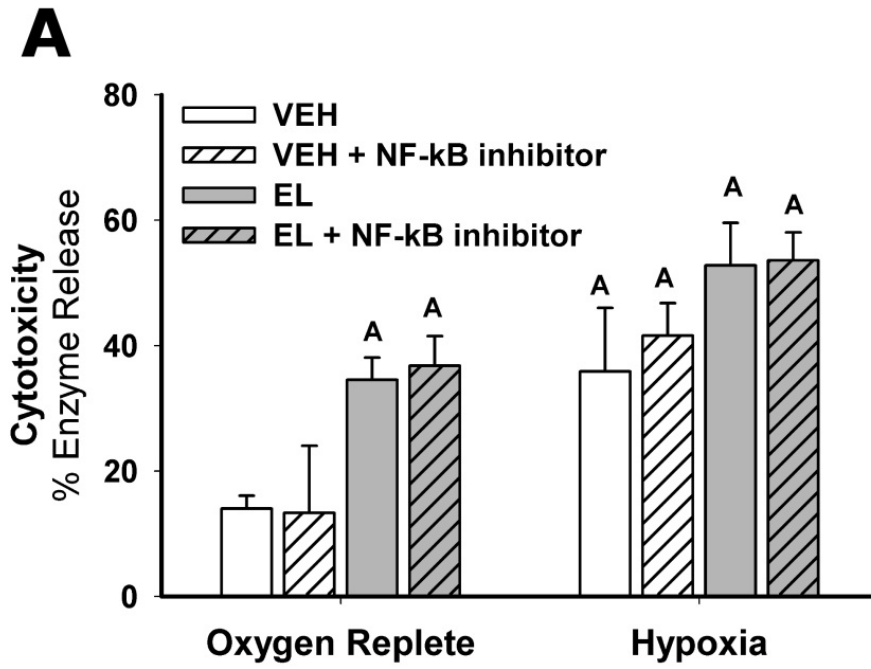
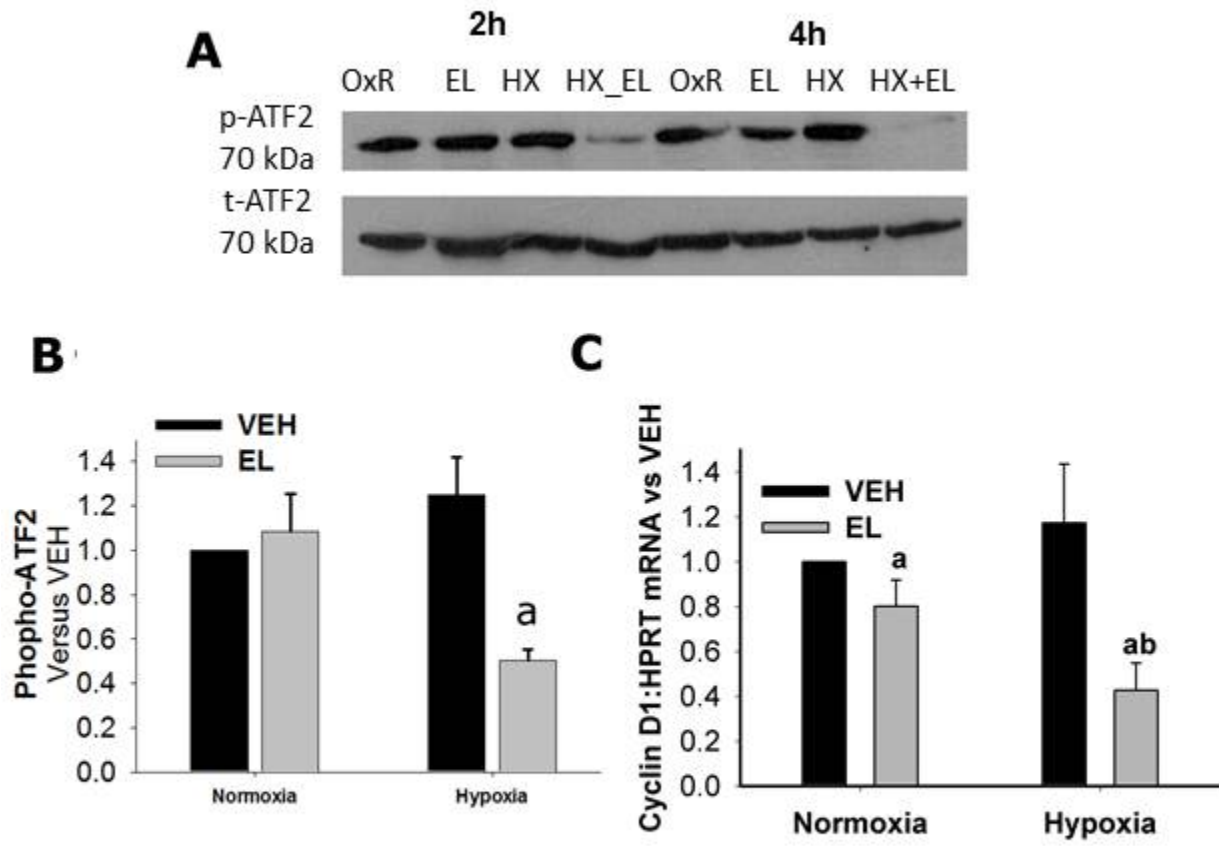


Figure 20: HX/EL cotreatment downregulates ATF2 activation and cyclin D1 expression. (A) Cells were treated for 2 and 4 hrs with EL, HX or HX/EL and whole cell lysates were probed for p-ATF2 and t-ATF2. (B) Quantification of p-ATF2 protein expression at 2h. Data represent the average p-ATF2:t-ATF2 \pm SEM of three separate experiments. A: $p < 0.05$ versus all other treatment groups. (C) Cells were treated with EL, HX or HX/EL for 8 hrs, and RNA was collected. Expression of Cyclin D1 and HPRT was measured. Data represent the average ratio of cyclin D1: HPRT \pm SEM of three separate experiments. A: $P < 0.05$ versus 0 U/mL in OxR; B: $P < 0.05$ versus 0 U/mL EL In HX.

Figure 20



3.5 Discussion

We have demonstrated that HX sensitizes Hepa1c1c7 cells to the cytotoxicity of EL, and that cotreatment with HX and EL results in a cytotoxic interaction that is dependent on p38 MAPK signaling, HIF-1 α , and lipid peroxidation (Chapter 2). In addition to the pathways mentioned, several other pathways to HX- or EL-induced cell death have been identified, including oxidative stress from ROS produced by mitochondria and XO, pro-apoptotic signaling induced by NF- κ B, calcium-induced cell death, and dysregulation of the cell cycle (Table 2).

Neither HX nor EL incited mitochondrial ROS production as measured by DCF fluorescence (Figure 16B). Also, the superoxide dismutase mimetic 4-OH Tempo did not prevent HX/EL-induced cell death (Figure 16A), suggesting that ROS are not involved. This is in contrast to previously published reports on the effects of EL and HX in other cell types.

It is well documented that EL incites ROS production in human fibroblasts (2), A549 respiratory epithelial cells (46) and bronchial epithelial cells (45). Furthermore, inhibition of the ETC with rotenone, the antioxidant DFX or radical scavenger dimethylthiourea attenuated ROS production and prevented EL-mediated cell death (45, 46). There is also extensive evidence that HX increases ROS production in many cell types (93), including the transformed liver cell lines Hep3B and HepG2 (15). A functional mitochondrial ETC is required for ROS generation during HX in HepG2 and Hep3B (15). Specifically, complex III of the ETC is the primary source of ROS (57, 95). Moreover, antioxidants protected both HepG2 and primary HPCs from HX-induced cell death (156). Thus, it is surprising that neither HX nor EL incited ROS in this system.

One potential reason for the lack of ROS production is the Warburg effect, in which many human cancer cell lines rely heavily on glycolysis, rather than oxidative phosphorylation, to produce ATP, even in the presence of adequate oxygen. Interestingly, hepatoma cells have an inherently higher level of ROS than normal hepatocytes (160). This suggests that it may be difficult to detect measurable changes in ROS production above this high baseline in Hepa1c1c7 cells. In a positive control experiment, the addition of 0.3% H₂O₂ to the cell culture well only increased DCF fluorescence by 1.25-fold (Figure 16B). Thus, because neither 2% O₂ nor 7.5 U/mL EL are greatly toxic on their own, the change in redox status may be too modest to detect, even in combination treatment. This is more likely than the Warburg effect, because others have successfully measured HX-induced ROS in Hepa1c1c7 (64) and HepG2 cells (16).

Another potential source of ROS is the activation of the enzyme XO. Both HX and EL increased XO activity compared to baseline, and there was an additive increase in XO activity in HX/EL-cotreated cells (Figure 16C). The mechanism by which HX enhances the activity of the enzyme is through conversion of XD to XO through reversible oxidation of sulfhydryl residues on the enzyme. EL can also convert XD to XO (88), and the mechanism is thought to be through proteolytic modification (135). Despite the increase in XO activity that was dependent on HX/EL cotreatment, XO inhibition with allopurinol did not prevent HX/EL-induced cell death (Figure 16D). These data suggest that XO activity does not contribute to cell death in this system, and is probably not an important source of ROS in this system. Another possible explanation

is that there is a limit in the availability of the substrate (xanthine) for the enzyme in the in vitro system, or that the stress of HX/EL cotreatment reduced xanthine production. Thus, perhaps XO was activated but did not have adequate substrate to catalyze into uric acid and produce ROS in the process.

To determine if HIF-1 α activation with nonhypoxic stimuli would interact with EL, Hepa1c1c7 cells were treated with either CoCl₂ or DFX and EL. CoCl₂ attenuated the cytotoxicity of EL and HX/EL cotreatment (Figure 18A), despite enhanced HIF-1 α activation, as marked by BNIP3 mRNA expression (Figure 18C). These data indicate that HIF-1 α activation by CoCl₂ is not sufficient for the interaction with EL, or that CoCl₂ has other HIF-1 α -independent effects in the cell. Consistent with our results, CoCl₂ has been reported to protect HepG2 cells (human hepatoma) from apoptosis induced by *tert*-butyl hydroperoxide (136).

The iron chelator DFX was also used to activate HIF-1 α . Iron chelation by DFX is thought to inhibit PHD and FIH activation, allowing HIF-1 α to accumulate and become transactivated. However, we saw no increase in BNIP3 mRNA expression with DFX treatment (Figure 18C) suggesting that the concentration used was not sufficient for HIF-1 α activation in Hepa1c1c7 cells. Furthermore, it did not interact with EL to cause cell death and had no effect on HX/EL-induced cell death. Interestingly, DFX has also been used extensively as an antioxidant, and has been shown to protect cells from EL-induced ROS and cell death (46). This supports other evidence that ROS are not involved in the mechanism of HX/EL-induced cell death (Figure 16).

We have demonstrated that HIF-1 α signaling is required for the interaction of HX/EL (Chapter 2, Figure 13). The data presented here appear to be in conflict with those findings, since neither method of HIF-1 α activation enhanced the cytotoxicity of EL, whereas HX does. However, it is important to point out that both CoCl₂ and DFX are not specific for HIF-1 α , and may have a variety of off-target effects. It is also possible that direct HIF-1 α activation is not sufficient for the interaction with EL, and that HX is activating other pathways in cells (such as MAPK and lipid peroxidation, as mentioned in Chapter 2), that are required in addition to HIF-1 α activation.

Inhibition of NF- κ B signaling with two different inhibitors had no effect on HX/EL-induced cytotoxicity (Figure 19), suggesting that it is not required for the interaction. Furthermore, chelation of intracellular calcium did not attenuate the interaction (Figure 17), indicating that calcium-activated cell death pathways do not contribute to cell death. It has been reported that calcium-dependent calpain activation can contribute to HX-mediated necrosis of HepG2 cells (94), but there is no evidence that calcium signaling plays a role in EL-induced cell death.

We also assessed activation of the transcription factor ATF2, which is normally activated downstream of p38 signaling. Interestingly, HX/EL cotreatment significantly decreased basal p-ATF2 levels, whereas neither HX nor EL alone had any effect on p-ATF2 (Figure 20B). The mechanism by which HX/EL cotreatment drastically reduces p-ATF2 is not known and requires further study. There is one report in which ERK can upregulate ATF2 activation after tolfenamic acid treatment in human colorectal cancer cells, leading to apoptosis (103). It is possible that the reduction in p-ERK caused by

HX/EL cotreatment (See Chapter 2, Figure 8) results in reduced ATF2, however this remains to be investigated. Furthermore, it remains to be seen if downregulation of ATF2 contributes to HX/EL-induced cell death, or if it is an epiphenomenon.

ATF2 upregulates the expression of a variety of cell cycle regulatory proteins, including cyclin D1. HX/EL-cotreatment reduced cyclin D1 mRNA expression 8 hrs after treatment (Figure 20C). Cyclin D1 plays a key role in the progression of the cell cycle by phosphorylating retinoblastoma protein and triggering HPCs to transition from G1 to S phase of the cell cycle. In vivo, disruption of cyclin D1 signaling can impair tissue repair following toxic insult or other injury, and can contribute to the development of liver failure (39). In vitro, downregulation of cyclin D1 expression induces cell cycle arrest and initiates apoptosis of the human hepatomas, HepG2 and Hep3B (127). Thus, one potential component of the mechanism of cell death by HX/EL might be inhibition of the cell cycle. These data suggest that HX/EL cotreatment might induce cell cycle arrest in Hepa1c1c7 cells via downregulation of cyclin D1 that can contribute to cell death signaling. Furthermore, this raises the possibility that HX and EL exposure in vivo might downregulate cyclin D1 in HPCs and thereby inhibit liver regeneration in models of injury in which HX and PMNs play a role.

As described in Section 1.2.4, HX can inhibit cell cycle progression through a variety of pathways. HIF-1 α directs transcription of the cyclin-dependent kinase inhibitors p21 and p27 (52). Cyclin D1 mRNA and protein expression are downregulated by HX in PC12 cells (23). Furthermore, HIF-1 α negatively regulates cyclin D1 expression; it binds to two HREs in the cyclin D1 promoter, and recruits histone deacetylase 7 to repress transcription of the gene (183). Thus, it is possible that the

downregulation of cyclin D1 caused by HX/EL cotreatment is a result of increased HIF-1 α activation, not downregulation of ATF2; this remains to be investigated.

To summarize, many of the pathways that have been implicated in HX- or EL-induced cell death alone were also investigated in this HX/EL-cotreatment model. Contrary to previously published reports, we observed no increases in HX- or EL-induced ROS production, and the water soluble antioxidants 4-OH Tempo (Figure 16A) and DFX (Figure 18B) did not protect cells from HX/EL cotreatment. These data suggest that ROS are either not produced or are undetectable, and that they do not play a role in cell death in this system. Intracellular calcium (Figure 17) and NF- κ B signaling (Figure 19) do not appear to contribute to cell death in this model. Interestingly, activation of HIF-1 α by treatment with CoCl₂ did not interact with EL to cause cell death, and CoCl₂ actually protected cells from HX/EL cotreatment. These data suggest that stabilization of HIF-1 α through non-hypoxic stimuli is not sufficient for an interaction with EL, and that HX contributes to cell death through additional pathways. HX/EL cotreatment reduced the activation of p-ATF2 (Figure 20A), however it is not known if this is involved in cell death. Finally, HX/EL cotreatment resulted in downregulation of cyclin D1 (Figure 20C), which may contribute to cell cycle arrest and subsequent cell death; however, this remains to be tested.

CHAPTER 4

Sparkenbaugh, E.M., Saini, Y., Greenwood, K.K., LaPres, J.J., Luyendyk, L.P., Copple, B.L., Maddox, J.F., Ganey, P.E., and Roth, R.A. (2011). The Role of Hypoxia Inducible Factor-1 alpha (HIF-1 α) in Acetaminophen Hepatotoxicity. *J Pharm Exp Ther.* 338(2)1-11.

4.1 Abstract

Hypoxia inducible factor-1 alpha (HIF-1 α) is a critical transcription factor that controls oxygen homeostasis in response to HX, inflammation and oxidative stress. HIF has been implicated in the pathogenesis of liver injury in which these events play a role, including APAP overdose, which is the leading cause of acute liver failure in the US. APAP overdose has been reported to activate HIF-1 α in mouse livers and isolated HPC downstream of oxidative stress. HIF-1 α signaling controls many factors that contribute to APAP hepatotoxicity, including mitochondrial cell death, inflammation, and hemostasis. Therefore, we tested the hypothesis that HIF-1 α contributes to APAP hepatotoxicity. Conditional HIF-1 α deletion was generated in mice using an inducible Cre-lox system. Control (HIF-1 α -sufficient) mice developed severe liver injury 6 and 24h after APAP overdose (400 mg/kg). HIF-1 α -deficient mice were protected from APAP hepatotoxicity at 6 hrs, but developed severe liver injury by 24 hrs, suggesting that HIF-1 α is involved in the early stage of APAP toxicity. In further studies, HIF-1 α -deficient mice had attenuated thrombin generation and reduced plasminogen activator inhibitor-1 (PAI-1) production compared to control mice, indicating that HIF-1 α signaling contributes to hemostasis in APAP hepatotoxicity. Finally, HIF-1 α -deficient animals had decreased hepatic PMN accumulation and plasma concentrations of IL-6, IL-8/KC and regulated upon activation normal T cell expressed and secreted (RANTES) compared to control mice, suggesting an altered inflammatory response. HIF-1 α contributes to hemostasis, sterile inflammation, and early hepatocellular necrosis during the pathogenesis of APAP toxicity.

4.2 Introduction

Hypoxia inducible factor (HIF) is the master regulator of oxygen homeostasis. It controls the expression of a large battery of genes involved in angiogenesis, erythropoiesis, glycolysis, inflammation, and cell death (102). As described in Section 1.2.3, the expression and activity of HIF-1 α is controlled at the level of protein stability. HIF-1 α expression and activation are also regulated by oxidative stress (95), inflammatory cytokines (180) and thrombin (54). HIF-regulated genes include PAI-1, VEGF, TNF α , IL-1 β , and cell death proteins such as BNIP3 and Nix (102, 123). Due to the many factors that can modulate HIF induction and the variety of downstream signaling targets, HIF has been identified as a key regulator of a generalized stress response (77).

HIF-1 α has been implicated in hepatocyte death in models of liver injury that have an inflammatory or oxidative stress component, such as sepsis (131), I-R (34), alcoholic liver disease (108) and fibrosis (28). Oxidative stress and mitochondrial dysfunction play a key role in APAP-induced liver injury. APAP overdose is the leading cause of drug-induced liver failure in the United States (104). At toxic doses, APAP is bioactivated by cytochrome P450 enzymes to *n*-acetyl-*p*-benzoquinone imine (NAPQI), which is reactive, depletes GSH and binds covalently to intracellular proteins, leading to mitochondrial dysfunction, production of ROS and hepatocellular necrosis (85).

Recent reports by James *et al.* (77) indicated that APAP overdose causes nuclear accumulation of HIF-1 α in mouse livers as early as 1h after treatment, which is before the onset of liver HX and hepatocellular injury. Furthermore, N-acetyl cysteine, which inactivates NAPQI (77) or CsA, which prevents MPT, prevented HIF-1 α

accumulation (17). Taken together, these data suggest that mitochondrial dysfunction and ROS are important contributors to early HIF-1 α stabilization in APAP overdose.

In addition to cellular necrosis caused by oxidative stress and mitochondrial dysfunction, APAP hepatotoxicity is also associated with disturbances to the hemostatic system in humans (79) and experimental animals (50). APAP overdose caused tissue factor-dependent activation of the coagulation system in mice, elevated circulating concentration of PAI-1 and fibrin deposition in liver (50). Inhibition of coagulation system activation through genetic or pharmacologic methods attenuated APAP-induced liver injury, suggesting a role for thrombin and the coagulation system in the pathogenesis. During injury progression, fibrin deposition can contribute to tissue ischemia and HX, which might enhance HIF-1 α accumulation above that caused by oxidative stress alone.

APAP hepatotoxicity is accompanied by a sterile inflammatory response (185), and concurrent inflammation can sensitize mice to APAP-induced liver injury (114). Mediators released from necrotic HPCs activate Kupffer cells (KCs), recruit and activate PMNs, and consequently produce cytokines that influence APAP-induced hepatocellular injury (31, 78). The role of PMNs in APAP hepatotoxicity remains controversial, with evidence both for and against a contribution of PMNs to injury progression (69). HIF-1 α plays a critical role in PMN function; it influences phagocytosis, motility, invasiveness, and apoptosis (32, 132, 180, 181). HIF-1 α also contributes to inflammatory cytokine production (191). Therefore, HIF-1 α might participate in the inflammatory response that accompanies APAP-induced liver injury.

In addition to the many factors mentioned above that associate APAP-induced liver injury with HX signaling, HIF-1 α can contribute directly to cell death of HPCs by upregulation of cell death genes. Nonetheless, it is currently unknown if HIF-1 α is involved causally in APAP-induced liver injury. To test the hypothesis that HIF-1 α contributes to the pathogenesis of APAP-induced liver injury, conditional HIF-1 α -deficient animals were generated and the role of HIF-1 α in APAP-induced hepatotoxicity, disruption of hemostasis, and inflammation was evaluated.

4.3 Materials and Methods

Materials

Unless otherwise stated, all reagents were purchased from Sigma Chemical Company (St. Louis, MO).

Generation of Conditional HIF-1 α -Deficient Animals

HIF-1 $\alpha^{\text{flox/flox}}$ mice (146) were a gift from Randall Johnson (University of California, San Diego), and UBC-Cre-ERT2 $^{+/-}$ mice were purchased from Jackson Laboratories (Bar Harbor, ME). The Cre-ERT2 is regulated by the ubiquitin C promoter and is expressed in virtually all cell types. Cre-ERT2 is a fusion protein composed of Cre recombinase and a mutated estrogen receptor that is selectively activated and targeted to the nucleus by (Z)-1-(p-Dimethylaminoethoxyphenyl)-1,2-diphenyl-1-butene, *trans*-2-[4-(1,2-Diphenyl-1-butenyl)phenoxy]-N,N-dimethylethylamine [Tamoxifen (TAM)] but not estrogen (145). C57Bl/6 HIF-1 $\alpha^{\text{flox/flox}}$ and UBC-Cre-ERT2 $^{+/-}$ transgenic mice were mated to generate UBC-Cre-ERT2 $^{+/-}$ /HIF-1 $\alpha^{\text{flox/flox}}$ mice capable of conditional recombination in the floxed HIF-1 α gene when treated with TAM. Male UBC-Cre-ERT2 $^{+/-}$ /HIF-1 $\alpha^{\text{flox/flox}}$ mice (4-5 weeks old) were treated once per day for 5 days with 200 $\mu\text{g/g}$ body weight TAM in corn oil (OIL) vehicle by oral gavage (145). TAM-treated UBC-Cre-ERT2 $^{+/-}$ /HIF-1 $\alpha^{\text{flox/flox}}$ mice were HIF-1 α deficient (denoted as HIF-1 $\alpha^{\Delta/\Delta}$) and OIL-treated animals were HIF-1 α sufficient (denoted as HIF-1 $\alpha^{+fl/+fl}$)

(Figure 21A). UBC-Cre-ERT2^{-/-}/HIF-1 α ^{flox/flox} littermate controls were treated with OIL or TAM to evaluate potential effects of TAM on APAP metabolism. Animals kept in a 12-hour light/dark cycle were fed a standard Rodent chow/Tek 8640 (Harlan Teklad; Madison, WI) and allowed access to water *ad libitum*. All procedures were performed according to the guidelines of the American Association for Laboratory Animal Science and the University Laboratory Animal Research Unit at Michigan State University.

Experimental Protocol

Eleven or twenty-one days after OIL or TAM administration, mice were fasted overnight then given 400 mg/kg APAP or saline (SAL) vehicle via intraperitoneal (i.p.) injection, and food was returned. Mice were anesthetized 2, 6 or 24 hours after APAP with sodium pentobarbital (50 mg/kg, i.p.), and blood was collected from the vena cava into a syringe containing sodium citrate (final concentration 0.76%) for preparation of plasma. The left lateral liver lobe was fixed in 10% formalin and paraffin-blocked for evaluation of histopathology. The left medial lobe was snap frozen in liquid nitrogen for protein, DNA and RNA analysis. The right medial lobe was embedded in Tissue-Tek O.C.T. compound and frozen in liquid nitrogen-cooled isopentane for immunohistochemical analyses.

Genotyping and Real-time PCR

Genotyping of mice was performed for the Cre transgene, HIF-1 α , and HIF-1 α ^{flox/flox} using previously published primer sequences (147). Genomic DNA was extracted from tail clippings using the Direct PCR extraction system (Viagen Biotech,

Los Angeles, CA) and was used to quantify the Cre transgene. Genotyping of livers from HIF-1 α ^{+fl/+fl} and HIF-1 α ^{Δ/Δ} mice was performed to determine the recombination efficiency. Genomic DNA was extracted using the Extract-N-Amp system (Sigma Aldrich, St. Louis, MO) per the manufacturer's instructions. PCR conditions were standardized for all alleles: denaturation at 94 °C for 3 min; 38 cycles of denaturation at 94 °C for 45 s, annealing at 60 °C for 45 s, and polymerization at 72 °C for 60 s followed by a 7-min extension at 72 °C.

Gene Expression Analysis

Liver tissue (50 mg) was homogenized in 1 mL of TRI reagent (Sigma Aldrich, St. Louis, MO) using a Precellys 24 Tissue Homogenizer (Cayman Chemicals, Ann Arbor, MI), and RNA was extracted. Total RNA was quantified spectrophotometrically using the NanoDrop 2000 (Thermo Fisher Scientific, Louisville, CO). Total RNA (1 μ g) was reverse-transcribed using iScript cDNA synthesis kit (Bio-Rad, Hercules, CA). The expression level of PAI-1, BNIP3 and HIF-1 α was analyzed by qRT-PCR using SYBR green (Applied Biosystems, Foster City, CA). Copy number was determined by comparison with standard curves of the respective genes. Expression level was normalized to the hypoxanthine guanine phosphoribosyl transferase (*HPRT*) gene. PCR primers were used as follows: mouse BNIP3: forward, 5'- tgcaggcacctttatcactctgct-3' and reverse 5'-cgcccgatttaagcagctttggat-3'; mouse Cre Transgene: forward, 5'-tgccacgaccaagtgcagcaatg-3' and reverse, 5'-agagacggaaatccatcgctcg-3'; mouse HIF-1 α : forward, 5'-cgtgtgagaaaacttctggatg-3' and reverse, 5'-catgtcgccgctcatctgtta-3'; and mouse HIF-1 α (flox): forward, 5'-ttggggatgaaaacatctgc-3' and reverse, 5'-

catgtcgccgtcatctgtta-3'; and HPRT: forward, 5'-aggagtcctggtgatgttgccagt-3' and reverse, 5'-gggacgcagcaactgacatttcta-3'.

Assessment of Hepatocellular Injury and Liver GSH Concentration

Hepatocellular injury was estimated from increases in plasma alanine aminotransferase (ALT) activity and from histopathologic evaluation of fixed tissue. ALT activity was determined spectrophotometrically using Infinity ALT Liquid Stable Reagent (Thermo Electron Corp; Louisville, CO). Paraffin sections of liver (5 μ m) were stained with hematoxylin-eosin and examined for evidence of hepatocellular necrosis. To measure GSH concentration, frozen liver samples (100 mg) were homogenized in 1 mL cold buffer (0.2 M 2-*N*-morpholino ethanesulfonic acid, 50 mM phosphate, and 1 mM EDTA; pH 6.0). Homogenates were spun at 10,000 x g for 15 minutes then deproteinated with metaphosphoric acid. Total hepatic GSH concentration was determined spectrophotometrically using a commercially available kit (Cayman Chemical Co.; Ann Arbor, MI).

Immunohistochemistry

Liver sections were stained immunohistochemically for HIF-1 α as described previously (147). Paraffin was removed from formalin-fixed liver sections (5 μ m) and endogenous peroxidase activity was quenched with 6% H₂O₂. Sections were probed with HIF-1 α antibody (1:500 dilution, NB100-479, Novus Biologicals; Littleton, CO), which was visualized with Rabbit Vector Elite ABC kit (Vector Laboratories; Burlingame, CA), and sections were counterstained with Nuclear Fast Red. The terminal

deoxynucleotidyl transferase-mediated dUTP nick-end labeling (TUNEL) assay was used to analyze DNA fragmentation. Liver sections were stained with the In Situ Cell Death Detection Kit, AP (Roche Diagnostics, Indianapolis, IN) per the manufacturer's instructions. Hepatic fibrin staining was performed as described previously (27). Dakocytomation rabbit anti-human/mouse fibrinogen (Dako North America; Carpinteria, CA) was the primary antibody, and a donkey anti-rabbit IgG conjugated to AlexaFluor 488 (Molecular Probes/Invitrogen; Carlsbad, CA) was used as the secondary antibody. Fibrin images were obtained with an Olympus IX71 inverted fluorescent microscope (Olympus, USA), and positive staining was quantified using Image J software (NIH; Bethesda, MD). Background staining in livers from SAL-treated mice was set as the threshold, and the percentage of pixels above threshold is presented. PMNs were stained as previously described (114), and PMN accumulation was quantified by counting the average number of PMNs in 20 randomly selected high-power fields (400x).

Detection of Bax

Frozen liver sections (5 μ m) were fixed in 4% paraformaldehyde for 30 minutes at room temperature. Fixed sections were washed 3 x 7 mins in phosphate buffered saline (PBS) and blocked in 10% donkey serum + 0.1% Triton X-100 (blocking buffer; BB) for 1 hour. Sections were incubated overnight at 4°C with the following primary antibodies [and their dilutions]: rabbit anti-Bax [1:200] (Cell Signaling Technology, Beverly, MA) and goat anti-cytochrome c oxidase subunit IV (Cox IV) [1:100] (Santa Cruz Biotechnology, Santa Cruz, CA) diluted in BB. After incubation, sections were washed 3 x 7 mins in PBS, blocked in BB for 1 hour, and washed 3 x 7 mins again.

Sections were incubated with donkey anti-rabbit Alexa Fluor 568 [1:1000] and donkey anti-goat Alexa Fluor 488 [1:1000] (Invitrogen, Carlsbad, CA) in BB, washed, then mounted with VectaShield Mounting Medium with DAPI (Vector Labs, Burlingame, CA). Slides were stored at -20°C prior to imaging.

Fluorescent slides were viewed with the Olympus FluoView 1000 confocal laser scanning microscope. Images were collected with Olympus FluoView 1000 software, version 2.0. Alexa Fluor 568 was detected with a 543 nm HeNeG laser with a BA 560-620 emission filter, and Alexa Fluor 488 was detected with a 488 nm Ar laser with a BA 505-525 emission filter. Images were scanned with sequential scan setting for the two lasers. A 60-X oil Plan/APO objective (NA 1.42) was used to acquire images. Five fields of view from each liver section were selected at random. Colocalization of Bax and Cox IV pixels was analyzed with Image J software (NIH, Bethesda, MD), and data are represented as the percentage of colocalized pixels in an image area.

Evaluation of Plasma and Intrahepatic Cytokine Concentrations

The plasma concentration of active PAI-1 was measured with a commercially available ELISA kit (Molecular Innovations; Novi, MI), following the manufacturer's instructions. The plasma concentrations of IFN γ , IL-1 β , IL-2, IL-4, IL-6, IL-10, IL-12 (p70), IL-8/KC, macrophage inflammatory protein (MIP)-1 α , RANTES, TNF- α , and VEGF were measured with a custom Milliplex MAP kit for mouse cytokines (Millipore Corporation; Billerica, MA) using the Bio-Plex 200 System (Bio-Rad Laboratories, Hercules, CA). For determination of hepatic cytokine concentrations, livers were homogenized in 0.1% Triton X-100 in PBS containing Halt Protease and Phosphatase

inhibitors (Thermo Fisher Scientific, Louisville, CO), and proteins were quantified by the BCA Assay. Concentrations of KC and RANTES were determined by ELISA (R&D Systems, Minneapolis, MN) and normalized to protein concentrations of the samples.

Statistical analyses

All data are represented as mean \pm SEM. Data which were not normally distributed were transformed via Box-cox power transformation. Two or three-way analysis of variance (ANOVA) was used as appropriate, and multiple comparisons were evaluated statistically with appropriate post-hoc tests. $P < 0.05$ was the criterion for significance.

4.4 Results

Effect of conditional deletion of HIF-1 α gene on liver HIF-1 α expression

Conditional HIF-1 α knockout mice were generated by mating HIF-1 $\alpha^{\text{flox/flox}}$ mice (146) with transgenic mice that express the Cre-recombinase transgene (145) under the control of the ubiquitin C promoter, and the HIF-1 α gene was inactivated upon TAM treatment (Figure 21A). Mice treated with TAM (HIF-1 $\alpha^{\Delta/\Delta}$ mice) displayed no obvious phenotypic differences compared to control animals. Expression of HIF-1 α protein in livers was evaluated immunohistochemically 2h after SAL or APAP treatment. SAL-treated HIF-1 $\alpha^{\text{+fl/+fl}}$ mice had minimal staining, whereas HIF-1 α staining was not observed in HIF-1 $\alpha^{\Delta/\Delta}$ mice (Figure 21B). APAP overdose increased hepatocellular HIF-1 α staining in HIF-1 $\alpha^{\text{+fl/+fl}}$ mice; the staining appeared to be cytoplasmic in most cells, with some nuclear staining. There was markedly less HIF-1 α staining in HIF-1 $\alpha^{\Delta/\Delta}$ mice treated with APAP, confirming successful deletion of HIF-1 α . There was significantly less expression of HIF-1 α mRNA in HIF-1 $\alpha^{\Delta/\Delta}$ mice compared to HIF-1 $\alpha^{\text{+fl/+fl}}$ controls (Table 4), demonstrating effective HIF-1 α deletion. At 24 hrs, APAP overdose increased expression of HIF-1 α mRNA at 24 hrs by 437-fold in HIF-1 $\alpha^{\text{+fl/+fl}}$. In HIF-1 $\alpha^{\Delta/\Delta}$ mice, there was a modest increase in HIF-1 α mRNA expression (by 26-fold) at 24 hrs. This supports previous evidence that APAP overdose caused HIF-1 α accumulation in mouse liver (17, 77).

Figure 21: Conditional HIF-1 α deletion in mice. (A) Five week old CRE-ERT2^(+/-) /HIF-1 α ^{flox/flox} mice were treated with OIL or 200 μ g/g TAM for five days to generate HIF-1 α ^{+fl/+fl} or HIF-1 α ^{Δ/Δ} mice. 21 days later, mice were treated with 400 mg/kg APAP or SAL intraperitoneally. Liver samples were taken 2 hrs after APAP administration. (B) Formalin-fixed livers were stained for HIF-1 α protein, which appears as dark brown stain. Arrows indicate positive staining. *For interpretation of the references to color in this and all other figures, the reader is referred to the electronic version of this dissertation.*

Figure 21

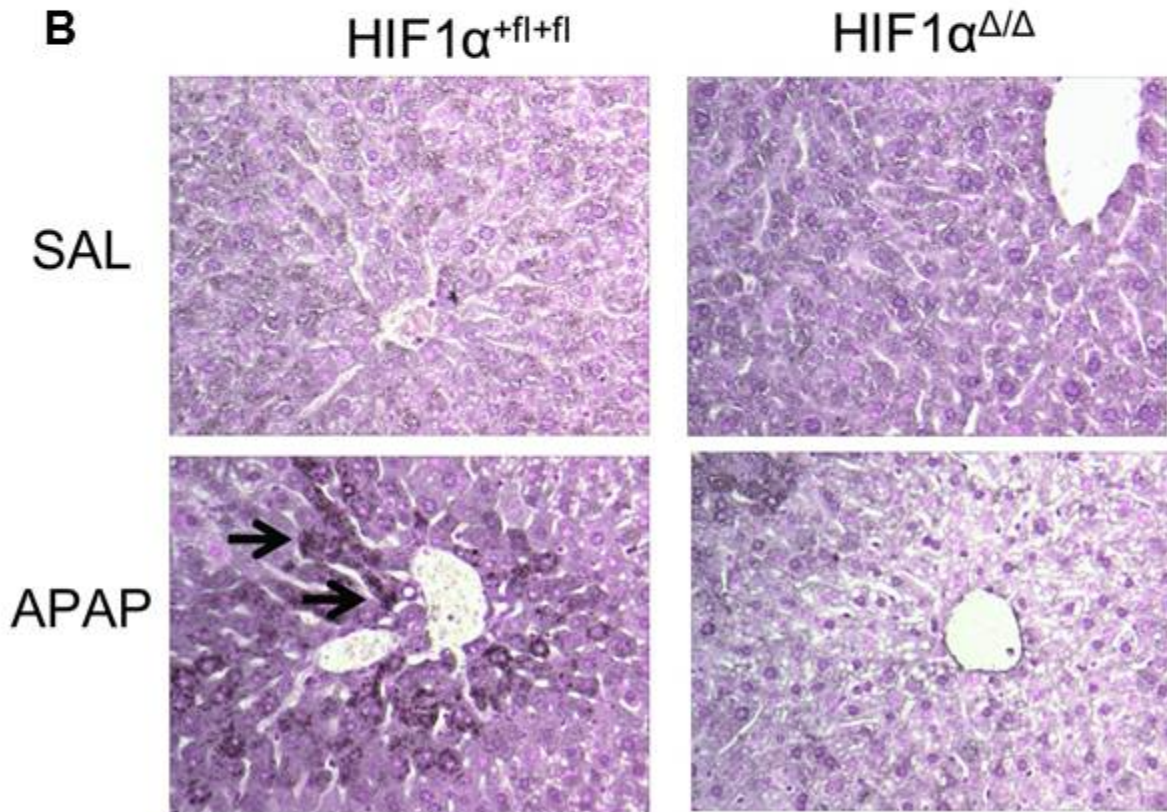
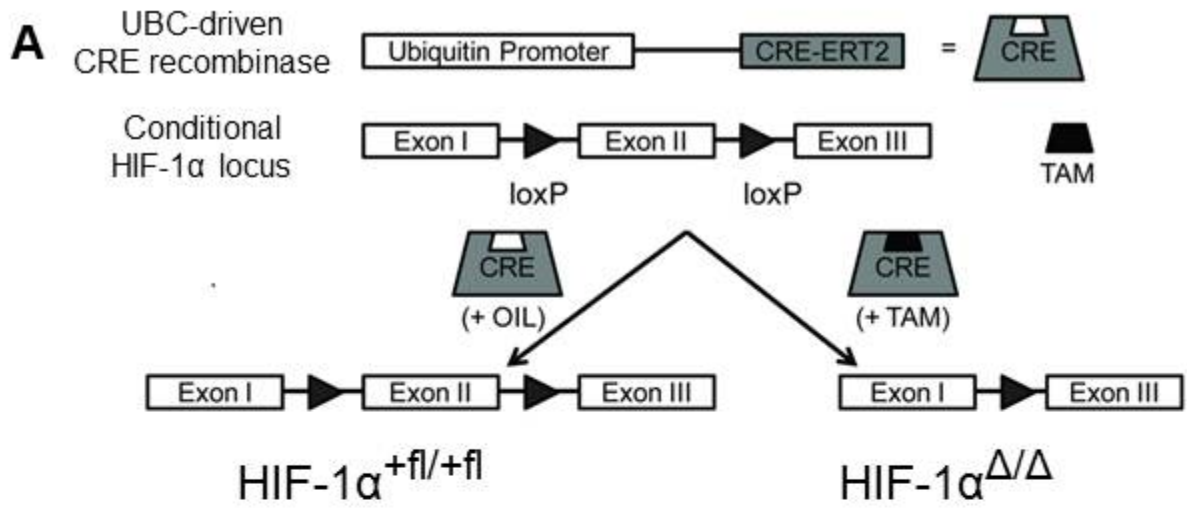


Table 4: Hepatic HIF-1 α mRNA expression after APAP overdose. HIF-1 α ^{+fl/+fl} and HIF-1 α ^{Δ/Δ} mice were treated with SAL or APAP then killed at 2 or 24 hrs. Real-time PCR was used to analyze liver tissue for expression of HIF-1 α mRNA. HIF-1 α mRNA was measured in liver tissue and is expressed as an average of the ratios of HIF-1 α :HPRT copy number normalized to SAL controls.

Table 4

<i>Genotype</i>	Real-time PCR (HIF-1 α :HPRT versus SAL-treated HIF-1 $\alpha^{+fl/+fl}$)			
	HIF-1 $\alpha^{+fl/+fl}$		HIF-1 $\alpha^{\Delta/\Delta}$	
<i>Treatment</i>	<u>2h</u>	<u>24h</u>	<u>2h</u>	<u>24h</u>
SAL	1 \pm 0.04	1 \pm 0.1	3E-2 \pm 2E-3 ^a	5.5E-3 \pm 4E-4 ^a
APAP	2.3 \pm 1.5 ^a	3.5E8 \pm 3E7 ^a	3E-2 \pm 1E-3 ^{ab}	6 \pm 3.8 ^a

HIF-1 α inactivation protects from early APAP hepatotoxicity

To determine whether TAM treatment could affect APAP hepatotoxicity, UBC-Cre-ERT2^(-/-)/HIF-1 α ^{flox/flox} mice, which do not express a functional Cre recombinase and cannot remove HIF-1 α , were treated with OIL or TAM for 5 days, and 3 weeks later were treated with saline (SAL) or 400 mg/kg APAP. Both OIL- and TAM-treated mice developed severe liver injury 6 hrs after treatment, indicating that TAM alone did not affect APAP hepatotoxicity (Figure 22). In contrast, when UBC-Cre-ERT2^{+/-}/HIF-1 α ^{flox/flox} mice, which are capable of TAM-induced Cre recombination, underwent the same treatments, OIL-treated UBC-Cre-ERT2^{+/-}/HIF-1 α ^{flox/flox} mice (HIF-1 α -sufficient) developed severe liver injury 6h after treatment, but injury was essentially absent in TAM-treated UBC-Cre-ERT2^{+/-}/HIF-1 α ^{flox/flox} mice (HIF-1 α -deficient) (Figure 22), indicating that the acute liver injury depended on HIF-1 α signaling. All subsequent experiments were performed in UBC-Cre-ERT2^{+/-}/HIF-1 α ^{flox/flox} mice.

HIF-1 α ^{+fl/+fl} mice treated with APAP had significantly greater plasma ALT activity at 2 hrs compared to SAL-treated animals, which developed into severe liver injury by 6 hrs and continued to increase through 24 hrs (Figure 23A). APAP treated HIF-1 α ^{Δ/Δ} mice had complete attenuation of liver injury at 2 hrs and 6 hrs, however plasma ALT activity was the same as in HIF-1 α ^{+fl/+fl} mice at 24 hrs. Histological analysis confirmed centrilobular hepatocellular necrosis in HIF-1 α ^{+fl/+fl} mice at 6 hrs and 24 hrs after APAP overdose and that HIF-1 α ^{Δ/Δ} mice had no necrosis at 6 hrs but significant lesions at 24

hrs (Figure 23B). Hepatic GSH depletion was used as an indication of APAP bioactivation. HIF-1 α ^{+fl/+fl} and HIF-1 α ^{Δ/Δ} mice treated with SAL had 4.4 \pm 0.5 and 5.3 \pm 0.6 μ mol glutathione/g liver, respectively. After APAP administration, glutathione concentration was reduced in HIF-1 α ^{+fl/+fl} and HIF-1 α ^{Δ/Δ} mice to 0.4 \pm 0.02 and 1.52 \pm 1.1 μ mol/g liver, respectively; these values were not significantly different from one another.

Figure 22: Effect of HIF-1 α deletion on APAP hepatotoxicity. Five week old CRE-ERT2^{-/-}/HIF-1 α ^{flox/flox} (labeled Cre (-)/HIF-1 α ^{fl/fl}) or CRE-ERT2^{+/-}/HIF-1 α ^{flox/flox} (labeled Cre (+)/HIF-1 α ^{fl/fl}) mice were treated with OIL or 200 μ g/g TAM daily for five days. 21 days later, mice were treated with APAP or SAL intraperitoneally. Plasma alanine aminotransferase (ALT) activity was measured 6h after APAP administration. Data represent means \pm SEM of n = 3-8 animals per group. *a* Significantly different from SAL-treated mice; *b* Significantly different from OIL-treated mice; *c* Significantly different from HIF-1 α ^{+fl/+fl} mice.

Figure 22

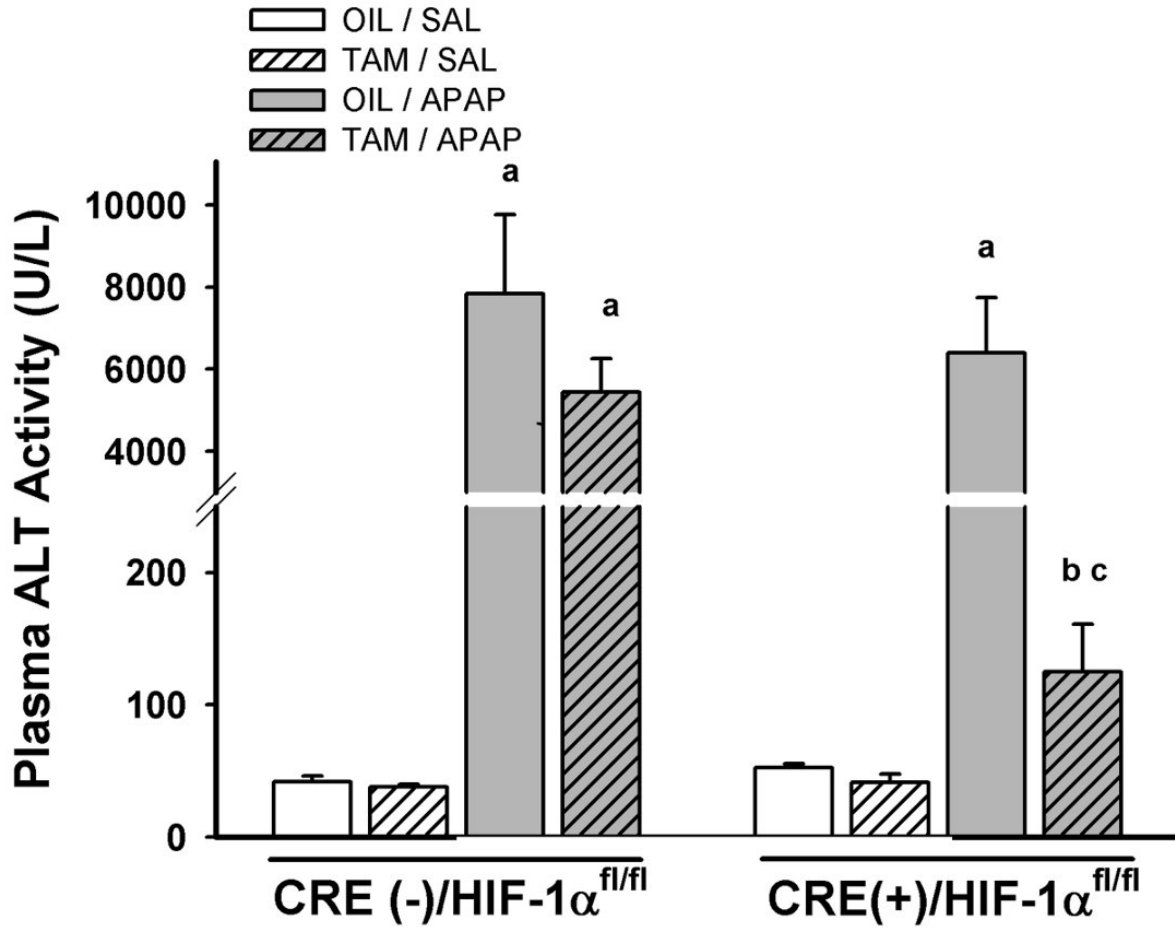
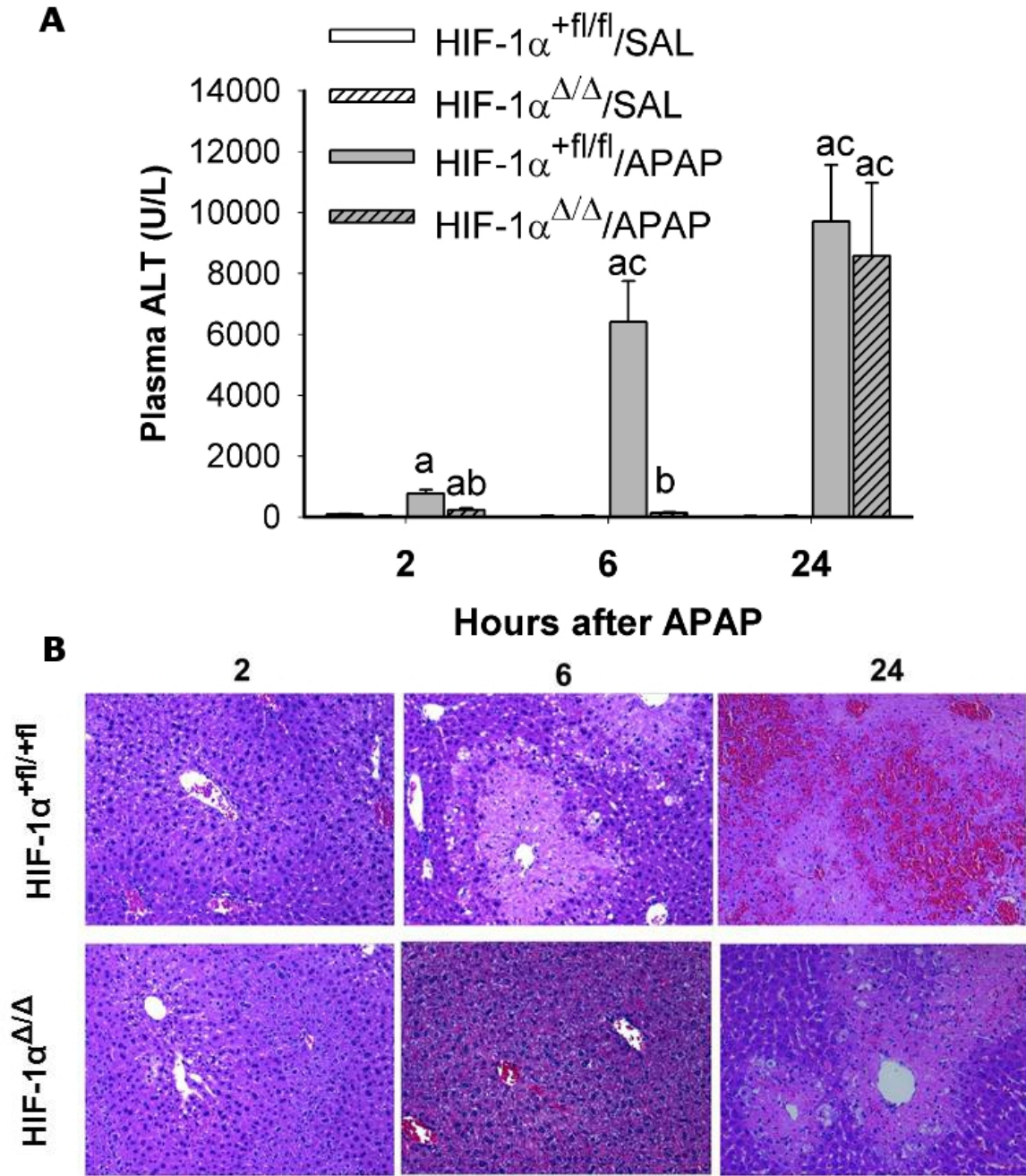


Figure 23: Time course of APAP-induced liver injury in HIF-1 α -deficient mice.

HIF-1 α ^{+fl/+fl} or HIF-1 α ^{Δ/Δ} mice were treated with APAP (400 mg/kg) or SAL, and plasma and liver samples were taken 2 hrs, 6 hrs and 24 hrs after later. (A) Liver injury was assessed from plasma ALT activity; data represent means \pm SEM of n = 3-8 animals per group. (B) Livers were processed for histology and stained with H&E. Sections are shown from mice with ALT values near the median. *a* Significantly different from SAL-treated mice; *b* Significantly different from APAP-treated HIF-1 α ^{+fl/+fl} mice; *c* Significantly different from same treatment at 2 hrs.

Figure 23



Expression of cell death proteins

The contribution of HIF-1 α to production of cell death proteins in APAP overdose was evaluated. APAP overdose did not affect the expression of BNIP3 mRNA in liver (Table 5) nor did it alter hepatic expression of BNIP3 protein (data not shown). Bax is a proapoptotic protein that translocates to the mitochondria upon activation and contributes to APAP-induced hepatocellular necrosis (7). In the livers of HIF-1 α ^{+fl/+fl} mice, APAP overdose increased the colocalization of Bax with Cox IV, a mitochondrial marker (Figure 24A-B). In contrast this effect was not observed in APAP-treated HIF-1 α ^{Δ/Δ} mice. APAP overdose caused DNA fragmentation in centrilobular HPC in HIF-1 α ^{+fl/+fl} mice at 6 and 24 hrs; this effect was attenuated upon HIF-1 α deletion (Figure 25).

Table 5: Hepatic BNIP3 mRNA expression after APAP overdose. HIF-1 α ^{+fl/+fl} and HIF-1 α ^{Δ/Δ} mice were treated with SAL or APAP then killed at 2, 6, or 24 hrs. Real-time PCR was used to analyze liver tissue for expression of BNIP3 mRNA. For each sample, the copy number of BNIP3 was normalized to that of HPRT, then further normalized to SAL-treated HIF-1 α ^{+fl/+fl} mice to account for variability in mRNA quantity at different time points. Data represents mean BNIP3:HPRT:SAL ratio \pm SEM of n=3-6 animals. a Significantly different from SAL-treated mice of same genotype; b Significantly different from corresponding HIF-1 α ^{+fl/+fl} mice.

Table 5

	Real-time PCR (BNIP3:HPRT versus SAL in HIF-1 α ^{+fl/+fl})					
	SAL			APAP		
Mouse	2 hrs	6 hrs	24 hrs	2 hrs	6 hrs	24 hrs
HIF- α ^{+fl/+fl}	1.0 \pm 0.02	1.0 \pm 0.02	1.0 \pm 0.1	0.72 \pm 0.13	0.33 \pm 0.04	0.4 \pm 0.7 ^a
HIF-1 α ^{Δ/Δ}	0.78 \pm 0.1	0.77 \pm 0.1	1.2 \pm 0.24	2.1 \pm 0.5 ^{ab}	0.77 \pm 0.26	0.32 \pm 0.1 ^a

Figure 24: Mitochondrial Bax translocation. Mice were treated with SAL or 400 mg/kg APAP, and 6 hrs later liver samples were taken. (A) Quantification of Bax: Cox IV colocalization was performed as described in Methods. (B) Representative 60X confocal fluorescent micrographs of frozen liver sections from 2-3 animals per group. There were no significant differences between SAL treated HIF-1 α ^{+fl/+fl} and HIF-1 α ^{Δ/Δ} mice, so they were combined for statistical purposes. ^a Significantly different from SAL-treated mice.

Figure 24

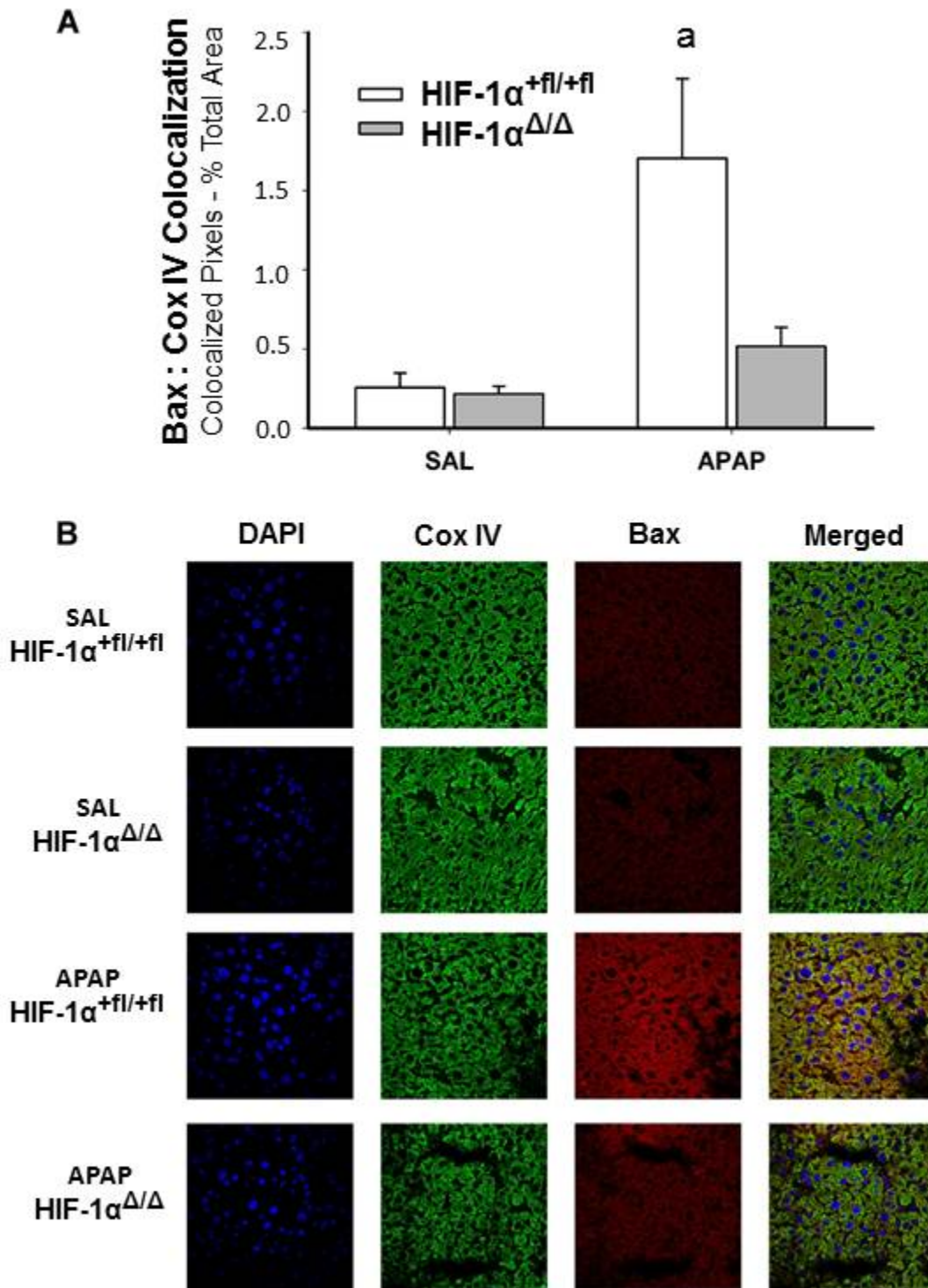
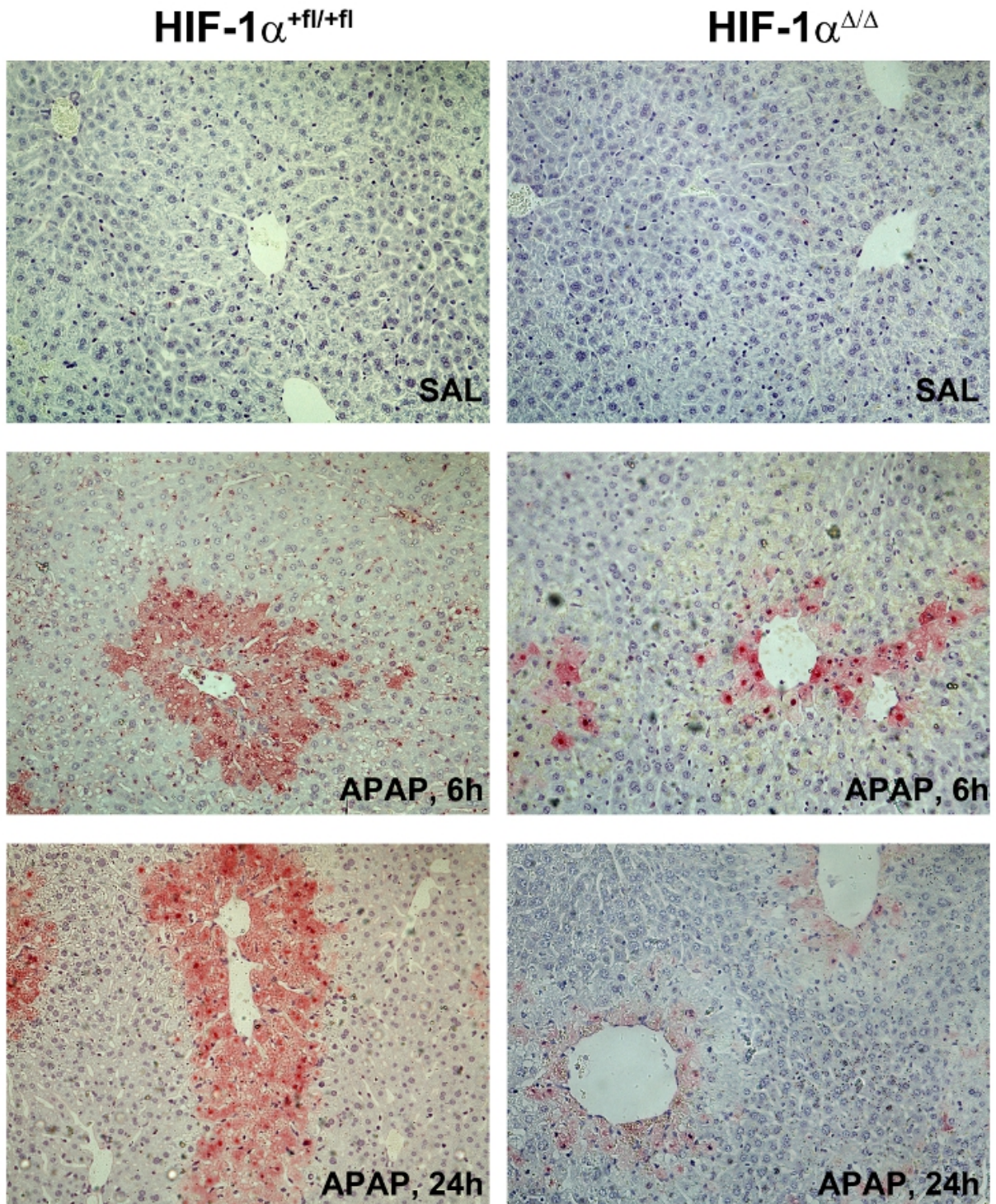


Figure 25: DNA fragmentation after APAP treatment. DNA fragmentation was evaluated by the TUNEL assay in $\text{HIF-1}\alpha^{\text{+fl/+fl}}$ and $\text{HIF-1}\alpha^{\Delta/\Delta}$ mice treated with SAL or 400 mg/kg APAP 6 or 24 hrs earlier (200x for all panels). TUNEL positive staining appears red.

Figure 25



HIF-1 α deletion attenuates coagulation system activation

Thrombin-antithrombin (TAT) concentration reflects the activation of thrombin in plasma. In HIF-1 α ^{+fl/+fl} mice, plasma TAT concentration was significantly increased by APAP overdose 2, 6 and 24 hrs after treatment, although it was somewhat less at 24 hrs. In HIF-1 α ^{Δ/Δ} mice, plasma TAT was elevated 2h after APAP, returned to baseline at 6 hrs, then increased significantly by 24 hrs to a concentration greater than the value in HIF-1 α ^{+fl/+fl} mice (Figure 26A). A consequence of thrombin activation in liver is deposition of fibrin, which was assessed by immunohistochemical staining. In HIF-1 α ^{+fl/+fl} mice, fibrin deposition was detected at 6h after overdose and increased significantly by 24 hrs. In contrast, there was no fibrin deposition in HIF-1 α ^{Δ/Δ} mice detected until 24 hrs after APAP (Figure 26B). In HIF-1 α ^{+fl/+fl} mice, fibrin deposition at 6 hrs appeared to be centrilobular and sinusoidal after APAP overdose (Figure 26C).

The fibrinolytic system consists of plasminogen and the plasminogen activators (PAs), tPA and uPA, which cleave plasminogen to plasmin to dissolve fibrin clots. PAI-1 is the endogenous inhibitor of PAs, and elevation of active PAI-1 in plasma suggests inhibition of fibrinolysis. Hepatic PAI-1 mRNA was measured 2, 6, and 24 hrs after treatment. In SAL-treated mice, basal PAI-1 mRNA expression was small (Table 6). In HIF-1 α ^{+fl/+fl} mice treated with APAP, hepatic PAI-1 mRNA was elevated by more than 10-fold as early as 2 hrs after APAP and remained so through 24 hrs. In HIF-1 α ^{Δ/Δ} mice, PAI-1 mRNA increased to the same level as HIF-1 α ^{+fl/+fl} mice 2 hrs after APAP,

then decreased to baseline at 6 hrs only to increase again by 24 hrs. The circulating concentration of active PAI-1 was also evaluated at 6 hrs and 24 hrs. In HIF-1 α ^{+fl/+fl} mice, APAP overdose increased the appearance of active PAI-1 in plasma at 6 hrs, and PAI-1 concentration increased further by 24 hrs (Figure 27). This increase in PAI-1 was attenuated in HIF-1 α ^{Δ/Δ} mice at 6 hrs but was similar to that seen in HIF-1 α ^{+fl/+fl} mice by 24 hrs.

The role of HIF-1 α in the inflammatory response to APAP

Plasma concentrations of cytokines were measured 6h after APAP exposure. Neither HIF-1 α deletion nor APAP overdose affected the plasma concentrations of IL-1 β , IL-2, IL-4, TNF α , MIP-1 α or VEGF at these times (Table 7). APAP overdose increased plasma concentrations of IL-6, RANTES, and KC in HIF-1 α ^{+fl/+fl} mice, and these increases were significantly attenuated upon HIF-1 α deletion (Table 7). Plasma concentrations of IL-6, KC and RANTES were evaluated 24 hrs after APAP treatment. APAP overdose increased IL-6 (Figure 28A) and KC (Figure 28B) in both HIF-1 α ^{+fl/+fl} and HIF-1 α ^{Δ/Δ} mice at 24 hrs, however there were no changes in RANTES (data not shown). Intrahepatic concentrations of IL-8/KC and RANTES were also determined. Hepatic RANTES was not altered by APAP (Figure 28C), but hepatic IL-8/KC was significantly increased 6 and 24 hrs after APAP overdose in HIF-1 α ^{+fl/+fl} mice, and by 24 hrs in HIF-1 α ^{Δ/Δ} mice (Figure 28D). IL-8/KC is a chemokine important for PMN infiltration, so hepatic PMNs were quantified. There were significantly fewer PMNs in

the livers of HIF-1 $\alpha^{\Delta/\Delta}$ mice 6 and 24 hrs after APAP administration compared to HIF-1 $\alpha^{+fl/+fl}$ mice (Figure 29).

Figure 26: Effect of HIF-1 α deletion on thrombin production and fibrin deposition.

SAL or 400 mg/kg APAP was administered to HIF-1 α ^{+fl/+fl} and HIF-1 α ^{Δ/Δ} mice, and plasma and liver samples were taken 2 hrs, 6 hrs and 24 hrs later. (A) Plasma TAT dimer was measured as a marker of thrombin generation. Frozen liver samples were stained immunohistochemically for fibrin. (B) Quantification of fibrin. (C): Representative liver sections from HIF-1 α ^{+fl/+fl} and HIF-1 α ^{Δ/Δ} mice treated with APAP. *a* Significantly different from SAL-treated mice; *b* Significantly different from APAP-treated HIF-1 α ^{+fl/+fl} mice.; *c* Significantly different from same group at 2 hrs and 6 hrs.

Figure 26

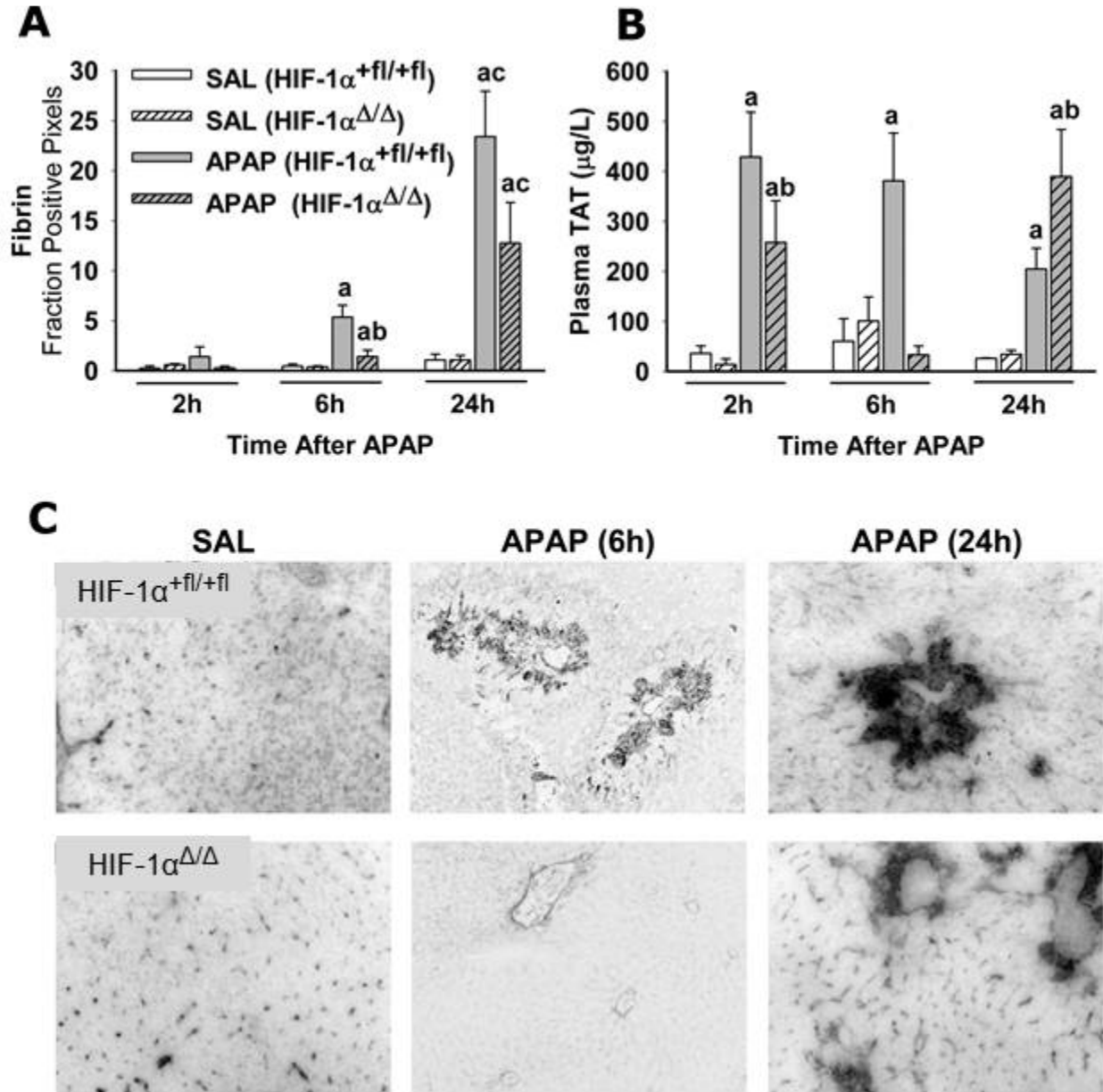


Table 6: Hepatic PAI-1 mRNA expression after APAP overdose in HIF-1 α ^{+fl/+fl} and HIF-1 α ^{Δ/Δ} mice. HIF-1 α ^{+fl/+fl} and HIF-1 α ^{Δ/Δ} mice were treated with SAL or APAP then killed after 2 hrs, 6 hrs, or 24 hrs. Real-time PCR was used to analyze liver tissue for the expression of PAI-1 mRNA. For each sample, the copy number of PAI-1 was normalized to that of HPRT. Data represent mean of the PAI-1:HPRT ratio \pm SEM of n=3-6. *a* Significantly different from SAL-treated mice of same genotype; *b* Significantly different from corresponding HIF-1 α ^{+fl/+fl} mice.

Table 6

	Real-time PCR (PAI-1:HPRT ratio) x 100					
	SAL			APAP		
Mouse	2 hrs	6 hrs	24 hrs	2 hrs	6 hrs	24 hrs
HIF1 α ^{+fl/+fl}	1.0±0.5	1.0±0.5	0.03±0.1	16±7 ^a	14±7 ^a	12±4 ^a
HIF1 α ^{Δ/Δ}	0.1±0.03 ^b	0.2±0.03 ^b	0.6±0.2	26±20 ^a	2.9±1 ^b	11±5 ^a

Figure 27: Effect of HIF-1 α deletion on PAI-1 production. 400 mg/kg APAP or SAL was administered to HIF-1 α ^{+fl/+fl} and HIF-1 α ^{Δ/Δ} mice, and plasma samples were taken after 2 hrs, 6 hrs or 24 hrs. Active PAI-1 protein was measured in plasma, and data represent means \pm SEM of n = 3-8 animals per group. *a* Significantly different from SAL-treated mice; *b* Significantly different from APAP-treated HIF-1 α ^{+fl/+fl} mice.

Figure 27

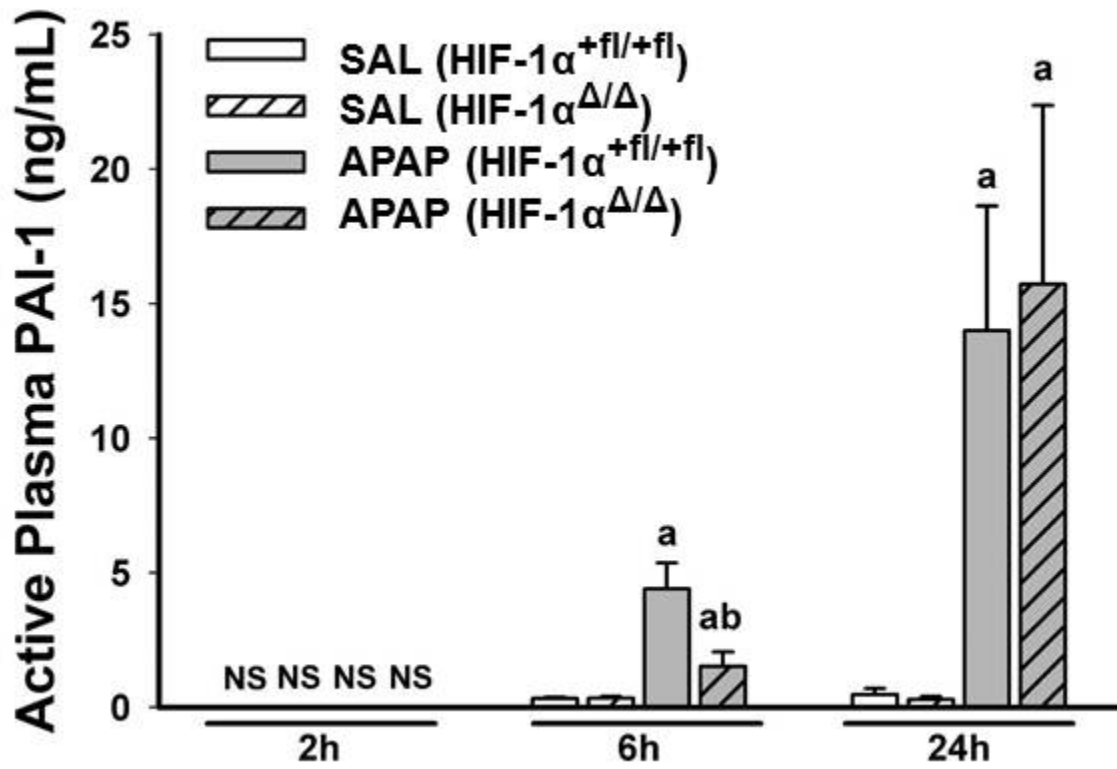


Table 7: Cytokine concentrations in plasma of APAP-treated HIF-1 α ^{+fl/+fl} and HIF-1 α ^{Δ/Δ} mice. HIF-1 α ^{+fl/+fl} and HIF-1 α ^{Δ/Δ} mice were treated with SAL or APAP and plasma was collected 6 hrs after administration and analyzed for cytokine concentrations using bead array. a significantly different from SAL-treated HIF-1 α ^{+fl/+fl} mice; b significantly different from APAP-treated HIF-1 α ^{+fl/+fl} mice

Table 7

Cytokine	Plasma cytokine (pg/mL)			
	SAL		APAP	
	HIF-1 α ^{+fl/+fl}	HIF-1 α ^{Δ/Δ}	HIF-1 α ^{+fl/+fl}	HIF-1 α ^{Δ/Δ}
IFN γ	15.9 \pm 1.0	17.3 \pm 1.4	17.4 \pm 1.5	17.6 \pm 0.5
IL-1 β	6.1 \pm 0.5	6.2 \pm 0.3	6.9 \pm 0.6	6.5 \pm 0.5
IL-2	4.0 \pm 0.4	3.8 \pm 0.2	5.8 \pm 0.9	4.4 \pm 0.3
IL-4	4.8 \pm 0.3	5.0 \pm 0.5	4.5 \pm 0.4	4.2 \pm 0.3
IL-6	23.5 \pm 3.0	27.8 \pm 3.7	231 \pm 45.1 ^a	38.2 \pm 5.6 ^b
IL-10	10.9 \pm 0.4	11.6 \pm 0.4	14.0 \pm 1.4	11.5 \pm 0.2
IL-12 (p70)	14.8 \pm 0.6	15.4 \pm 0.2	14.6 \pm 0.5	14.4 \pm 0.3
IL-8/KC	49.8 \pm 7.4	40.3 \pm 8.0	573 \pm 372 ^a	110 \pm 25.5 ^b
MIP-1 α	11.5 \pm 0.5	12.1 \pm 0.3	12.4 \pm 0.7	12.0 \pm 0.3
RANTES	28.5 \pm 4.0	27.3 \pm 1.5	52.9 \pm 10.9 ^a	33.2 \pm 3.2 ^b
TNF α	17.9 \pm 0.4	18.4 \pm 0.5	20.0 \pm 1.0	18.3 \pm 0.4
VEGF	19 \pm 0.4	20.5 \pm 0.6	19.1 \pm 0.6	19.5 \pm 0.6

Figure 28: Hepatic and plasma concentration of cytokines. Plasma concentration of IL-6 and IL-8/KC were measured at 6 and 24 hrs, and liver lysates were prepared and the concentrations of KC and RANTES determined 6 and 24 hrs after SAL or APAP. Data represent means \pm SEM of n = 3-8 animals per group. (A) Plasma IL-6 concentration at 6 and 24 hrs. (B) Plasma IL-8/KC concentration at 6 and 24 hrs. (C) Hepatic RANTES concentration. (D) Hepatic KC concentration. *a* Significantly different from SAL-treated mice; *b* Significantly different from APAP-treated HIF-1 α ^{+fl/+fl} mice; *c* Significantly different from same treatment at 6 hrs.

Figure 28

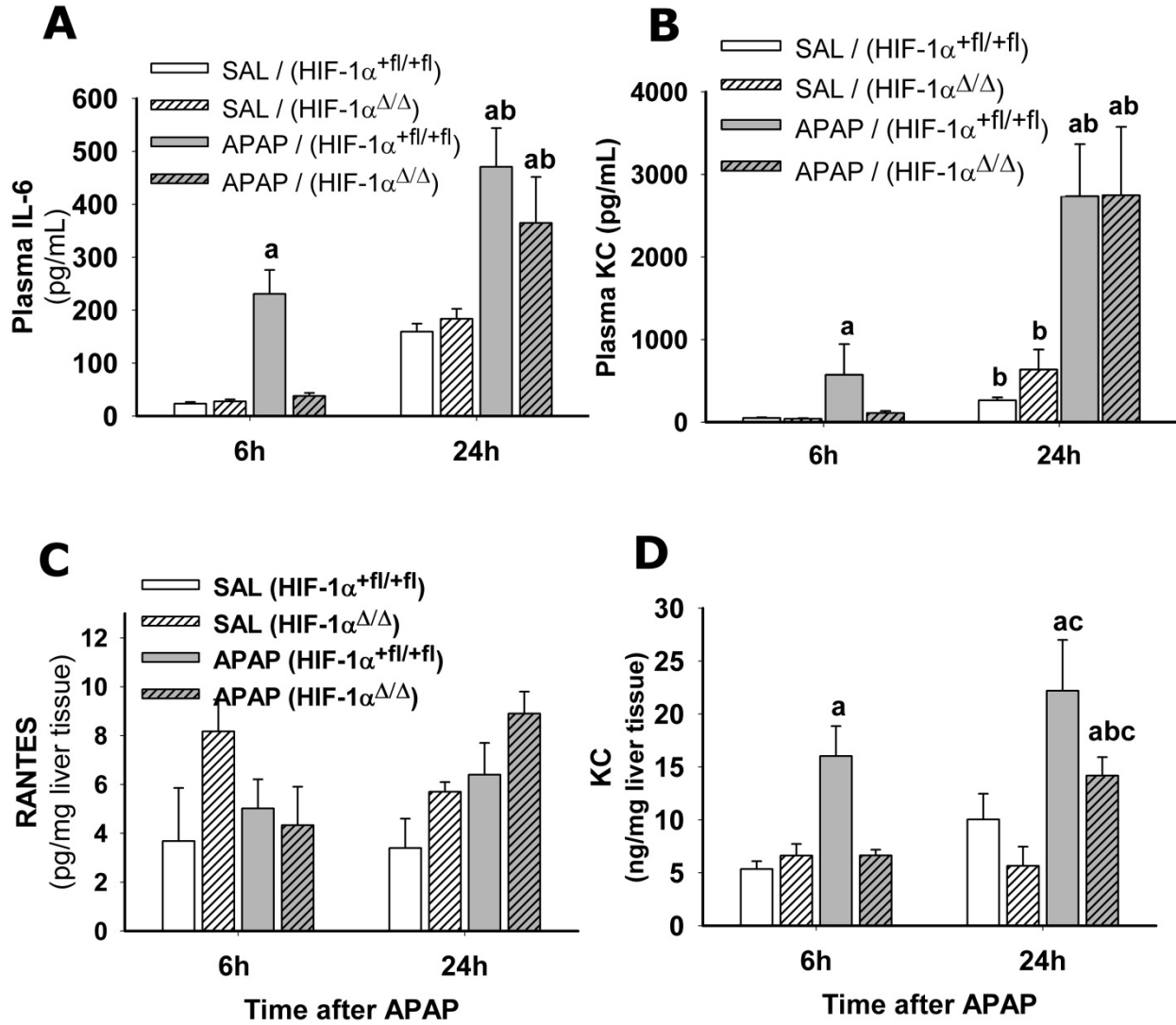
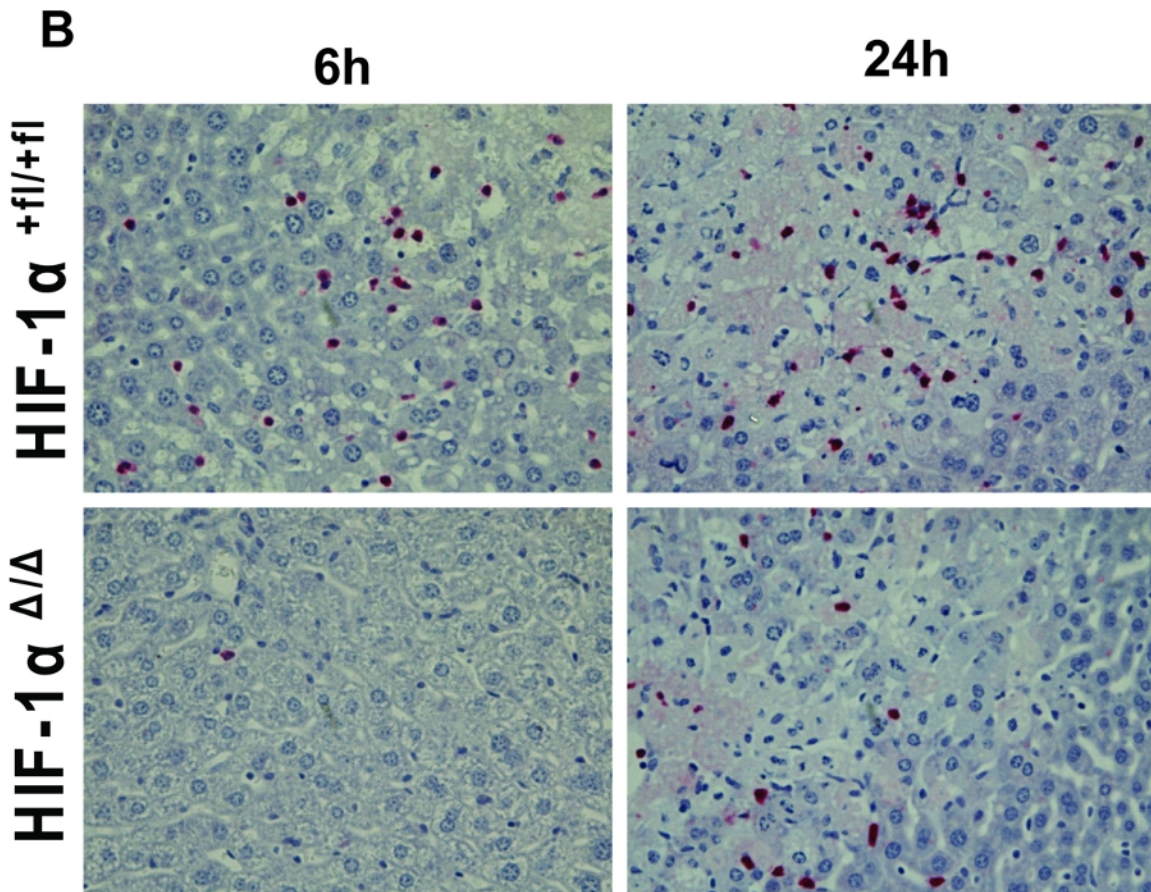
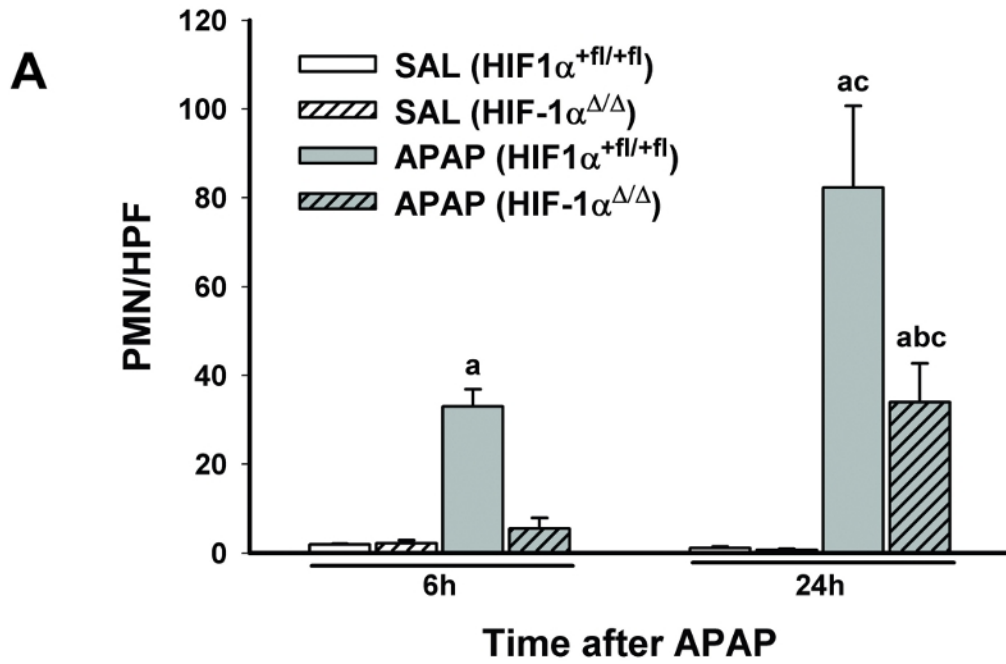


Figure 29: Hepatic PMN accumulation after APAP treatment in HIF-1 α ^{+fl/+fl} and HIF-1 α ^{Δ/Δ} mice. (A) PMNs were quantified in 20 randomly selected high-power fields (HPF; 400x). Data represent means \pm SEM of n = 3-8 animals per group. *a* Significantly different from SAL; *b* Significantly different from APAP-treated HIF-1 α ^{+fl/+fl} mice; *c* Significantly different from same group at 6 hrs. (B) Representative sections from HIF-1 α ^{+fl/+fl} and HIF-1 α ^{Δ/Δ} mice. PMNs appear red.

Figure 29



4.6 Discussion

HIF-1 α deletion protected mice from early APAP-induced liver injury, but it did not prevent the development of severe liver injury 24 hrs after overdose (Figure 23). The protection from toxicity at 2 and 6 hrs was not due to decreased bioactivation, since the depletion of GSH was similar in HIF-1 α ^{+fl/+fl} and HIF-1 α ^{Δ/Δ} mice. These data suggest that HIF-1 α has dual roles in the pathogenesis of APAP-induced liver injury. HIF-1 α appears to have a damaging role in early progression of injury, possibly through its contribution to insertion of Bax into the mitochondria (Figure 24), hemostasis (Figure 26 and Figure 27), and/or the inflammatory response (Table 7, Figure 28, Figure 29). The loss of protection at 24 hrs suggests that HIF-1 α has a protective role at later times, or that its absence delays the onset of liver injury. The former suggestion is consistent with a recently published report indicating that HPC exposed to moderate HX were protected from APAP-induced cell death (188). The protective effect of HX was attributed to hypoxic preconditioning, because HIF-1 α can induce the transcription of protective factors, such as heme oxygenase-1 or EPO (11). Furthermore, Kato *et al* (90) found that the HIF-1 α -regulated gene VEGF is important in liver repair from APAP overdose.

APAP overdose increased hepatic HIF-1 α protein at 2 hrs in HIF-1 α ^{+fl/+fl} mice (Figure 21C), an effect that was attenuated in HIF-1 α ^{Δ/Δ} mice. This is consistent with recently published reports that APAP overdose caused nuclear accumulation of HIF-1 α in liver extracts and isolated mouse HPC 1 hr after treatment, an effect which was maintained through 12 hrs (17, 77). HIF-1 α accumulation occurred prior to the development of HX in the liver (17), suggesting that the initial mechanism by which HIF-

1 α is stabilized is independent of HX. However, the coagulation system is activated and fibrin deposits in the liver beginning 2 hrs after administration of APAP (50) and tissue HX becomes apparent between 2 and 4 hrs (17); accordingly coagulation-dependent HX could contribute to prolonged stabilization of HIF-1 α during the progression of liver injury.

APAP overdose caused HIF-1 α -dependent translocation of Bax to the mitochondrial membrane (Figure 24). APAP overdose causes JNK-dependent Bax insertion into the mitochondrial membrane beginning 1 hr after treatment (148), and Bax^{-/-} mice were protected from APAP hepatotoxicity at 6 hrs, but not 12 hrs (7). Bajt et al., (7) hypothesized that Bax contributes to early MPT formation and release of mitochondrial intermembrane proteins that initiate DNA fragmentation and hepatocellular necrosis, but that continuous oxidative stress supplants this mechanism to cause cell damage at later times. Our observation that HIF-1 $\alpha^{\Delta\Delta}$ mice had reduced Bax translocation (Figure 24) at 6 hrs after APAP is consistent with this hypothesis. Additionally, APAP-induced DNA fragmentation was attenuated in HIF-1 $\alpha^{\Delta\Delta}$ mice compared to HIF-1 $\alpha^{+fl/+fl}$ animals (Figure 25). These data suggest that HIF-1 α is necessary for early Bax translocation and DNA fragmentation, however other APAP-induced signaling overcomes this protection by 24 hrs.

In addition to its role in cell death signaling, HIF-1 α might contribute to APAP-induced liver injury by modulating the hemostatic system. APAP overdose activates the coagulation system and results in sinusoidal fibrin deposition in mice (50), and it is associated with alterations in plasma hemostatic factors in humans (79). Furthermore,

reduction in coagulation attenuated liver injury 6 hrs, but not 24 hrs after APAP overdose in mice (50), similar to our current finding in HIF-1 $\alpha^{\Delta/\Delta}$ mice (Figure 23). In the absence of HIF-1 α expression, there was significant attenuation of thrombin generation (Figure 26A) and fibrin deposition (Figure 26B) at 6 hrs. By 24 hrs, thrombin generation in HIF-1 $\alpha^{\Delta/\Delta}$ mice had exceeded that seen HIF-1 $\alpha^{+fl/+fl}$ mice at the same time, and there was significant sinusoidal fibrin (Figure 26B). This raises the possibility that the protection afforded by HIF-1 α deletion is mediated by its ability to delay thrombin generation and fibrin deposition, thereby delaying the development of liver injury. However, it is also possible that in the absence of liver injury in HIF-1 $\alpha^{\Delta/\Delta}$ mice at 2 and 6 hrs, there is not a stimulus for activation of thrombin.

HIF-1 α also plays a role in fibrinolysis through regulation of PAI-1 expression (28). In the present study, hepatic PAI-1 mRNA and plasma protein were elevated at all times measured in APAP-treated HIF-1 $\alpha^{+fl/+fl}$ mice (Table 6), consistent with previous findings (8, 50). In contrast, in HIF-1 $\alpha^{\Delta/\Delta}$ mice PAI-1 mRNA was elevated at 2 hrs, returned to baseline by 6 hrs, then increased to the same level as HIF-1 $\alpha^{+fl/+fl}$ mice by 24 hrs (Table 6). The appearance of active PAI-1 in the plasma followed a similar pattern (Figure 27). This results raises the possibility that during APAP overdose, PAI-1 expression is a consequence of hepatocellular death and hemostasis, rather than due to a direct regulatory role by HIF-1 α ; indeed other transcription factors such as egr-1 and HIF-2 α contribute to PAI-1 expression (28). PAI-1 $^{-/-}$ mice had enhanced liver necrosis and increased mortality after administration of 200 mg/kg APAP compared to

control animals, suggesting a protective role for PAI-1; the enhanced liver injury in PAI-1^{-/-} mice was associated with decreased expression of proliferating cell nuclear antigen (PCNA) and was therefore attributed to delayed tissue repair (8).

Appropriate tissue repair is necessary for recovery from liver injury (119), and the HIF-1 α -regulated gene VEGF has recently been identified as an important mediator of tissue repair after APAP hepatotoxicity (40, 90). We found no increase in plasma VEGF at 6 hrs (Table 7), which is in contrast with previously published reports in which hepatic VEGF protein was increased starting 8 hrs after APAP overdose (40, 90). VEGF is produced by HPCs and acts locally on sinusoidal endothelial cells, therefore it might not have reached detectable concentrations in plasma. VEGF plays an important role in hepatocyte regeneration and restoration of liver microvasculature, through activation of repair pathways (40) and angiogenesis (90). Since VEGF is regulated by HIF-1 α , it is possible that the progression of liver injury between 6 and 24 hrs in HIF-1 $\alpha^{\Delta/\Delta}$ mice occurs because of loss of regeneration and other repair mechanism that are initiated by VEGF.

APAP overdose is associated with increases in inflammatory cytokines, and the role of HIF-1 α in the production of cytokines is well documented in other conditions. Mice with HIF-1 α -deficient monocytes produced less TNF α , IL-6, IL-12, IL-1 α and IL-1 β in response to LPS compared to wild type animals (131). In human patients, large plasma concentrations of IL-6, IL-8 and MCP-1 correlated with the severity of liver injury due to APAP overdose (78). Furthermore, APAP overdose increased plasma concentrations of IL-1 β , IL-6, KC, MCP-1, MIP-2 and TNF α in mice (66, 67). In our

study, APAP overdose caused an increase in plasma concentrations of IL-6, KC, and RANTES at 6 hrs in HIF-1 α ^{+fl/+fl} mice, which was attenuated by deletion of HIF-1 α (Table 7). Additionally, APAP overdose increased hepatic concentration of IL-8/KC 6 hrs and 24 hrs after treatment in HIF-1 α ^{+fl/+fl} mice, and 24 hrs after treatment in HIF-1 α ^{Δ/Δ} mice (Figure 28). IL-8/KC is a chemokine important for the recruitment of PMNs to the liver. HIF-1 α ^{Δ/Δ} mice had smaller plasma concentrations of IL-8/KC and RANTES at 6 hrs (Table 4.4), which was associated with fewer hepatic PMNs 6 and 24 hrs after APAP compared to HIF-1 α ^{+fl/+fl} mice (Figure 29).

The role of PMNs in APAP-induced liver injury remains controversial (69). There is evidence that PMNs promote liver injury (69, 110) in APAP overdose, however more recent evidence suggests that they accompany the sterile inflammatory response but do not contribute to injury (69, 185). PMNs are necessary for the phagocytosis of necrotic HPCs in APAP hepatotoxicity (101). HIF-1 α -deficient monocytes have reduced phagocytic capacity and reduced release of antimicrobial proteins and granule proteases such as elastase and cathepsin G (32, 191), raising the possibility that HIF-1 α ^{Δ/Δ} mice might have reduced ability to phagocytose necrotic HPC and thus reduced tissue repair capacity. This might explain why hepatocellular injury appears to return by 24 hrs.

In summary, deletion of HIF-1 α protects mice from early progression of APAP-induced liver injury, but does not afford lasting protection. At early times, HIF-1 α regulates Bax translocation to the mitochondria and consequent DNA fragmentation that

results in hepatocellular necrosis. It also contributes to regulation of the coagulation and fibrinolytic systems, as well as to the production of inflammatory mediators that can influence the pathogenesis of APAP-induced liver injury. At later times, HIF-1 α deletion does not protect from severe liver injury, possibly through regulation of factors that support tissue repair and regeneration, such as PMN infiltration, VEGF and PAI-1. Our results suggest that HIF-1 α has dual roles in APAP-induced liver injury, promoting damage early and conferring protection later during the pathogenesis.

CHAPTER 5

Summary and Conclusions

5.1 Summary of research

5.1.2 The role of HX and HIF-1 α in an in vitro model of liver injury

The hypothesis to be tested in this dissertation was that HX sensitizes HPCs to EL-mediated cell death dependent on ROS, MAPK and HIF-1 α . In initial experiments, an EL-concentration response curve was generated in primary rat HPCs in either an OxR or HX environment (Figure 6A). Concentrations of EL up to 17 U/mL were not cytotoxic to HPCs after 8 hrs of treatment. Exposure of HPCs to HX (5% O₂) for 8 hrs was not cytotoxic, however cotreatment of cells with HX and EL (either 8.5 U/mL or 17 U/mL) resulted in a synergistic cytotoxicity. This was consistent with previously published results [Figure 5B, published in (112)]. This interaction was also observed in Hepa1c1c7 cells. Concentrations of EL of 15 U/mL and greater were cytotoxic to Hepa1c1c7 cells after 24 hrs. Exposure to HX (2% O₂) was modestly cytotoxic, however cotreatment of HX with EL concentrations of 7.5 U/mL EL and greater resulted in synergistic cytotoxicity (Figure 6B). In all subsequent studies discussed in this section, a concentration of 7.5 U/mL EL and 2% O₂ were utilized to study the mechanism of the interaction.

In order to determine the type of cell death caused by the HX/EL interaction, apoptosis was assessed in HX/EL cotreated cells. However, neither caspase 3/7 signaling (Figure 7B) nor mitochondrial permeability transition (Figure 7C) was involved in the interaction, indicating that the mode of cell death is not apoptosis.

MAPK signaling is critical to cytotoxicity caused by both HX and EL in various cell types. EL reduced ERK signaling in both OxR- and HX-treated cells (Figure 8A); ERK inhibition actually potentiated EL-mediated cell death, yet had no effect on the HX/EL interaction (Figure 9A). This indicated that EL might inhibit ERK signaling in Hepa1c1c7 cells, and that ERK might play a protective role in cells exposed to EL, but that it is not involved in the interaction of HX/EL. There were no treatment-related effects on JNK phosphorylation, and JNK inhibition did not protect cells from the HX/EL interaction (Figure 8B, Figure 9B). Both HX and EL induced p38 phosphorylation, and there was an additive increase in phospho-p38 in HX/EL-cotreated cells (Figure 8C). Inhibition of p38 signaling attenuated cell death caused by HX/EL cotreatment, yet had no effect on either treatment alone (Figure 9C). These data suggested that p38 is important to the mechanism of cell death caused by HX/EL interaction in Hepa1c1c7 cells.

HIF-1 α is a critical transcription factor in the cellular response to HX and can direct the transcription of cell death genes such as BNIP3 and Nix. We tested the hypothesis that HIF-1 α is involved in the HX/EL interaction. EL had no effect on the accumulation or nuclear translocation of HIF-1 α 1 hr after treatment. HX increased nuclear HIF-1 α accumulation that was further enhanced by cotreatment with EL (Figure 10). HIF-1 α activity was assessed by measuring BNIP3 and Nix mRNA 8 hrs after treatment. EL did not affect Nix expression. HX increased Nix mRNA which was further enhanced by cotreatment with EL (Figure 11A). BNIP3 mRNA expression was increased by both EL and HX alone, and cotreatment resulted in a synergistic increase in BNIP3 mRNA (Figure 11B). BNIP3 protein was assessed 12 hrs after treatment, and it followed a pattern similar to mRNA expression (Figure 12).

In order to determine if HIF signaling was required for the cytotoxicity of HX and EL, the HIF-1 β /ARNT-deficient HepaC4 cell line was utilized. Interestingly, EL caused modest cytotoxicity in HepaC4 cells, however HX was not cytotoxic, and it did not enhance EL-mediated cell death (Figure 13). Furthermore, neither HX nor HX/EL cotreatment increased BNIP3 mRNA (Figure 14A) or protein (Figure 14B) in these cells. These data suggested that HIF-1 α signaling is involved in the interaction of HX/EL, possibly through its role in production of the cell death protein BNIP3 and Nix.

One mechanism by which p38 MAPK might contribute to HX/EL cell death is through phosphorylation of HIF-1 α , which increases its transactivation and gene transcription. Indeed, inhibition of p38 signaling attenuated HX/EL-induced BNIP3 mRNA and protein expression (Figure 11B and Figure 12B). Interestingly, p38 inhibition only attenuated BNIP3 mRNA and protein in cotreated cells, having had no effect on BNIP3 produced by either treatment alone, suggesting that p38 is crucial to the signaling required for the interaction.

Another pathway that was investigated in the mechanism of HX/EL-mediated cell death was oxidative stress. However, increased ROS were not detected in Hepa1c1c7 cells treated with EL, HX or HX/EL (Figure 16B), and neither the water-soluble antioxidant 4-OH Tempo (Figure 16A) nor the antioxidant and iron chelator DFX protected Hepa1c1c7 cells from the HX/EL interaction (Figure 18B). Interestingly, the lipid soluble antioxidant Vitamin E did protect cells from the HX/EL interaction (Figure 15), which suggested that membrane lipid peroxidation could be involved in the mechanism of cell death. HX/EL increased TBARS, which was attenuated by Vitamin E (Table 3). Interestingly, the increase in TBARS caused by HX/EL cotreatment was also

partially attenuated by p38 inhibition (Table 3), which suggests that p38 contributes to cell death through modulation of lipid peroxidation. The increase in TBARS caused by HX/EL cotreatment was not attenuated in HepaC4 cells, indicating that the mechanism by which HIF-1 α contributes to cell death is independent of lipid peroxidation.

Another pathway of potential interest in the interaction of HX/EL is the transcription factor ATF2 and its gene product cyclin D1, which is involved in cell cycle regulation. HX/EL cotreatment resulted in significant reduction in activated ATF2 compared to either treatment alone (Figure 20A), and there was significantly less cyclin D1 mRNA expression in HX/EL cotreated cells compared to treatment with HX or EL alone (Figure 20B). This suggests that HX/EL cotreatment inhibits cell cycle progression.

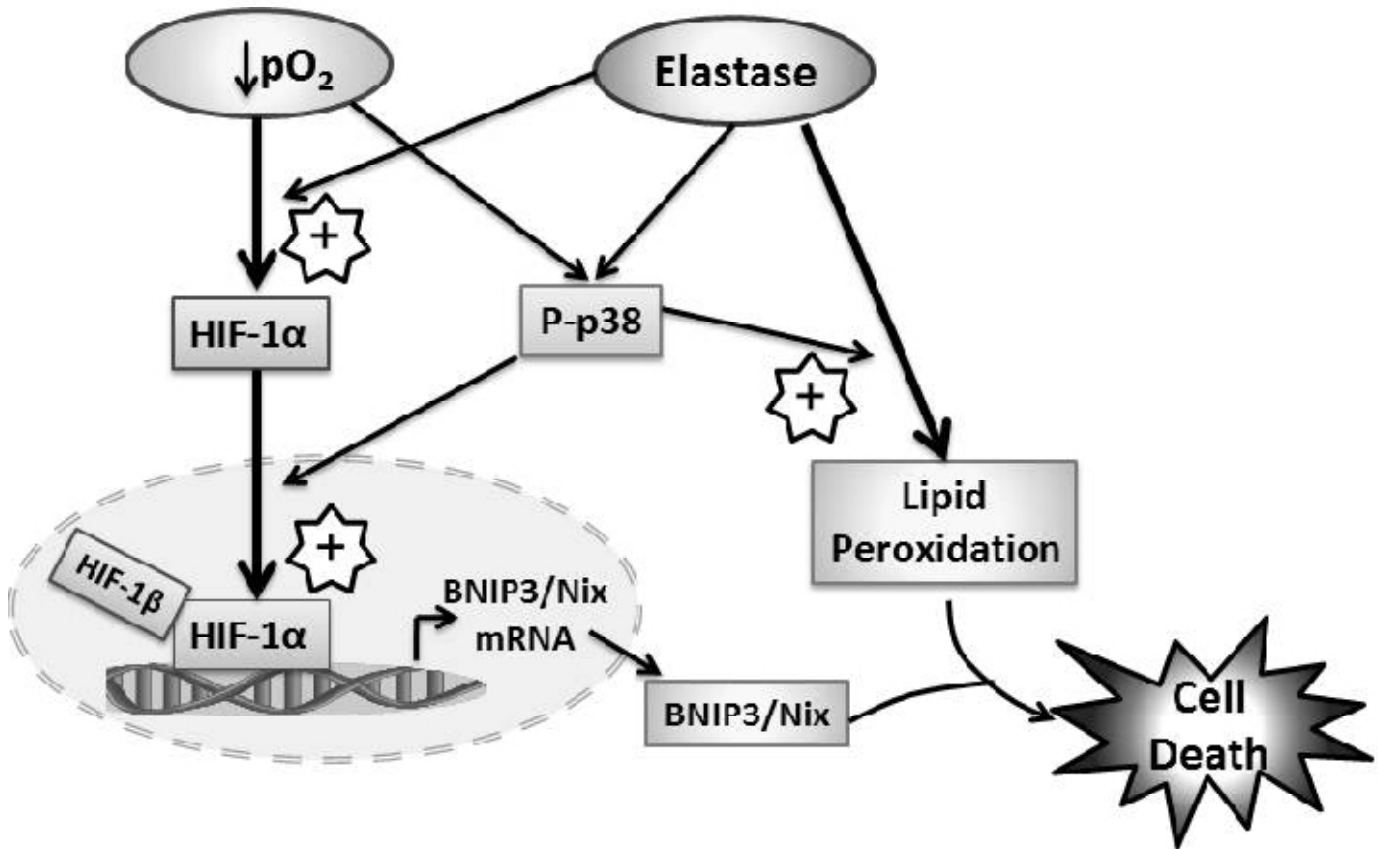
I also investigated other pathways and their potential role in the HX/EL interaction. Despite increased XO activity in HX/EL-treated cells compared to either treatment alone, XO signaling was not required for the interaction (Figure 16C-D). Furthermore, neither calcium nor NF- κ B signaling contributed to the interaction (Figure 17 and Figure 19). Interestingly, HIF-1 α activation with the “HX mimetic” CoCl₂ did not interact with EL to cause cell death, and protected the cells from the HX/EL interaction (Figure 18). This suggests that HIF-1 α activation is not sufficient for the interaction of HX and EL, and that HX must activate additional pathways that contribute to cell death.

To summarize, HX interacts with EL in Hepa1c1c7 cells to cause cell death that is dependent on p38 activation, HIF-1 α signaling, and lipid peroxidation. Furthermore,

p38 contributes to both HIF-1 α signaling and lipid peroxidation. Based on the results, a proposed pathway of HX/EL-induced cell death is outlined in Figure 30.

Figure 30: Proposed pathway to HX/EL-induced hepatocyte injury. See Section 5.1 for a detailed explanation of the pathways involved.

Figure 30

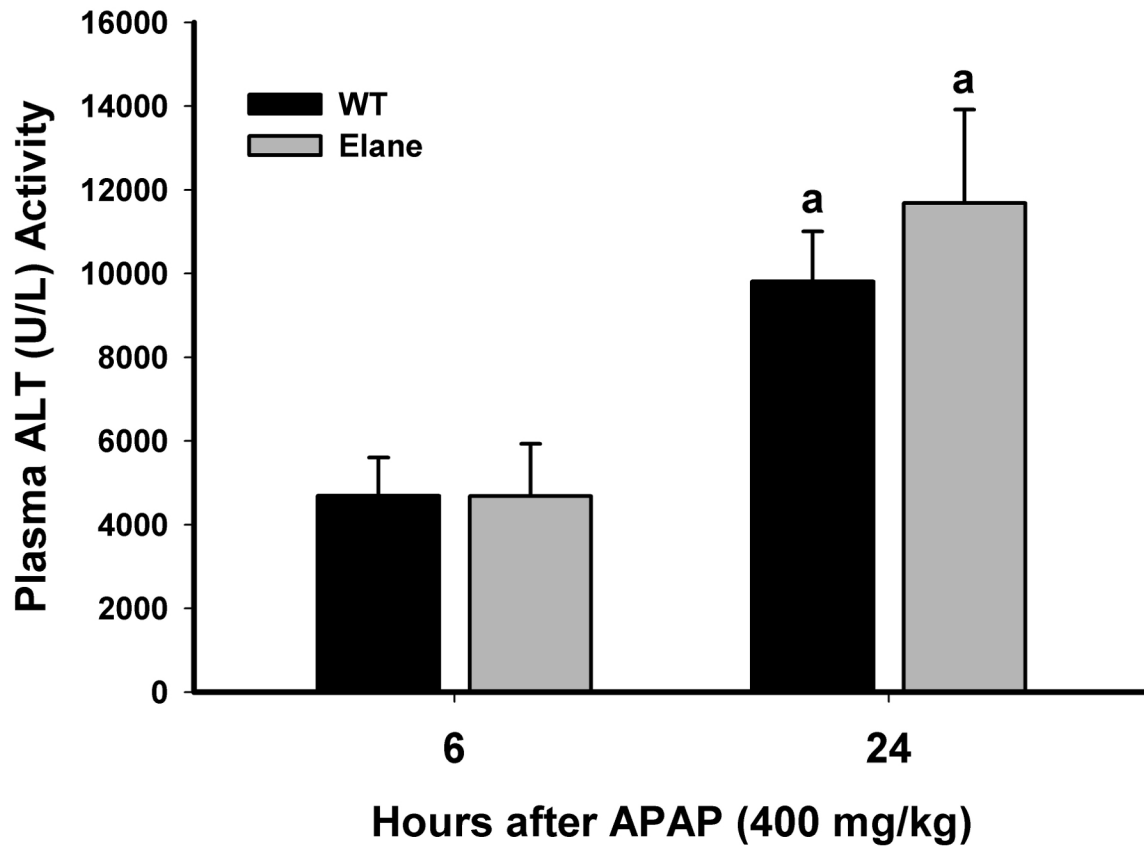


5.1.2 The role of HIF-1 α in an in vivo model of liver injury

The data presented in Chapter 2 indicated that EL and HX are critical to hepatocyte cell death in an in vitro model of liver injury. Furthermore, HIF-1 α appears to be an important mediator of cell death. As described in Chapter 1, EL and HX are implicated in the pathogenesis of hepatocyte death in a variety of liver conditions such as sepsis, I-R, and inflammation/drug models of idiosyncratic liver injury. However, neither EL nor HIF-1 α have been investigated in a widely-studied model of liver injury, APAP overdose. The role of PMNs in APAP-induced liver injury is controversial (described in Section 4.5), yet it is accepted that they are involved in removal of dead cells and HPC regeneration after APAP overdose. To determine if EL contributes to HPC necrosis and liver failure after APAP overdose, EL knockout mice (available from Jackson Laboratories) were treated with 400 mg/kg APAP, and liver injury was assessed at 6 and 24 hrs. EL knockout did not protect mice from APAP overdose (Figure 31). This indicates that EL does not contribute to HPC necrosis in APAP overdose and is consistent with previous reports that PMNS are not involved in the progression of liver injury (68, 185).

Figure 31: Genetic knockout of neutrophil EL does not protect from APAP overdose. Eight week old male C57/BL6/J and Elane (EL -/-) mice were fasted overnight and treated with 400 mg/kg APAP ip. Blood was collected 6 and 24 hrs after treatments and plasma was assessed for alanine aminotransferase (ALT) activity. Data represents mean \pm SEM of n=5 animals per group. a: $p < 0.05$ vs same genotype at 6 hrs.

Figure 31



There is evidence in the literature that HX, and specifically HIF-1 α , might play a role in APAP overdose. Activation of the coagulation system, which can result in liver ischemia and consequent tissue hypoxia, is important to the progression of APAP-induced hepatotoxicity [discussed in Chapter 4 and (50)]. Furthermore APAP overdose caused hepatic HIF-1 α accumulation (77) and HX (17). Therefore, I tested the hypothesis that HIF-1 α contributes to the progression of APAP-induced liver injury.

HIF-1 α deletion significantly protected mice from APAP overdose 6 hrs after treatment, however animals developed severe liver injury by 24 hrs (Figure 23), suggesting that HIF-1 α might play a damaging role in the progression of liver injury, but a protective role at later times. Interestingly, APAP overdose did not increase hepatic BNIP3 expression, and HIF-1 α deletion had no effect on BNIP3 (Table 5), suggesting that HIF-1 α does not contribute to hepatocyte death through transcription of a cell death protein in this model. Bax-mediated MPTP and release of nonspecific endonucleases is important to the mechanism of APAP hepatotoxicity (7). HIF-1 α deletion attenuated APAP-induced translocation of Bax to the mitochondria (Figure 24) and also attenuated DNA fragmentation (Figure 25).

The role of HIF-1 α in coagulation system activation by APAP overdose was also assessed. HIF-1 α deletion attenuated thrombin generation and hepatic fibrin deposition caused by APAP overdose (Figure 26), suggesting that HIF-1 α is involved in thrombin generation directly, or that it is required for hepatocyte (or other cell) injury that stimulates the activation of the intrinsic coagulation cascade. Furthermore, HIF-1 α deletion attenuated the expression of PAI-1 6 hrs after overdose (Figure 27 and Table

6). PAI-1 inhibits fibrinolysis and thus stabilizes fibrin clots, which might partially explain why there is less fibrin deposition in HIF-1 α deficient mice.

As noted above, the role of inflammation and PMNs in APAP overdose is controversial. However, HIF-1 α is an important mediator of cytokine production (32) and PMN function (132) and its role in the sterile inflammatory response caused by APAP overdose was investigated. HIF-1 α signaling contributes to the production of proinflammatory cytokines TNF α , IL-6, IL-12, and IL-1 α and IL-1 β in monocytes and macrophages (131). HIF-1 α deletion reduced both plasma and hepatic concentrations of the chemokine IL-8/KC (Table 7 and Figure 27) and the pro-inflammatory cytokine IL-6 (Table 7). Furthermore, hepatic PMN accumulation was attenuated in HIF-1 α -deficient mice compared to wild type controls 6 and 24 hrs after APAP overdose (Figure 29). These data suggest that HIF-1 α might contribute to the inflammatory response that accompanies APAP overdose.

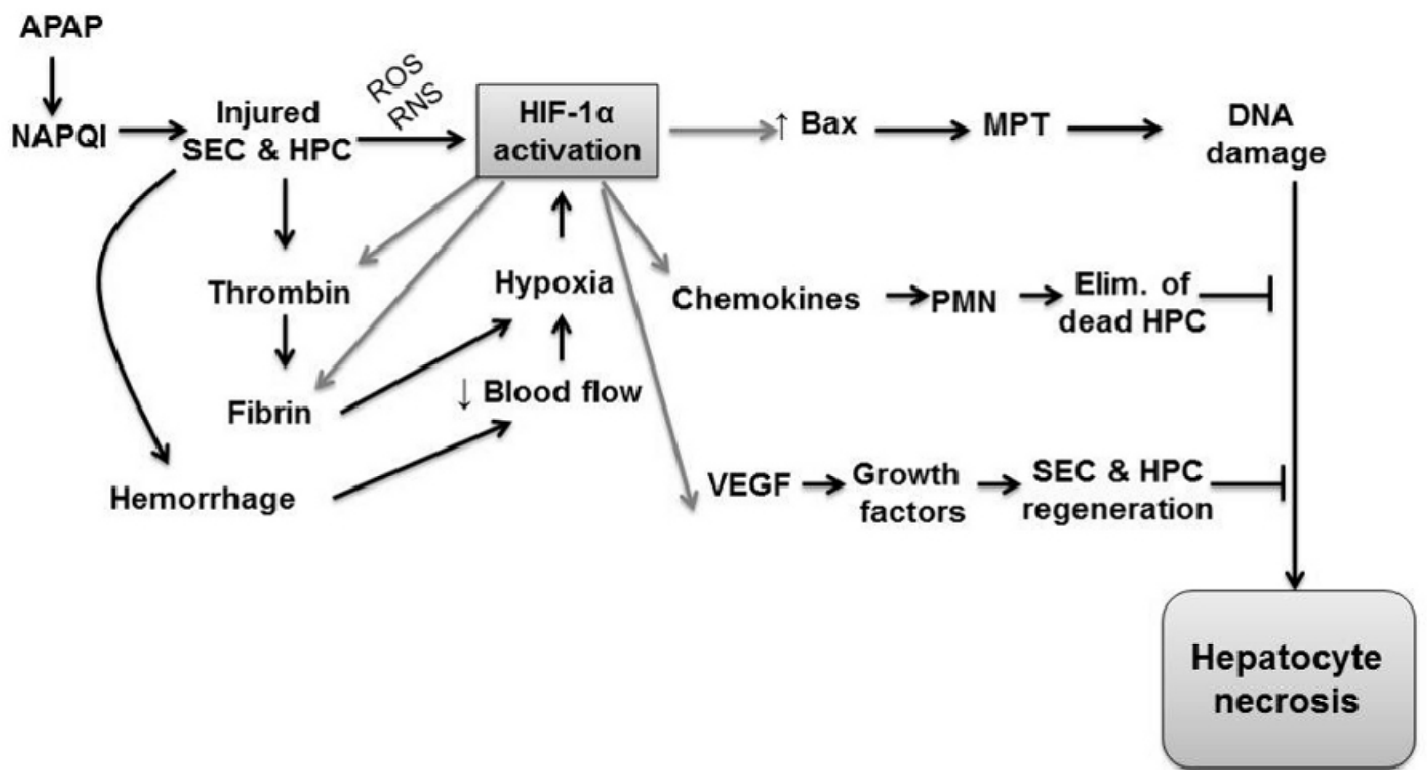
Although HIF-1 α deficiency was associated with less injury 6 hr after APAP exposure, there was significant liver injury in HIF-1 α -deficient mice 24 hrs after APAP overdose that was not different from animals with normal HIF-1 α expression (Figure 23). This suggested that HIF-1 α might have a dual role in APAP overdose. Initially, it contributes to the progression of injury through modulation of the pathways described above. HIF-1 α deletion might merely delay the progression of APAP hepatotoxicity, which may explain severe liver injury seen in HIF-1 α deficient mice at 24 hrs. Alternatively, we hypothesized that at later times, HIF-1 α is involved in the initiation of repair and regeneration after APAP overdose. Hepatic PMN accumulation during APAP overdose contributes phagocytosis of dead hepatocytes and initiation of hepatic repair

pathways. HIF-1 α signaling is required for PMN phagocytic function (132), and there were fewer PMNs in the livers of APAP-treated HIF-1 α -deficient mice at 24 hrs (Figure 29), suggesting reduced tissue repair capacity in these animals. Another pathway that is important for recovery from APAP overdose is VEGF signaling. Others have demonstrated that APAP overdose increased hepatic VEGF expression and that activation of the VEGF receptor activates regeneration pathways (40). VEGF production is mediated in part by HIF-1 α , and it is possible that there is reduced VEGF signaling in HIF-1 α -deficient animals.

To summarize, HIF-1 α deletion protected mice from APAP-induced hepatocellular injury (Figure 23), Bax activation (Figure 24), DNA damage (Figure 25), coagulation system activation (Figure 26) and inflammation (Figure 27 and Figure 29) at 6 hrs, yet no protection was evident by 24 hrs, suggesting that HIF-1 α has a dual role. The proposed role for HIF-1 α in APAP overdose is presented in Figure 32 .

Figure 32: The proposed dual role of HIF-1 α in APAP overdose. See section 5.1.2 for a detailed description of the signaling pathways depicted.

Figure 32



5.2 Considerations for in vitro and cell culture experiments

The initial intent of this dissertation was to study the mechanism of the interaction of HX and EL in primary rat HPCs, not a transformed hepatocyte cell line. However, primary HPCs proved to be a difficult model in which to work. For instance, there was a lot of day-to-day inconsistency in the viability of isolated HPCs. This led to variability among experiments and loss of productivity. This caused me to look for a more consistent model in which to study the HX/EL interaction, and I began to research transformed hepatic cell lines.

I initially began working with the human hepatoma HepG2. These cells had been used extensively to study HX signaling, especially regarding the role of HX in mitochondrial ROS production and HIF-1 α activation (described in detail in Section 1.2.4). However, initial experiments indicated that they were not sensitive to the HX/EL-interaction, so they were not similar to primary rat HPCs.

I then moved onto Hepa1c1c7 cells line, which is a murine hepatoma cell line. The role of HX and HIF-1 α signaling had been characterized in Hepa1c1c7 cells, and the advantage to these cells is that the HIF-1 β /ARNT-deficient derivative, HepaC4 cell line, is commercially available. Initial experiments indicated that Hepa1c1c7 cells were sensitive to EL-mediated cell death at EL concentrations that were relevant to the studies in primary HPCs. Furthermore, HX enhanced the cytotoxicity of EL, which suggested that these would be a valuable model to utilize.

The Hepa1c1c7 cells initially proved to be a very consistent experimental model. There was some variability in the strength of the interaction between HX and EL,

however, this was later attributed to passage number. We found that the HX/EL interaction was most consistent and robust between passages 12 and 20. Unfortunately, there have been prolonged periods of time in which the HX/EL interaction model did not reproduce. During these times, every component of the model system was assessed for consistency, including the growth medium and fetal bovine serum used for cell maintenance, the enzyme activity of EL, the reagents used in the cell death assay, and the calibration of the hypoxia chambers. We later determined that our cell culture room had a modest contamination issue involving mycoplasma and other bacteria. The microbial contamination was not detectable by visual inspection of cultures using phase contrast microscopy. Once the contamination was resolved and new cell culture stocks were obtained, the interaction between HX and EL returned and results were consistent.

This indicates the importance of maintaining sterile conditions in a shared tissue culture facility. Despite using aseptic techniques and maintaining separate bottles of growth medium, cell stocks and incubator space, my cultures and frozen stocks became contaminated, and this affected the outcome of my experiments for a prolonged period of time. Currently, cell cultures are monitored for signs of contamination after they are thawed from frozen stocks and before experiments are initiated.

The studies presented in Chapter 2 and Chapter 3 indicate that transformed hepatocyte lines can be a useful experimental tool. However, it is important to monitor cell passage number and do experiments within a small window of passages for consistent results. Furthermore, sterile tissue culture technique is crucial to successful in vitro studies.

5.3 Major findings and implications

1. HX interacts with EL to cause cell death in Hepa1c1c7 cells. This observation has been published in primary rat HPCs (112). However, the development of this model in a murine cell line demonstrates that this phenomenon is not species-specific. It also demonstrates that a transformed cell line is a suitable model for in vitro studies involving HX.

2. EL enhances HX-mediated HIF-1 α accumulation and transcription of the cell death gene BNIP3. This suggests that BNIP3 might be a critical mediator of HPC death in models of liver injury in which HX and PMNs play a role. I-R increased hepatic BNIP3 protein, and knockdown protected mice from I-R injury (120). BNIP3 mRNA was also upregulated in the livers of LPS/RAN-treated rats (113) and LPS/monocrotaline (24), however it is not known if it contributes to liver injury in these models.

3. HX enhances EL-induced lipid peroxidation in Hepa1c1c7 cells, and a lipid soluble antioxidant attenuates lipid peroxidation and attenuates cell death. This indicates that lipid peroxidation is an important mediator of HPC injury, and its role could be investigated in sepsis, I-R and DILI.

4. P38 MAPK appears to be a central mediator of the interaction between HX and EL in hepatocytes. p38 signaling contributed to the cytotoxicity of HX/EL cotreatment, by enhancing HIF-1 α transactivation and lipid peroxidation. This indicates that p38 contributes to cell death signaling through modulation of multiple pathways, and is a potential therapeutic target for liver injury.

5. HIF-1 α contributes to the progression of HPC injury during APAP overdose through modulation of the hemostatic system, sterile inflammatory response, and mitochondrial cell death signaling. APAP overdose did not upregulate hepatic BNIP3 expression. This is interesting in light of evidence that EL is not involved in liver injury after APAP overdose and suggests that BNIP3 might play a more critical role in liver injury in models in which both HX and PMNs are involved, and be less important in situations where HX and HIF-1 α are involved without PMNs.

6. The data presented in Chapter 3 and 4 offers insight into the mechanism of HPC death caused by exposure to EL and HX. These findings are of particular interest to the treatment and prevention of liver injury in pathological conditions where PMNs and tissue HX are implicated, such as sepsis, I-R, cholestasis and drug-induced liver injury (see Section 1.5 for a more detailed discussion and listing of these conditions).

5.4 Knowledge gaps and future studies

The research described in Chapters 3 and 4 provide mechanistic insight into the mode of cell death caused by coexposure of hepatocytes to HX and EL. These findings provide information on modes of hepatocyte death in I-R, sepsis, drug-induced liver injury and other models of liver disease, and may offer therapeutic targets for the prevention of liver failure. The mechanism of this interaction was worked out entirely in the Hepa1c1c7 cell line, and it would be interesting to determine if these pathways play the same roles in primary human, rat and mouse HPCs.

The findings presented indicate that HIF-1 α signaling contributes to cell death after HX/EL cotreatment, and that it is required for BNIP3 production. However, it is unknown if BNIP3 signaling leads to cell death. Future studies could examine the role of BNIP3 in this interaction in vitro, and its role could also be investigated in inflammation/drug interaction models of idiosyncratic liver injury.

Another finding which requires further research is examination of lipid peroxidation. Oxidative stress was not observed in HX/EL-cotreated cells, thus the source of radicals for lipid peroxidation is not known. It is possible that a non-oxygen-centered radical is being produced and oxidizing lipids. Furthermore, it is unknown if lipid peroxidation is involved in liver injury after inflammation/drug coexposure.

The role of ATF2 and cyclin D1 in cell death caused by HX/EL cotreatment also requires further investigation. The mechanism by which HX/EL cotreatment selectively reduces phospho-ATF2 is not known. Furthermore, a direct link between AFT2 and cyclin D1 has not been established in these cells. There is also evidence in the

literature that HIF-1 α is a negative regulator of cyclin D1. Thus, it is important to determine the stimulus for downregulation of cyclin D1. Finally, the loss of cyclin D1 and dysregulation of the cell cycle has not been linked to cell death in this in vitro model. These pathways could also be investigated in in vivo models, and could indicate whether cell cycle dysregulation can contribute to liver injury.

The findings presented in Chapter 4 indicate that HIF-1 α can play multiple roles in liver injury and can contribute to early cell death signaling and progression events in APAP overdose. Furthermore, we hypothesized that HIF-1 α might be required for successful regeneration and repair after insult, through modulation of PMN function and VEGF-mediated hepatocyte growth. However, this role for HIF-1 α has not been investigated specifically. First, markers of hepatic regeneration, such as PCNA could be measured in HIF-1 α -deficient animals 24-48 hrs after APAP overdose. Second, hepatic VEGF mRNA and protein should be measured in HIF-1 α deficient animals 24 hrs after APAP. If VEGF is lower in HIF-1 α deficient animals compared to wild type controls, then animals could be treated with VEGF to determine if it rescues hepatic repair mechanisms.

It would also be interesting to determine the role of HIF-1 α in the various cell types involved in APAP overdose. In unpublished observations, a colleague has found that HPC-specific HIF-1 α deletion does not protect animals from APAP-induced liver injury (B. Copple, personal communication). The data presented in Chapter 4 indicate that HIF-1 α is important in cytokine production, PMN infiltration, and coagulation system activation. This suggests that HIF-1 α signaling plays an important role in nonparenchymal cell types and requires further investigation. Thus it would be

interesting to dissect its role by selective deletion of HIF-1 α in various liver cell types, such as KCs, PMNs and SECs.

REFERENCES

REFERENCES

1. **Andrade DR, Jr., Andrade DR, and dos Santos SA.** Study of Rat Hepatocytes in Primary Culture Submitted to Hypoxia and Reoxygenation: action of the cytoprotectors prostaglandin E1, superoxide dismutase, allopurinol, and verapamil. *Experimental Gastroenterology* 46: 333-340, 2009.
2. **Aoshiha K, Yasuda K, Yasui S, Tamaoki J, and Nagai A.** Serine proteases increase oxidative stress in lung cells. *American Journal of Physiology Lung Cellular and Molecular Biology* 281: L556-L564, 2001.
3. **Araki Y, Matsumiya M, Matsuura T, Kaibori M, Okumura T, Nishizawa M, and Kwon AH.** Sivelestat Suppresses iNOS Gene Expression in Proinflammatory Cytokine-Stimulated Hepatocytes. *DigDisSci* 2011.
4. **Arii S, Teramoto K, and Kawamura T.** Current progress in the understanding of and therapeutic strategies for ischemia and reperfusion injury of the liver. *Journal of Hepatobiliary and Pancreatic Surgery* 10: 189-194, 2003.
5. **Arteel GE, Iimuro Y, Yin M, Raleigh JA, and Thurman RG.** Chronic enteral ethanol treatment causes hypoxia in rat liver tissue in vivo. *Hepatology* 25: 920-926, 1997.
6. **Arteel GE, Raleigh JA, Bradford BU, and Thurman RG.** Acute alcohol produces hypoxia directly in rat liver tissue in vivo: role of Kupffer cells. *Am J Physiol* 271: G494-500, 1996.
7. **Bajt ML, Farhood A, Lemasters JJ, and Jaeschke H.** Mitochondrial bax translocation accelerates DNA fragmentation and cell necrosis in a murine model of acetaminophen hepatotoxicity. *JPharmacolExpTher* 324: 8-14, 2008.
8. **Bajt ML, Yan H-M, Farhood A, and Jaeschke H.** Plasminogen Activator Inhibitor-1 Limits Liver Injury and Facilitates Regeneration after Acetaminophen Overdose. *Toxicological Sciences* 104: 419-427, 2008.
9. **Barrett KE, Barman SM, Boitano S, and Brooks H.** *Ganong's Review of Medical Physiology*. The McGraw-Hill Companies, Inc., 2010.
10. **Belaouaj A, McCarthy R, Baumann M, Gao Z, Ley T, Abraham S, and Shapiro S.** Mice lacking neutrophil elastase reveal impaired host defense against gram negative bacterial sepsis. *Nature Medicine* 4: 615-618, 1998.
11. **Bernhardt WM, Warnecke C, Willam C, Tanaka T, Wiesener MS, and Eckardt KU.** Organ protection by hypoxia and hypoxia-inducible factors. *Methods Enzymol* 435: 221-245, 2007.

12. **Bhoumik A, Lopez-Bergami P, and Ronai Z.** ATF2 on the double - activating transcription factor and DNA damage response protein. *Pigment Cell Research* 20: 498-506, 2007.
13. **Birrer R, Takuda Y, and Takara T.** Hypoxic hepatopathy: pathophysiology and prognosis. *InternMed* 46: 1063-1070, 2007.
14. **Carmeliet P, Dor Y, Herbert JM, Fukumura D, Brusselmans K, Dewerchin M, Neeman M, Bono F, Abramovitch R, Maxwell P, Koch CJ, Ratcliffe P, Moons L, Jain RK, Collen D, and Keshert E.** Role of HIF-1alpha in hypoxia-mediated apoptosis, cell proliferation and tumour angiogenesis. *Nature* 394: 485-490, 1998.
15. **Chandel N, Maltepe E, Goldwasser E, Mathieu C, Simon M, and Schumacker P.** Mitochondrial reactive oxygen species trigger hypoxia-induced transcription. *Proceedings of the National Academy of Sciences* 95: 11715-11720, 1998.
16. **Chandel N, McClintock DS, Feliciano CE, Wood TM, Melendez JA, Rodriquez AM, and Schwacha M.** Reactive oxygen species generated at mitochondrial complex III stabilize hypoxia-inducible factor-1alpha during hypoxia: a mechanism of O₂ sensing. *Journal of Biological Chemistry* 275: 25130-25138, 2000.
17. **Chaudhuri S, McCullough SS, Hennings L, Letzig L, Simpson PM, Hinson JA, and James LP.** Acetaminophen hepatotoxicity and HIF-1alpha induction in mice occur without hypoxia. *Toxicology and Applied Pharmacology* 252: 211-220, 2011.
18. **Chen HC, Lin HC, Liu CY, Wang CH, Hwang T, Huang TT, Lin CH, and Kuo HP.** Neutrophil elastase induces IL-8 synthesis by lung epithelial cells via the mitogen-activated protein kinase pathway. *JBiomedSci* 11: 49-58, 2004.
19. **Chien KR, Abrams J, Serroni A, Martin JT, and Farber JL.** Accelerated phospholipid degradation and associated membrane dysfunction in irreversible, ischemic liver cell injury. *Journal of Biological Chemistry* 253: 4809-4817, 1978.
20. **Choi SM, Oh H, and Park H.** Microarray analyses of hypoxia-regulated genes in an aryl hydrocarbon receptor nuclear translocator (Arnt)-dependent manner. *FEBS Journal* 275: 5618-5634, 2008.
21. **Chu W, Li X, Li C, Wan L, Shi H, Song X, Liu X, Chen X, Zhang C, Shan H, Lu Y, and Yang B.** TGFBR3, a potential negative regulator of TGF-beta signaling, protects cardiac fibroblasts from hypoxia-induced apoptosis. *Journal of Cellular Physiology* 226: 2586-2594, 2011.
22. **Chua YL, Dufour E, Dassa EP, Rustin P, Jacobs HT, Taylor CT, and Hagen T.** Stabilization of hypoxia-inducible factor-1alpha protein in hypoxia occurs independently of mitochondrial reactive oxygen species production. *The Journal of Biological Chemistry* 285: 31277-31284, 2010.

23. **Conrad PW, Rust RT, Han J, Millhorn DE, and Beitner-Johnson D.** Selective activation of p38alpha and p38gamma by hypoxia. Role in regulation of cyclin D1 by hypoxia in PC12 cells. *JBiolChem* 274: 23570-23576, 1999.
24. **Copple B, Rondelli C, Maddox J, Hoglen N, Ganey P, and Roth R.** Modes of Cell Death in Rat Liver after Monocrotaline Exposure. *Toxicological Sciences* 77: 172-182, 2004.
25. **Copple BL.** Hypoxia stimulates hepatocyte epithelial to mesenchymal transition by hypoxia-inducible factor and transforming growth factor-beta-dependent mechanisms. *Liver Int* 30: 669-682, 2010.
26. **Copple BL, Bai S, and Moon JO.** Hypoxia-inducible factor-dependent production of profibrotic mediators by hypoxic Kupffer cells. *HepatoRes* 40: 530-539, 2010.
27. **Copple BL, Banes A, Ganey PE, and Roth RA.** Endothelial cell injury and fibrin deposition in rat liver after monocrotaline exposure. *ToxicoSci* 65: 309-318, 2002.
28. **Copple BL, Bustamante J, Welch T, Kim ND, and Moon JO.** Hypoxia-inducible factor-dependent production of profibrotic mediators by hypoxic hepatocytes. *Liver International* 29: 1010-1021, 2009.
29. **Copple BL, Roth R, and Ganey P.** Anticoagulation and inhibition of nitric oxide synthase influence hepatic hypoxia after monocrotaline exposure. *Toxicology* 225: 128-137, 2006.
30. **Copple BL, Woolley B, Rondelli C, Ganey P, and Roth R.** Activation of signal transduction pathways in hepatic parenchymal cells are required for neutrophil-dependent killing. *The Toxicologist* 98: 200, 2003.
31. **Cover C, Liu J, Farhood A, Malle E, Waalkes MP, Bajt ML, and Jaeschke H.** Pathophysiological role of the acute inflammatory response during acetaminophen hepatotoxicity. *Toxicology and Applied Pharmacology* 216: 98-107, 2006.
32. **Cramer T, Yamanishi Y, Clausen B, Forster I, Pawlinski R, Mackman N, Haase V, Jaenisch R, Corr M, Nizet V, Firestein G, Gerber HP, and Ferrar N.** HIF-1alpha Is Essential for Myeloid Cell-Mediated Inflammation. *Cell* 112: 645-657, 2003.
33. **Cummins EP, and Taylor CT.** Hypoxia-responsive transcription factors. *European Journal of Physiology* 450: 363-371, 2005.
34. **Cursio R, Miele C, Filippa N, Van OE, and Gugenheim J.** Liver HIF-1 alpha induction precedes apoptosis following normothermic ischemia-reperfusion in rats. *TransplantProc* 40: 2042-2045, 2008.

35. **Dahm LJ, Schultze AE, and Roth RA.** An antibody to neutrophils attenuates alpha-naphthylisothiocyanate-induced liver injury. *JPharmacolExpTher* 256: 412-420, 1991.
36. **Deng X, Liguori M, Sparkenbaugh E, Waring J, Blomme EAG, Ganey P, and Roth R.** Gene Expression Profiles in Livers from Diclofenac-Treated Rats Reveal Intestinal Bacteria-Dependent and -Independent Pathways Associated with Liver Injury. *Journal of Pharmacology and Experimental Therapeutics* 327: 634-644, 2008.
37. **Deng X, Luyendyk J, Zou W, Lu J, Malle E, Ganey P, and Roth R.** Neutrophil Interaction with the Hemostatic System Contributes to Liver Injury in Rats Cotreated with Lipopolysaccharide and Ranitidine. *Journal of Pharmacology and Experimental Therapeutics* 322: 552-861, 2007.
38. **Deng X, Stachlewitz R, Liguori M, Blomme EAG, Waring J, Luyendyk J, Maddox J, Ganey P, and Roth R.** Modest Inflammation Enhances Diclofenac Hepatotoxicity in Rats: Role of Neutrophils and Bacterial Translocation. *Journal of Pharmacology and Experimental Therapeutics* 319: 1-9, 2006.
39. **Devi SS, and Mehendale HM.** Disrupted G1 to S phase clearance via cyclin signaling impairs liver tissue repair in thioacetamide-treated type 1 diabetic rats. *Toxicology and Applied Pharmacology* 207: 89-102, 2005.
40. **Donahower B, McCullough SS, Kurten R, Lamps LW, Simpson P, Hinson JA, and James LP.** Vascular endothelial growth factor and hepatocyte regeneration in acetaminophen toxicity. *AmJPhysiol GastrointestLiver Physiol* 291: G102-G109, 2006.
41. **Dugan CM, MacDonald AE, Roth RA, and Ganey PE.** A mouse model of severe halothane hepatitis based on human risk factors. *JPharmacolExpTher* 333: 364-372, 2010.
42. **Fairbanks KD, and Tavill AS.** Liver disease in alpha 1-antitrypsin deficiency: a review. *AmJGastroenterol* 103: 2136-2141, 2008.
43. **Faurschou M, and Borregaard N.** Neutrophil granules and secretory vesicles in inflammation. *Microbes and Infection* 5: 1317-1327, 2003.
44. **Fernandez-Checa JC.** Redox regulation and signaling lipids in mitochondrial apoptosis. *BiochemBiophysRes Commun* 304: 471-479, 2003.
45. **Fischer BM, Cuellar JG, Diehl ML, deFreytas AM, Zhang J, Carraway KL, and Voynow JA.** Neutrophil elastase increases MUC4 expression in normal human bronchial epithelial cells. *Am JPhysiol Lung Cell MolPhysiol* 284: L671-L679, 2003.
46. **Fischer BM, and Voynow JA.** Neutrophil elastase induces MUC5AC gene expression in airway epithelium via a pathway involving reactive oxygen species. *Am*

JRespirCell MolBiol 26: 447-452, 2002.

47. **Fong CC, Zhang Q, Shi YF, Wu R, Fong WF, and Yang M.** Effect of hypoxia on RAW264.7 macrophages apoptosis and signaling. *Toxicology* 235: 52-61, 2007.

48. **Fouassier L, Beaussier M, Schiffer E, Rey C, Barbu V, Mergey M, Wendum D, Callard P, Scoazec JY, Lasnier E, Stieger B, Lienhart A, and Housset C.** Hypoxia-induced changes in the expression of rat hepatobiliary transporter genes. *AmJPhysiol GastrointestLiver Physiol* 293: G25-G35, 2007.

49. **Gando S, Hayakawa M, Sawamura A, Hoshino H, Oshiro A, Kubota N, and Jesmin S.** The activation of neutrophil elastase-mediated fibrinolysis is not sufficient to overcome the fibrinolytic shutdown of disseminated intravascular coagulation associated with systemic inflammation. *ThrombRes* 121: 67-73, 2007.

50. **Ganey P, Luyendyk J, Newport SW, Eagle TM, Maddox J, Mackman N, and Roth R.** Role of the coagulation system in acetaminophen-induced hepatotoxicity in mice. *Hepatology* 46: 1177-1186, 2007.

51. **Ginzberg H, Shannon PT, Suzuki T, Hong O, Vachon E, Moraes T, Herrera Abreu MT, Cherepanov V, Wang X, Chow CW, and Downey GP.** Leukocyte elastase induces epithelial apoptosis: role of mitochondrial permeability changes and Akt. *American Journal of Physiology Gastrointestinal and Liver Physiology* 287: G286-G298, 2004.

52. **Goda N, Ryan HE, Khadivi B, McNulty W, Rickert RC, and Johnson RS.** Hypoxia-inducible factor 1alpha is essential for cell cycle arrest during hypoxia. *MolCell Biol* 23: 359-369, 2003.

53. **Gonzalez-Rubio S, Hidalgo AB, Ferrin G, Bello RI, Gonzalez R, Gahete MD, Ranchal I, Rodriguez BA, Barrera P, Aguilar-Melero P, Linares CI, Castano JP, Victor VM, De la Mata M, and Muntane J.** Mitochondrial-driven ubiquinone enhances extracellular calcium-dependent nitric oxide production and reduces glycochenodeoxycholic acid-induced cell death in hepatocytes. *Chemical research in toxicology* 22: 1984-1991, 2009.

54. **Gorlach A, Diebold I, Schini-Kerth VB, Berchner-Pfannschmidt U, Roth U, Brandes RP, Kietzmann T, and Busse R.** Thrombin activates the hypoxia-inducible factor-1 signaling pathway in vascular smooth muscle cells: Role of the p22(phox)-containing NADPH oxidase. *CircRes* 89: 47-54, 2001.

55. **Gujral J, Bucci T, Farhood A, and Jaeschke H.** Mechanism of Cell Death During Warm Hepatic Ischemia-Reperfusion in Rats: Apoptosis or Necrosis. *Hepatology* 33: 397-405, 2001.

56. **Gujral J, Farhood A, Bajt ML, and Jaeschke H.** Neutrophils Aggravate Acute Liver Injury During Obstructive Cholestasis in Bile Duct-Ligated Mice. *Hepatology* 38: 355-363, 2003.
57. **Guzy RD, Hoyos B, Robin E, Chen H, Liu L, Mansfield KD, Simon MC, Hammerling U, and Schumacker P.** Mitochondrial Complex III is required for hypoxia-induced ROS production and cellular oxygen sensing. *Cell Metabolism* 1: 401-408, 2005.
58. **Harbrecht BG, Billiar T, Curran RD, Stadler J, and Simmons RL.** Hepatocyte injury by activated neutrophils in vitro is mediated by proteases. *Annals of Surgery* 218: 120-128, 1993.
59. **Herman B, Nieminen AL, Gores GJ, and Lemasters JJ.** Irreversible injury in anoxic hepatocytes precipitated by an abrupt increase in plasma membrane permeability. *FASEB J* 2: 146-151, 1988.
60. **Heutinck KM, ten BI, Hack CE, Hamann J, and Rowshani AT.** Serine proteases of the human immune system in health and disease. *MolImmunol* 47: 1943-1955, 2010.
61. **Hill DA, and Roth RA.** Alpha-naphthylisothiocyanate causes neutrophils to release factors that are cytotoxic to hepatocytes. *ToxicolAppPharmacol* 148: 169-175, 1998.
62. **Hirsila M, Koivunen P, Xu L, Seeley T, Kivirikko KL, and Myllyharu J.** Effect of desferrioxamine and metals on the hydroxylases in the oxygen sensing pathway. *FASEB J* 19: 1308, 2005.
63. **Ho J, Buchweitz J, Roth RA, and Ganey P.** Identification of factors from rat neutrophils responsible for cytotoxicity to isolated hepatocytes. *Journal of Leukocyte Biology* 59: 716-724, 1996.
64. **Holme JA, Gorria M, Arlt VM, Ovrebo S, Solhaug A, Tekpli X, Landvik NE, Huc L, Fardel O, and Lagadic-Gossmann D.** Different mechanisms involved in apoptosis following exposure to benzo[a]pyrene in F258 and Hepa1c1c7 cells. *Chemico-Biological Interactions* 167: 41-55, 2007.
65. **Hughes SJ, Yang W, Juszczak M, Jones GL, Powis SH, Seifalian AM, and Press M.** Effect of inspired oxygen on portal and hepatic oxygenation: effective arterialization of portal blood by hyperoxia. *Cell Transplant* 13: 801-808, 2004.
66. **Ishida Y, Kondo T, Ohshima T, Fujiwara H, Iwakura Y, and Mukaida N.** A Pivotal Involvement of IFN-gamma in the Pathogenesis of Acetaminophen-induced Acute Liver Injury. *FASEB J* 16: 1227-1236, 2002.

67. **Ishida Y, Kondo T, Tsuneyama K, Lu P, Takayasu T, and Mukaida N.** The pathogenic roles of tumor necrosis factor receptor p55 in acetaminophen-induced liver injury in mice. *Journal of Leukocyte Biology* 75: 59-67, 2004.
68. **Jaeschke H.** How relevant are Neutrophils for Acetaminophen Hepatotoxicity. *Hepatology* 43: 1191-1194, 2006.
69. **Jaeschke H.** Innate Immunity and Acetaminophen -Induced Liver Injury: Why So Many Controversies? *Hepatology* 48: 699-701, 2008.
70. **Jaeschke H.** Mechanisms of Liver Injury. II. Mechanisms of neutrophil-induced liver cell injury during hepatic ischemia-reperfusion and other acute inflammatory conditions. *American Journal of Physiology Gastrointestinal and Liver Physiology* 290: G1083-G1088, 2006.
71. **Jaeschke H.** Molecular Mechanisms of hepatic ischemia-reperfusion injury and preconditioning. *American Journal of Physiology Gastrointestinal and Liver Physiology* 284: G15-G26, 2003.
72. **Jaeschke H.** Toxic Responses of the Liver. In: *Cassarett and Doull's Toxicology - The Basic Science of Poisons*, edited by Klaassen CDMcGraw-Hill, 2008, p. 557-582.
73. **Jaeschke H, and Bajt ML.** REVIEW: Intracellular Signaling Mechanisms of Acetaminophen-Induced Liver Cell Death. *Toxicological Sciences* 89: 31-41, 2006.
74. **Jaeschke H, Farhood A, Fisher MA, and Smith CW.** Sequestration of neutrophils in the hepatic vasculature during endotoxemia is independent of beta 2 integrins and intercellular adhesion molecule-1. *SHOCK* 6: 351-356, 1996.
75. **Jaeschke H, and Lemasters JJ.** Apoptosis Versus Oncotic Necrosis in Hepatic Ischemia/Reperfusion Injury. *Gastroenterology* 125: 1246-1257, 2003.
76. **Jaeschke H, and Smith CW.** Mechanisms of neutrophil-induced parenchymal cell injury. *Journal of Leukocyte Biology* 61: 647-653, 1997.
77. **James LP, Donahower B, Burke A, McCullough S, and Hinson JA.** Induction of the nuclear factor HIF-1alpha in acetaminophen toxicity: Evidence for oxidative stress. *Biochemical and Biophysical Research Communication* 343: 171-176, 2006.
78. **James LP, Simpson PM, Farrar HC, Kearns GL, Wasserman GS, Blumer JL, Reed MD, Sullivan JE, and Hinson JA.** Cytokines and Toxicity in Acetaminophen Overdose. *Journal of Clinical Pharmacology* 45: 1165-1171, 2005.
79. **James LP, Wells E, Beard RH, and Farrar HC.** Predictors of outcome after acetaminophen poisoning in children and adolescents. *The Journal of Pediatrics* 140: 522-526, 2002.

80. **James PE, Madhani M, Roebuck W, Jackson S, and Swartz H.** Endotoxin-Induced Liver Hypoxia: Defective Oxygen Delivery Versus Oxygen Consumption. *Nitric Oxide* 6: 18-28, 2002.
81. **Jeong H-J, Hong S-H, Park R-K, Shin T, An N-H, and Kim H-M.** Hypoxia-induced IL-6 production is associated with activation of MAP kinase, HIF-1, and NF- κ B on HEI-OC1 cells. *Hearing Research* 207: 59-67, 2005.
82. **Jewell UR, Kvietikova I, Scheid A, Bauer C, Wenger RH, and Gassmann M.** Induction of HIF-1 α in response to hypoxia is instantaneous. *FASEB J* 15: 1312-1314, 2001.
83. **Jin K, Mao XO, Zhu Y, and Greenberg D.** MEK and ERK protect hypoxic cortical neurons via phosphorylation of Bad. *J Neurochem* 80: 119-125, 2002.
84. **Johnson GL, and Lapadat R.** Mitogen-Activated Protein Kinase Pathways Mediated by ERK, JNK, and p38 Protein Kinases. *Science* 298: 1911-1912, 2002.
85. **Jollow DJ, Mitchell JR, Potter WZ, Davis DC, Gillette JR, and Brodie BB.** Acetaminophen-induced hepatic necrosis. II. Role of covalent binding in vivo. *JPharmacolExpTher* 187: 195-202, 1973.
86. **Joo JH, Kim JW, Lee Y, Yoon SY, Kim JH, Paik SG, and Choe IS.** Involvement of NF- κ B in the regulation of S100A6 gene expression in human hepatoblastoma cell line HepG2. *Biochemical and Biophysical Research Communications* 307: 274-280, 2003.
87. **Jungermann K, and Kietzmann T.** Oxygen: Modulator of Metabolic Zonation and Disease of the Liver. *Hepatology* 31: 255-260, 2000.
88. **Kakita T, Suzuki M, Takeuchi H, Unno M, and Matsuno S.** Significance of xanthine oxidase in the production of intracellular oxygen radicals in an in-vitro hypoxia-reoxygenation model. *J Hepatobiliary Pancreat Surg* 9: 249-255, 2002.
89. **Karhausen J, Haase VH, and Colgan SP.** Inflammatory Hypoxia: Role of Hypoxia-Inducible Factor. *Cell Cycle* 4: 256-268, 2005.
90. **Kato T, Ito Y, Hosono K, Suzuki T, Tamaki H, Minamino T, Kato S, Sakagami H, Shibuya M, and Majima M.** Vascular endothelial growth factor receptor-1 signaling promotes liver repair through restoration of liver microvasculature after acetaminophen hepatotoxicity. *ToxicolSci* 120: 218-229, 2011.
91. **Kewley RJ, Whitelaw ML, and Chapman-Smith A.** The mammalian basic-helix-loop-helix/PAS family of transcriptional regulators. *The International Journal of Biochemistry and Cell Biology* 36: 189-204, 2004.

92. **Khan S, and O'Brien PJ.** Modulating hypoxia-induced hepatocyte injury by affecting intracellular redox state. *Biochimica et Biophysica Acta* 1269: 153-161, 1995.
93. **Kietzmann T, and Gorkach A.** Reactive oxygen species in the control of hypoxia-inducible factor-mediated gene expression. *Seminars in Cell & Developmental Biology* 16: 474-486, 2005.
94. **Kim MJ, Oh SJ, Park SH, Kang HJ, Won MH, Kang TC, Hwang IK, Park JB, Kim JI, Kim J, and Lee JY.** Hypoxia-induced cell death of HepG2 cells involves a necrotic cell death mediated by calpain. *Apoptosis* 12: 707-718, 2007.
95. **Klimova TA, and Chandel N.** Mitochondrial Complex III regulates hypoxia activation of HIF. *Cell Death and Differentiation* 15: 660-666, 2008.
96. **Kodali P, Wu P, Lahiji PA, Brown EJ, and Maher JJ.** ANIT toxicity toward mouse hepatocytes in vivo is mediated primarily by neutrophils via CD18. *Am J Physiol Gastrointest Liver Physiol* 291: G355-G363, 2006.
97. **Korkmaz B, Moreau T, and Gauthier F.** Neutrophil elastase, proteinase 3, and cathepsin G: Physicochemical properties, activity and physiopathological functions. *Biochimie* 90: 227-242, 2008.
98. **Kuwahara I, Lillehoj EP, Lu W, Singh IS, Isohama Y, Miyata T, and Kim KC.** Neutrophil elastase induces IL-8 gene transcription and protein release through p38/NF- κ B activation via EGFR transactivation in a lung epithelial cell line. *Am J Physiol Lung Cell Mol Physiol* 291: L407-L416, 2006.
99. **Kwon AH, and Qiu Z.** Neutrophil elastase inhibitor prevents endotoxin-induced liver injury following experimental partial hepatectomy. *Br J Surg* 94: 609-619, 2007.
100. **Lasnier E, Blanc MC, Housset C, Rey C, Roch-Arveiller M, and Vaubourdolle M.** Cytotoxic response of sinusoidal endothelial cells to polymorphonuclear leukocytes and its potential implication in hypoxia-reoxygenation injury. *Liver* 22: 495-500, 2002.
101. **Lawson JA, Farhood A, Hopper RD, Bajt ML, and Jaeschke H.** The Hepatic Inflammatory Response after Acetaminophen Overdose: Role of Neutrophils. *Toxicological Sciences* 54: 509-516, 2000.
102. **Lee K, Roth R, and LaPres J.** Hypoxia, drug therapy and toxicity. *Pharmacology and Therapeutics* 113: 229-246, 2007.
103. **Lee SH, Bahn JH, Whitlock NC, and Baek SJ.** Activating transcription factor 2 (ATF2) controls tolfenamic acid-induced ATF3 expression via MAP kinase pathways. *Oncogene* 29: 5182-5192, 2010.

104. **Lee WM.** Acetaminophen toxicity: changing perceptions on a social/medical issue. *Hepatology* 46: 966-970, 2007.
105. **Leeper-Woodford S, and Detmer K.** Acute hypoxia increases alveolar macrophage tumor necrosis factor activity and alters NF-kB expression. *American Journal Physiology: Lung Cellular and Molecular Biology* 20: L909-L916, 1999.
106. **Lemasters J, Qian T, Bradham CA, Brenner D, Cascio WE, Trost LC, Nishimura Y, Nieminen AL, and Herman B.** Mitochondrial Dysfunction in the Pathogenesis of Necrotic and Apoptotic Cell Death. *Journal of Bioenergetics and Biomembranes* 31: 305-319, 1999.
107. **Lemasters JJ, DiGuseppi J, Nieminen AL, and Herman B.** Blebbing, free Ca²⁺ and mitochondrial membrane potential preceding cell death in hepatocytes. *Nature* 325: 78-81, 1987.
108. **Li L, Chen SH, Zhang Y, Yu CH, Li SD, and Li YM.** Is the hypoxia-inducible factor-1 alpha mRNA expression activated by ethanol-induced injury, the mechanism underlying alcoholic liver disease? *HepatobiliaryPancreatDisInt* 5: 560-563, 2006.
109. **Li Z, and Diehl AM.** Innate immunity in the liver. *Curr Opin Gastroenterol* 19: 565-571, 2003.
110. **Liu Z-X, Han D, Gunawan B, and Kaplowitz N.** Neutrophil Depletion Protects Against Murine Acetaminophen Hepatotoxicity. *Hepatology* 43: 1220-1230, 2006.
111. **Lluis J, Morales A, Blasco C, Colelle A, Mari M, Garcia-Ruiz C, and Fernandez-Checa J.** Critical role of mitochondrial glutathione in the survival of hepatocytes during hypoxia. *The Journal of Biological Chemistry* 280: 3224-3232, 2005.
112. **Luyendyk J, Shaw P, Green C, Maddox J, Ganey P, and Roth R.** Coagulation-Mediated Hypoxia and Neutrophil-Dependent Hepatic Injury in Rats Given Lipopolysaccharide and Ranitidine. *Journal of Pharmacology and Experimental Therapeutics* 314: 1023-1031, 2005.
113. **Luyendyk JP, Lehman-McKeeman LD, Nelson DM, Bhaskaran VM, Reilly TP, Car BD, Cantor GH, Maddox JF, Ganey PE, and Roth RA.** Unique gene expression and hepatocellular injury in the lipopolysaccharide-ranitidine drug idiosyncrasy rat model: comparison with famotidine. *Toxicol Sci* 90: 569-585, 2006.
114. **Maddox JF, Amuzie CJ, Li M, Newport SW, Sparkenbaugh E, Cuff CF, Pestka JJ, Cantor GH, Roth RA, and Ganey PE.** Bacterial- and viral-induced inflammation increases sensitivity to acetaminophen hepatotoxicity. *JToxicolEnvironHealth A* 73: 58-73, 2010.

115. **Majmundar AJ, Wong WJ, and Simon MC.** Hypoxia-Inducible Factors and the Response to Hypoxic Stress. *Molecular Cell* 40: 294-309, 2010.
116. **Majno G, and Joris I.** Apoptosis, Oncosis, and Necrosis. *American Journal of Pathology* 146: 3-15, 1995.
117. **Mansfield KD, Simon MC, and Keith B.** Hypoxic reduction in cellular glutathione levels requires mitochondrial reactive oxygen species. *JApplPhysiol* 97: 1358-1366, 2004.
118. **Mavier P, Preaux AM, Guigui B, Lescs MC, Zafrani ES, and Dhumeaux D.** In vitro toxicity of polymorphonuclear neutrophils to rat hepatocytes: evidence for a proteinase-mediated mechanism. *Hepatology* 8: 254-258, 1988.
119. **Mehendale HM.** Tissue repair: an important determinant of final outcome of toxicant-induced injury. *Toxicologic Pathology* 33: 41-51, 2005.
120. **Metukuri M, Beer-Stolz D, Namas RA, Dhupar R, Torres A, Loughran P, Jefferson BS, Tsung A, Billiar T, Vodovotz Y, and Zamora R.** Expression and subcellular localization of BNIP3 in hypoxic hepatocytes and liver stress. *American Journal of Physiology Gastrointestinal and Liver Physiology* 296: G499-G509, 2009.
121. **Minet E, Michel G, Mottet D, Raes M, and Michiels C.** Transduction Pathways Involved in Hypoxia-Inducible Factor-1 Phosphorylation and Activation. *Free Radical Biology & Medicine* 31: 847-855, 2001.
122. **Mollen KP, McCloskey CA, Tanaka H, Prince JM, Levy RM, Zuckerbraun BS, and Billiar TR.** Hypoxia activates c-Jun N-terminal kinase via Rac1-dependent reactive oxygen species production in hepatocytes. *SHOCK* 28: 270-277, 2007.
123. **Murdoch C, Muthana M, and Lewis C.** Hypoxia Regulates Macrophage Functions in Inflammation. *The Journal of Immunology* 175: 6257-6263, 2005.
124. **Nakano Y, Kondo T, Matsuo R, Murata S, Fukunaga K, and Ohkohchi N.** Prevention of leukocyte activation by the neutrophil elastase inhibitor, sivelestat, in the hepatic microcirculation after ischemia-reperfusion. *JSurgRes* 155: 311-317, 2009.
125. **Nath B, Levin I, Csak T, Petrasek J, Mueller C, Kodys K, Catalano D, Mandrekar P, and Szabo G.** Hepatocyte-specific hypoxia-inducible factor-1alpha is a determinant of lipid accumulation and liver injury in alcohol-induced steatosis in mice. *Hepatology* 53: 1526-1537, 2011.
126. **Niknahad H, Khan S, and O'Brien PJ.** Hepatocyte injury resulting from the inhibition of mitochondrial respiration at low oxygen concentrations involves reductive stress and oxygen activation. *Chemico-Biological Interactions* 98: 27-44, 1995.

127. **Nishimura D, Ishikawa H, Matsumoto K, Shibata H, Motoyoshi Y, Fukuta M, Kawashimo H, Goto T, Taura N, Ichikawa T, Hamasaki K, Nakao K, Umezawa K, and Eguchi K.** DHMEQ, a novel NF-kappaB inhibitor, induces apoptosis and cell-cycle arrest in human hepatoma cells. *Int J Oncol* 29: 713-719, 2006.
128. **Okajima K, Harada N, Uchiba M, and Mori M.** Neutrophil elastase contributes to the development of ischemia-reperfusion-induced liver injury by decreasing endothelial production of prostacyclin in rats. *AmJPhysiol GastrointestLiver Physiol* 287: G1116-G1123, 2004.
129. **Okajima K, Harada N, Uchiba M, and Mori M.** Neutrophil elastase contributes to the development of ischemia-reperfusion-induced liver injury by decreasing endothelial production of prostacyclin in rats. *American Journal of Physiology Gastrointestinal and Liver Physiology* 287: G1116-G1123, 2004.
130. **Perng DW, Wu YC, Tsai MC, Lin CP, Hsu WH, Perng RP, and Lee YC.** Neutrophil elastase stimulates human airway epithelial cells to produce PGE2 through activation of p44/42 MAPK and upregulation of cyclooxygenase-2. *American Journal of Physiology Lung Cellular and Molecular Physiology* 285: L925-L930, 2003.
131. **Peyssonnaud C, Cejudo-Martin P, Doedens A, Zinkernagel A, Johnson RS, and Nizet V.** Cutting Edge: Essential Role of Hypoxia Inducible Factor 1a in Development of Lipopolysaccharide-Induced Sepsis. *The Journal of Immunology* 178: 7516-7519, 2007.
132. **Peyssonnaud C, Datta V, Cramer T, Doedens A, Theodorakis E, Gallo R, Hurtado-Ziola N, Nizet V, and Johnson RS.** HIF-1a expression regulates the bactericidal capacity of phagocytes. *The Journal of Clinical Investigation* 115: 1806-1815, 2005.
133. **Pham CTN.** Neutrophil serine proteases: specific regulators of inflammation. *Nature Immunology* 6: 541-550, 2006.
134. **Phan SH, Gannon DE, Varani J, Ryan US, and Ward PA.** Xanthine oxidase activity in rat pulmonary artery endothelial cells and its alteration by activated neutrophils. *American Journal of Pathology* 134: 1201-1211, 1989.
135. **Phan SH, Gannon DE, Ward PA, and Karmiol S.** Mechanism of neutrophil-induced xanthine dehydrogenase to xanthine oxidase conversion in endothelial cells: evidence of a role for elastase. *AmJRespirCell MolBiol* 6: 270-278, 1992.
136. **Piret JP, Mottet D, Raes M, and Michiels C.** CoCl₂, a Chemical Inducer of Hypoxia-Inducible Factor-1, and Hypoxia Reduce Apoptotic Cell Death in Hepatoma Cell Line HepG2. *Annals of the NY Academy of Science* 973: 443-447, 2006.

137. **Poellinger L.** HIF-1 and hypoxic response: the plot thickens. *Current Opinion in Genetics and Development* 14: 85, 2004.
138. **Preston GA, Zarella CS, Pendergraft WF, III, Rudolph EH, Yang JJ, Sekura SB, Jennette JC, and Falk RJ.** Novel effects of neutrophil-derived proteinase 3 and elastase on the vascular endothelium involve in vivo cleavage of NF-kappaB and proapoptotic changes in JNK, ERK, and p38 MAPK signaling pathways. *JAm Soc Nephrol* 13: 2840-2849, 2002.
139. **Ramaiah SK, and Jaeschke H.** Role of Neutrophils in the Pathogenesis of Acute Inflammatory Liver Injury. *Toxicologic Pathology* 35: 757-766, 2007.
140. **Recio JA, and Merlino G.** Hepatocyte growth factor/scatter factor activates proliferation in melanoma cells through p38 MAPK, ATF-2 and cyclin D1. *Oncogene* 21: 1000-1008, 2002.
141. **Rink RD, Short BL, and Pennington C.** Hepatic oxygen supply and plasma lactate and glucose in endotoxic shock. *CircShock* 5: 105-113, 1978.
142. **Rodell TC, Cheronis JC, and Repine JE.** Endothelial cell xanthine oxidase-derived toxic oxygen metabolites contribute to acute lung injury from neutrophil elastase. *Chest* 93: 146S, 1988.
143. **Rosser BG, and Gores GJ.** Liver Cell Necrosis: Cellular Mechanisms and Clinical Implications. *Gastroenterology* 108: 252-275, 1995.
144. **Roth RA, and Ganey PE.** Intrinsic versus idiosyncratic drug-induced hepatotoxicity--two villains or one? *JPharmacolExpTher* 332: 692-697, 2010.
145. **Ruzankina Y, Pinzon-Guzman C, Asare A, Ong T, Pontano L, Cotsarelis G, Zediak VP, Velez M, Bhandoola A, and Brown EJ.** Deletion of the developmentally essential gene ATR in adult mice leads to age-related phenotypes and stem cell loss. *Cell Stem Cell* 1: 113-126, 2007.
146. **Ryan HE, Lo J, and Johnson RS.** HIF-1a is required for solid tumor formation and embryonic vascularization. *The EMBO Journal* 17: 3005-3015, 1998.
147. **Saini Y, Harkema JR, and LaPres J.** HIF1a is essential for normal intrauterine differentiation of alveolar epithelium and surfactant production in the newborn lung of mice. *Journal of Biological Chemistry* 283: 33650-33657, 2008.
148. **Saito C, Lemasters JJ, and Jaeschke H.** c-Jun N-terminal kinase modulates oxidant stress and peroxynitrite formation independent of inducible nitric oxide synthase in acetaminophen hepatotoxicity. *ToxicolApplPharmacol* 246: 8-17, 2010.
149. **Salceda S, Beck I, and Caro J.** Absolute Requirement of Aryl Hydrocarbon Receptor Nuclear Translocator Protein for Gene Activation by Hypoxia. *Arch Biochem*

Biophys 334: 389-394, 1996.

150. **Sanjuan-Pla A, Cervera A, Apostolova N, Garcia-Bou R, Victor V, Murphy M, and McCreath K.** A targeted antioxidant reveals the importance of mitochondrial reactive oxygen species in the hypoxic signaling of HIF-1a. *FEBS Letters* 579: 2669-2674, 2005.
151. **Schaeffer HJ, and Weber MJ.** Mitogen-Activated Protein Kinases: Specific Messages from Ubiquitous Messengers. *Molecular and Cellular Biology* 19: 2435-2444, 1999.
152. **Schofield C, and Ratcliffe P.** Oxygen Sensing by HIF Hydroxylases. *Nature Reviews: Molecular Cell Biology* 5: 343-354, 2004.
153. **Semenza G.** HIF-1, O₂, and the 3 PHDs: How Animal Cells Signal Hypoxia to the Nucleus (Minireview). *Cell* 107: 1-3, 2001.
154. **Semenza GL.** HIF-1: mediator of physiological and pathophysiological responses to hypoxia. *JApplPhysiol* 88: 1474-1480, 2000.
155. **Seta KA, Spicer Z, Yuan Y, Lu G, and Millhorn DE.** Responding to hypoxia: lessons from a model cell line. *SciSTKE* 2002: re11, 2002.
156. **Shan X, Jones DP, Hashmi M, and Anders MW.** Selective depletion of mitochondrial glutathione concentrations by (R,S)-3-hydroxy-4-pentenoate potentiates oxidative cell death. *ChemRes Toxicol* 6: 75-81, 1993.
157. **Shaw P, Hopfensperger MJ, Ganey P, and Roth R.** Lipopolysaccharide and Trovafloxacin Coexposure in Mice Causes Idiosyncrasy-Like Liver Injury Dependent on Tumor Necrosis Factor-Alpha. *Toxicological Sciences* 100: 259-266, 2007.
158. **Shaw PJ, Fullerton AM, Scott MA, Ganey PE, and Roth RA.** The role of the hemostatic system in murine liver injury induced by coexposure to lipopolysaccharide and trovafloxacin, a drug with idiosyncratic liability. *ToxicolApplPharmacol* 236: 293-300, 2009.
159. **Shaw PJ, Ganey PE, and Roth RA.** Trovafloxacin enhances the inflammatory response to a Gram-negative or a Gram-positive bacterial stimulus, resulting in neutrophil-dependent liver injury in mice. *JPharmacolExpTher* 330: 72-78, 2009.
160. **Shi DY, Xie FZ, Zhai C, Stern JS, Liu Y, and Liu SL.** The role of cellular oxidative stress in regulating glycolysis energy metabolism in hepatoma cells. *Molecular Cancer* 8: 32, 2009.
161. **Shingu K, Eger EI, 2nd, and Johnson BH.** Hypoxia may be more important than reductive metabolism in halothane-induced hepatic injury. *Anesth Analg* 61: 824-

827, 1982.

162. **Snyder CM, and Chandel NS.** Mitochondrial Regulation of Cell Survival and Death During Low-Oxygen Conditions. *Antioxidants and Redox Signaling* 11: 2673-2683, 2009.

163. **Sowter HM, Ratcliffe PJ, Watson P, Greenberg AH, and Harris AL.** HIF-1-dependent regulation of hypoxic induction of the cell death factors BNIP3 and NIX in human tumors. *Cancer Res* 61: 6669-6673, 2001.

164. **Stanley AJ, MacGregor IR, Dillon JF, Bouchier IA, and Hayes PC.** Neutrophil activation in chronic liver disease. *EurJGastroenterolHepatol* 8: 135-138, 1996.

165. **Suzuki T, Moraes T, Vachon E, Ginzberg H, Huang TT, Matthay M, Hollenberg M, Marshall J, McCulloch C, Herrera Abreu MT, Chow CW, and Downey G.** Proteinase-Activated Receptor-1 Mediates Elastase-Induced Apoptosis of Human Lung Epithelial Cells. *American Journal of Respiratory Cell and Molecular Biology* 33: 231-247, 2005.

166. **Suzuki T, Moraes TJ, Vachon E, Ginzberg H, Huang TT, Matthay M, Hollenberg MD, Marshall J, McCulloch CAG, Abreu MRH, Chow CW, and Downey GP.** Proteinase-Activated Receptor-1 Mediates Elastase-Induced Apoptosis of Human Lung Epithelial Cells. *American Journal of Respiratory Cell Molecular Biology* 33: 231-247, 2005.

167. **Suzuki T, Yamashita C, Zemans RL, Briones N, Van LA, and Downey GP.** Leukocyte elastase induces lung epithelial apoptosis via a PAR-1-, NF-kappaB-, and p53-dependent pathway. *AmJRespirCell MolBiol* 41: 742-755, 2009.

168. **Takai S, Kimura K, Nagaki M, Satake S, Kakimi K, and Moriwaki H.** Blockade of neutrophil elastase attenuates severe liver injury in hepatitis B transgenic mice. *JVirol* 79: 15142-15150, 2005.

169. **Taylor C.** Mitochondria and cellular oxygen sensing in the HIF pathway. *Biochemical Journal* 409: 19-26, 2008.

170. **Tiniakos DG.** Liver biopsy in alcoholic and non-alcoholic steatohepatitis patients. *Gastroenterol Clin Biol* 33: 930-939, 2009.

171. **Tsujimoto H, Ono S, Majima T, Kawarabayashi N, Takayama E, Kinoshita M, Seki S, Hiraide H, Moldawer LL, and Mochizuki H.** Neutrophil elastase, MIP-2, and TLR-4 expression during human and experimental sepsis. *SHOCK* 23: 39-44, 2005.

172. **Uchida Y, Freitas MC, Zhao D, Busuttill RW, and Kupiec-Weglinski JW.** The inhibition of neutrophil elastase ameliorates mouse liver damage due to ischemia and reperfusion. *Liver Transplantation* 15: 939-947, 2009.

173. **Uhlmann D, Pietsch UC, Ludwig S, Hess J, Armann B, Gaebel G, Escher E, Schaffranietz L, Tannapfel A, Fiedler M, Hauss J, and Witzigmann H.** Assessment of hepatic ischemia-reperfusion injury by simultaneous measurement of tissue pO₂, pCO₂, and pH. *MicrovascRes* 67: 38-47, 2004.
174. **van Uden P, Kenneth NS, and Rocha S.** Regulation of hypoxia-inducible factor-1a by NF-kB. *Biochemical Journal* 412: 477-484, 2008.
175. **Varani J, Ginsburg I, Schuger L, Gibbs DF, Bromberg J, Johnson KJ, Ryan US, and Ward PA.** Endothelial cell killing by neutrophils. Synergistic interaction of oxygen products and proteases. *AmJPathol* 135: 435-438, 1989.
176. **Varani J, and Ward PA.** Mechanisms of neutrophil-dependent and neutrophil-independent endothelial cell injury. *BiolSignals* 3: 1-14, 1994.
177. **Vengellur A, Phillips JM, Hogenesch JB, and LaPres J.** Gene expression profiling of hypoxia signaling in human hepatocellular carcinoma cells. *Physiological Genomics* 22: 308-318, 2005.
178. **Vovenko EP, and Chuikin AE.** Tissue Oxygen Tension Profiles Close to Brain Arterioles and Venules in the Rat Cerebral Cortex during the Development of Acute Anemia. *Neuroscience and Behavioral Physiology* 40: 723-731, 2010.
179. **Wakabayashi Y, Shimizu H, Kimura F, Yoshidome H, Ohtsuka M, Kato A, and Miyazaki M.** Mechanism of neutrophil accumulation in sinusoids after extrahepatic biliary obstruction. *Hepatology* 55: 1179-1183, 2008.
180. **Walmsley S, Cadwallader K, and Chilvers E.** The role of HIF-1a in myeloid cell inflammation. *TRENDS in Immunology* 26: 434-439, 2005.
181. **Walmsley S, Print C, Farahi N, Peyssonnaud C, Cramer T, Sobolewski A, Condliffe A, Cowburn A, Johnson N, and Chilvers E.** Hypoxia-induced neutrophil survival is mediated by HIF-1a-dependent NF-kB activity. *The Journal of Experimental Medicine* 201: 105-115, 2005.
182. **Walsh DE, Greene CM, Carroll TP, Taggart CC, Gallagher PM, O'Neill SJ, and McElvaney NG.** Interleukin-8 up-regulation by neutrophil elastase is mediated by MyD88/IRAK/TRAF-6 in human bronchial epithelium. *JBiolChem* 276: 35494-35499, 2001.
183. **Wen W, Ding J, Sun W, Wu K, Ning B, Gong W, He G, Huang S, Ding X, Yin P, Chen L, Liu Q, Xie W, and Wang H.** Suppression of Cyclin D1 by Hypoxia-Inducible Factor-1 via Direct Mechanism Inhibits the Proliferation and 5-Fluorouracil-Induced Apoptosis of A549 cells. *Cancer Res* 70: 2010-2019, 2010.
184. **Wiedow O, and Meyer-Hoffert U.** Neutrophil serine proteases: potential key regulators of cell signalling during inflammation. *Journal of Internal Medicine* 257: 319-

328, 2005.

185. **Williams CD, Bajt ML, Farhood A, and Jaeschke H.** Acetaminophen-induced hepatic neutrophil accumulation and inflammatory liver injury in CD18-deficient mice. *Liver Int* 30: 1280-1292, 2010.

186. **Wu K, Urano T, Ihara H, Takada Y, Fujie M, Shikimori M, Hashimoto K, and Takada A.** The cleavage and inactivation of plasminogen activator inhibitor type 1 by neutrophil elastase: the evaluation of its physiologic relevance in fibrinolysis. *Blood* 86: 1056-1061, 1995.

187. **Yajima D, Motani H, Hayakawa M, Sato Y, Sato K, and Iwase H.** The relationship between cell membrane damage and lipid peroxidation under the condition of hypoxia-reoxygenation: analysis of the mechanism using antioxidants and electron transport inhibitors. *Cell Biochem Funct* 27: 338-343, 2009.

188. **Yan H-M, Ramachandran A, Bajt ML, Lemasters JJ, and Jaeschke H.** The Oxygen Tension Modulates Acetaminophen-Induced Mitochondrial Oxidant Stress and Cell Injury in Cultured Hepatocytes. *Toxicological Sciences* 117: 525-523, 2010.

189. **Yang JJ, Kettritz R, Falk RJ, Jennette JC, and Gaido ML.** Apoptosis of endothelial cells induced by the neutrophil serine proteases proteinase 3 and elastase. *AmJPathol* 149: 1617-1626, 1996.

190. **Zegura B, Lah TT, and Filipic M.** The role of reactive oxygen species in microcystin-LR-induced DNA damage. *Toxicology* 200: 59-68, 2004.

191. **Zinkernagel A, Johnson RS, and Nizet V.** Hypoxia inducible factor (HIF) in innate immunity and infection. *Journal of Molecular Medicine* 85: 1339-1346, 2007.

192. **Zou W, Beggs KM, Sparkenbaugh EM, Jones AD, Younis HS, Roth RA, and Ganey PE.** Sulindac metabolism and synergy with tumor necrosis factor-alpha in a drug-inflammation interaction model of idiosyncratic liver injury. *JPharmacolExpTher* 331: 114-121, 2009.

193. **Zou W, Devi SS, Sparkenbaugh E, Younis HS, Roth RA, and Ganey PE.** Hepatotoxic interaction of sulindac with lipopolysaccharide: role of the hemostatic system. *ToxicolSci* 108: 184-193, 2009.